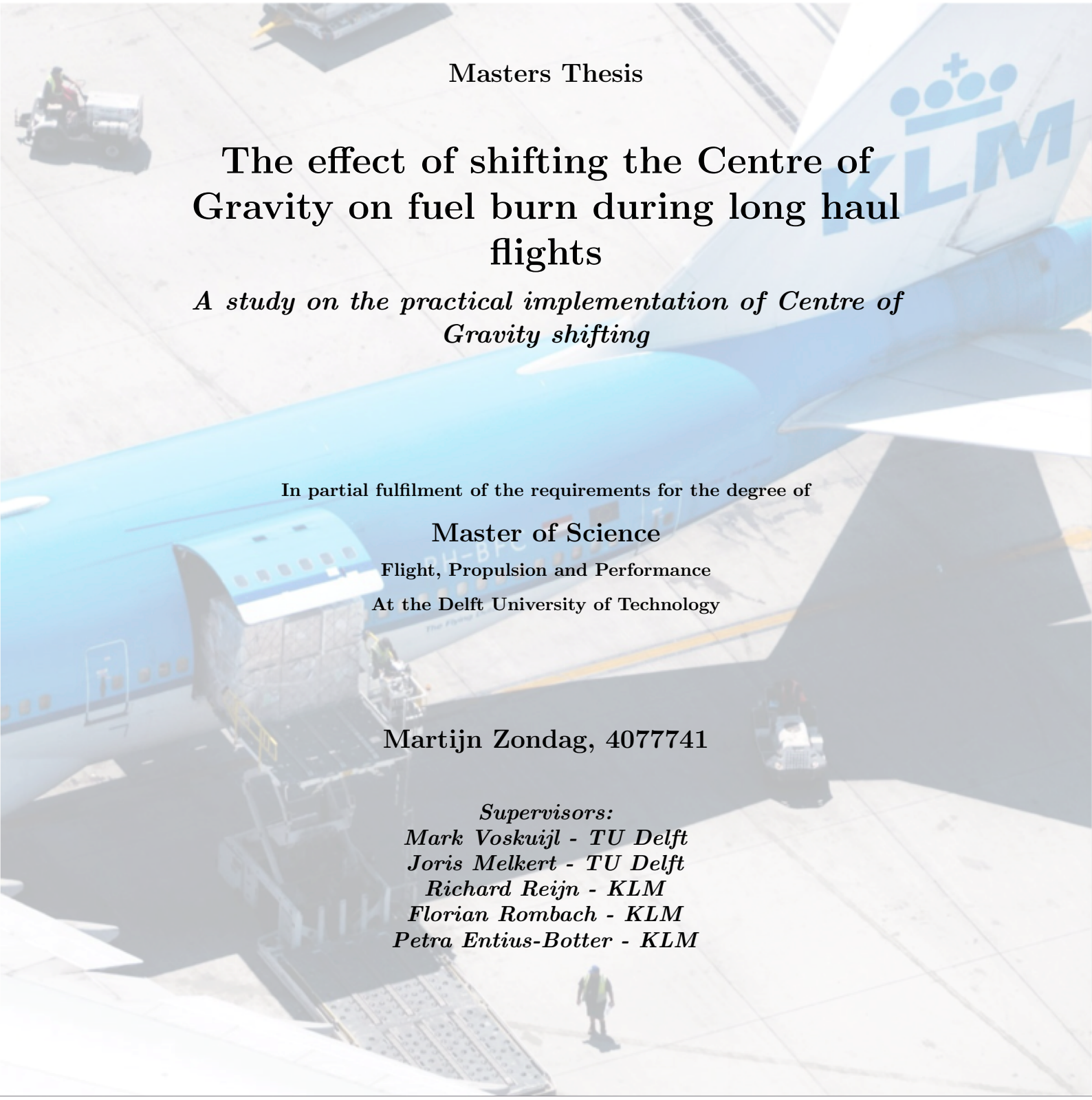

Masters Thesis

The effect of shifting the Centre of Gravity on fuel burn during long haul flights

A study on the practical implementation of Centre of Gravity shifting

In partial fulfilment of the requirements for the degree of

Master of Science

Flight, Propulsion and Performance

At the Delft University of Technology

Martijn Zondag, 4077741

Supervisors:
Mark Voskuijl - TU Delft
Joris Melkert - TU Delft
Richard Reijn - KLM
Florian Rombach - KLM
Petra Entius-Botter - KLM

Challenge the future

Preface

By handing in this report, I will finalise my Masters degree Flight, Preformance and Propuslion at the Technical University in Delft. This research is conducted at Koninklijke Luchtvaart Maatschappij. This thesis contributes to the effect of the Centre of Gravity on the fuel consumption.

Enabling this thesis, I would like to thank KLM for allowing me to perform this research. Special thanks go to Richard Reijn, Petra Entius-Botter and Florian Rombach, for helping me shape and perform this research. The aid in obtaining the required data is much appreciated. I would also like to thank all other colleagues that I worked with during the course of this research.

In addition, I would like to thank Mark Voskuijl for guiding me, even during the busy period due to changing jobs. As such, I would also like to thank Joris Melkert, for taking over these tasks from Mark Voskuijl at the very last stages of my graduation.

Next to the aforementioned persons helping me during my graduation, I would like to thank Bernice Hofland. Your help and feedback, next to those of KLM and the TU Delft, proved a welcome and fresh addition.

Finally, I would like to thank my parents and family, for supporting me throughout my university years.

Martijn Zondag,
Delft, September 2018

Word of Caution

This report contains the research performed at KLM. Due to confidentiality, numbers and figures are adjusted to give an indication. Calculated and input values are multiplied by undisclosed factors and rounded, while figures do not provide values. Exception to this are values that can easily be obtained from literature or other sources, and are not confidential.

Care has been to ensure any discussed values show behaviour similar to those encountered during the research. Nonetheless, coherence between input and output can be absent. The same can be said of coherence between certain plots, since values were checked for their representation of those encountered in the research. Finally, some data has been removed, since it is not deemed required to understand the report.

A division has been made considering the multiplication factors. Values related to Boeing and Airbus each have their own factor, while KLM data also has its own factor, but also contains exaggerations and a subtraction. As such, if one has access to one of each, the factors can be derived, making it possible to replicate that research. The derivation of the constants is not necessary, since anyone having access to all KLM data can also access the original research report. This way, replication of this report is possible for someone with access to KLM data. Competitors will be unable to determine confidential data from KLM using this method.

Summary

This report contains the research of the practical effect of shifting the Centre of Gravity (CG) of an aircraft aft. The relation between fuel savings and CG location is a means to reduce fuel burn. Due to increasing fuel prices, this relation has obtained attention of aircraft operators. Despite literature discussing the relation between aft CG and fuel burn, no readily available method to derive a quantification is available. Therefore, the main focus of this research is put on giving insight on this relation and quantifying the potential fuel savings. Some discussion is provided on other effects related to the CG, which were encountered during the research.

In practice, it shows that while developing the load plan of an aircraft, loadcontrollers are prompted with logistical requirements stating a preference of loading certain parts first. However, loading all heavy cargo in the rear of an aircraft will shift the CG aft, making the aircraft fly more efficiently. Due to this, conflicts arise, leaving loadcontrollers without an indication of what will be less favourable for the company. As such, the loadcontrol department of Koninklijke Luchtvaart Maatschappij (KLM) wished to get a better knowledge of the consequences of aft CG placement. To create a complete picture, other effects related to CG shifting were included in the research. The results will enable a better understanding by KLM, while easing managerial decisions.

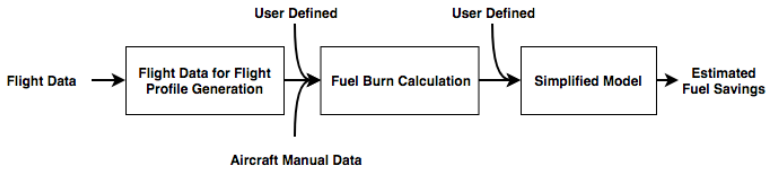

Figure 0.1.: The Three Modules Used Throughout the Research

To research the relation between the CG and fuel burn, a fuel computation program was made. This enabled accurate fuel predictions based on the major influences, such that the included CG effects could be further investigated. Three modules were defined to facilitate this research, which are depicted in figure 0.1.

Using flight data, the first module will generate an average flight profile, serving as input for the second module, the fuel burn module. Together with aircraft specific data and user defined input, the total fuel consumption can be calculated. The resulting fuel burn is used with the Zero-Fuel Weight (ZFW) and Zero Fuel Weight CG location expressed as a percent of Mean Aerodynamical Chord (ZFWMAC) to determine a function for the fuel burn. The coefficients of this function are saved to the simplified model.

In more detail, the first module generates an average flight profile for each route. It consists of normalised routes being averaged for their wind, flight speed, flight levels and ambient temperatures, while discarding outliers. For each profile, the average take-off fuel burn, zero fuel weight, take-off weight and distance is determined. Since the flight route is dependent on the season, aircraft type and origin-destination combination, the analysis is done for all possible sets of these three variables.
The second module, which takes the flight profile, calculates the fuel burn by including aircraft performance data and user defined ZFW and ZFWMAC. The Performance Engineers Manual (PEM) and literature provided by Ruijgrok, Anderson and Torenbeek provided means to numerically compute climb, cruise and descending fuel burn.
The last module takes the results to generate a simplified tool. This was developed by varying the ZFW and the accompanying ZFWMAC location for each route set in the second module. Through the coefficients of the derived function, the simplified tool is able to quickly provide a user the expected savings of a shifted ZFWMAC.

Having developed the three modules, validation was performed to see if the modules provided logical and accurate data. Validating the first two, it was found that they predicted the fuel burn within 2% on average over a whole month, with the largest difference being 4%, compared to actual flights. Doing the same, only using the average flight profile as input, resulted in a 1% difference between a flight with inputs comparable to the average. The third module, or the simplified module, proved to provide values within 4%, on average, of the extensive calculations performed in the first two modules.

Running the first and second modules shows that the CG indeed influences the fuel burn. By introducing the simplified module, an airline like KLM can save on fuel costs. Seven different aircraft have been analysed, namely the Boeing 747-400, 747-400 Combi, 777-200ER, 777-300ER, 787-9, Airbus A330-200 and A330-300.

Evaluating flights of the considered aircraft, with varying CG locations and ZFWs, the fuel savings of an aft CG were found. Over all aircraft, the longest flights heading west, especially during winter, had the highest savings potential. Due to the parabolic nature of the CG-fuel burn relation, variations in the ranking can occur if a flight performs poorly on its average CG. The ZFW had an influence on the ranking too, with empty aircraft having a percentage wise higher savings potential with an aft CG, but heavy flights having a larger absolute savings. As indication, fuel savings between 200kg and 3000kg were encountered.

Concluding, shifting the CG has an impact on the fuel burn of an aircraft. A more aft CG will result in a lower consumption. Typically, savings of 0 to 5% of the total fuel are found for a 5 percentage point shift in ZFWMAC, depending on the aircraft. From an operational point of view, this shift of 5 percentage points is not directly achievable due to operational and logistical limitations. Nonetheless, this can save KLM €5.5 to €7 million in fuel costs annually, excluding costs due to non-compliance with current logistical requirements. However, while shifting the CG, an operator must stay within the design limits, to ensure safe flight. With the results, theory is expanded by obtaining insight on the theoretical relation between CG location and fuel burn.

Contents

List of Acronyms viii

List of Symbols x

1 Introduction and Background 2
- 1.1 Problem Introduction . . . 3
- 1.2 Aims and Objectives . . . 4
- 1.3 Research Outline . . . 5
- 1.4 Conclusion . . . 5

2 Theoretical Framework 6
- 2.1 Forces, Moments and Accelerations . . . 6
- 2.2 Equations of Motion . . . 8
- 2.3 Drag . . . 10
  - 2.3.1 Centre of Gravity Related Drag . . . 10
  - 2.3.2 Total Drag . . . 12
- 2.4 Wind . . . 12
- 2.5 Theoretical Gain . . . 13
- 2.6 Limitations . . . 17
- 2.7 Conclusion . . . 19

3 Methodology 20
- 3.1 Flight Data Module . . . 20
  - 3.1.1 Initial, Constant Variables . . . 21
  - 3.1.2 Flight Varying Variables . . . 22
- 3.2 Fuel Burn Module . . . 25
  - 3.2.1 Aircraft Design Data . . . 26
  - 3.2.2 Airbus Data . . . 27
  - 3.2.3 Fuel Burn . . . 27
  - 3.2.4 Drag Coefficient Details . . . 30
  - 3.2.5 Centre of Gravity Implementation . . . 31
- 3.3 Simplified Model . . . 33
- 3.4 Assumptions . . . 35
- 3.5 Conclusion . . . 36

4 Validation and Verification **37**
4.1 Flight Data Module . . . 37
4.1.1 Flight Varying Variables . . . 38
4.1.2 Initial, Constant Variables . . . 41
4.1.3 Aircraft Manual Data . . . 41
4.2 Fuel Burn Module . . . 42
4.2.1 Cruise . . . 42
4.2.2 Step Climb . . . 43
4.2.3 Climb . . . 44
4.2.4 Descent . . . 45
4.2.5 CG Effects . . . 47
4.2.6 Whole Flight . . . 49
4.2.7 Standard Flight . . . 50
4.3 Simplified Model . . . 51
4.4 Verification . . . 53
4.5 Conclusion . . . 53

5 Results **55**
5.1 Savings Potential . . . 55
5.1.1 Boeing 777-200ER . . . 55
5.1.2 Whole Fleet . . . 57
5.1.3 Short Range . . . 65
5.2 A330 Trim Tank . . . 65
5.3 Snowball Effect . . . 66
5.4 Conclusion . . . 67

6 Flight Planning Process **69**

7 Conclusion, Discussion and Recommendations **75**
7.1 Conclusion . . . 75
7.2 Discussion and Recommendations . . . 75
7.2.1 Flight Data Module . . . 76
7.2.2 Fuel Burn Module . . . 76
7.2.3 Simplified Model . . . 77
7.2.4 Further Research . . . 78

References **79**

Appendix A Additional Theoretical Framework **84**
A.1 Forces and Moments . . . 84
A.2 Additional Modelling Details . . . 85
A.2.1 Flaps and Landing Gear . . . 86
A.2.2 Takeoff and Landing Procedure . . . 86
A.2.3 Turns and Sideslip . . . 86
A.2.4 Altitude offset airport . . . 86
A.2.5 Fuel Penalties . . . 87
A.3 Additional Details . . . 87
A.3.1 Fuel Build-up . . . 87

Appendix B Fuel Burn Validation **89**
B.1 Standard Flight Fuel Consumption . . . 89

Appendix C Largest Potential Route Results **90**

Appendix D Results per Season **91**

Appendix E Lift-Horizontal Tail Drag Relation **92**

Appendix F Problem and Research Question **95**
F.1 Research Objective . . . 96
F.2 Research Question . . . 96
F.2.1 Sub-questions . . . 96

Appendix G Use of Tool **98**
G.1 How To Run . . . 98
G.2 Input Data . . . 98

List of Acronyms

AC	Aerodynamical Center.
AFM	Aircraft Flight Manual.
APU	Auxiliary Power Unit.
ATC	Air Traffic Control.
BADA	Base of Aircraft Data.
CAS	Calibrated Airspeed.
CG	Centre of Gravity.
EoM	Equations of Motion.
EOM	Equations of Motion.
FCOM	Flight Crew Operating Manual.
FL	Flight Level.
FPP	Flight Performance and Propulsion.
FPPM	Flight Planning and Performance Manual.
FTP	Fuel Temperature Prediction.
IATA	International Air Transport Association.
IFP	In Flight Performance.
ISA	International Standard Atmosphere.
KLM	Koninklijke Luchtvaart Maatschappij.
KLM E&M	KLM Engineering and Maintenance.
LEMAC	Leading Edge Mean Aerodynamic Chord.
LERC	Leading Edge Reference Chord.
MAC	Mean Aerodynamic Chord.
MTOW	Maximum Take-off Weight.
MZFW	Maximum Zero-Fuel Weight.

NOTAM	Notices to Airmen.
NP	Neutral Point.
OCC	Operations Control Centre.
OEM	Original Equipment Manufacturer.
OEW	Operating Empty Weight.
PEM	Performance Engineers Manual.
PEP	Performance Engineers Program.
RC	Reference Chord.
ROC	Rate of Climb.
ROCD	Rate of Climb/Descent.
ROD	Rate of Descent.
SM	Static Margin.
TAS	True Airspeed.
TOC	Top of Climb.
TOD	Top of Descent.
TOW	Take-off Weight.
TSFC	Thrust Specific Fuel Consumption.
ZFW	Zero-Fuel Weight.
ZFWMAC	Zero Fuel Weight CG location expressed as a percent of Mean Aerodynamical Chord.

List of Symbols

Sign	Description	Unit
a	Speed of Sound	m/s
A	Aspect Ratio	-
$\bar{c}$	Average Chord Length	m
C_D	Drag Coefficient	-
C_{D_0}	Zero-lift Drag Coefficient	-
C_{D_i}	Induced Drag Coefficient	-
C_L	Lift Coefficient	-
C_m	Moment Coefficient	-
c_T	Specific Fuel Consumption	-
D	Drag	N
e	Oswald Efficiency Factor	-
E	Endurance	s
F	Fuel Weight Flow	N/s
g	Gravitational Acceleration	m/s^2
h	Geometric Altitude	m
L	Lift	N
m	Mass	kg
$\dot{m}$	Mass Flow	kg/s
M	Mach Number	-
M	Moment	Nm
p	Pressure	Pa
R	Mean Earth Radius	m
R	Gas Constant for Air	$\frac{J}{kgK}$
S	Wing Area	m^2
$S.M.$	Static Margin	
t	Time	s
T	Thrust	N
T	Temperature	K
V	Velocity	m/s
W	Weight	N
W	Wind Velocity	m/s
x	Location	-
X	x-direction	-
Z	z-direction	-

Sign	Description	Unit
	Greek Alphabet	
α_T	Thrust Angle of Attack	α_T
α	Angle of Attack	deg
γ	Flight Path Angle	deg
γ	Heat Capacity Ratio of Air	-
δ	Pressure Ratio	-
η	Thrust Setting	%
θ	Temperature Ratio	-
θ	Pitch Angle	deg
κ	Temperature Lapse Rate	$^oC/m$
λ	Lattitude	DMS
μ	Bank Angle	deg
ρ	Density	kg/m^3
τ	Longitude	DMS
ϕ	Bank Angle	deg
χ	Velocity Heading Angle	deg
	Subscripts	
0	Sea Level Conditions	
ac	Aerodynamic Center	
h	Horizontal tail contribution	
$A-h$	Tailless aircraft contribution	
b	Body Reference	
cg	Center of Gravity	
e	East Component	
e	Earth Reference	
end	Ending/terminating point	
f	Fuel	
g	Ground Relative Contribution	
h	Horizontal Tail Contribution	
h	Upward Component	
$init$	Initial/starting point	
max	Maximum	
$mindrag$	Minimal drag condition	
n	North Component	
np	Neutral Point	
Re	Reynolds Number	
s	Airmass Relative Contribution	
s	Quasi-steady flight condition	
SL	Sea Level Condition	
T	Thrust Contribution	
$trim$	Trim Contribution	
w	Wind Relative Contribution	

Sign	Description	Unit
$wing$	Wing Contribution	
x	X_e-direction Contribution	
z	Z_e-direction Contribution	
∞	Free-stream Condition	

1. Introduction and Background

Due to the complexity of aviation, airlines are struggling to stay profitable (Jara-Díaz, Cortés & Mora, 2012). One of the main contributions of the total cost is the fuel consumption of the fleet. According to the International Air Transport Association (IATA), this can amount to 33% of the total costs (International Air Transport Association, 2017). The Koninklijke Luchtvaart Maatschappij (KLM) states a similar percentage of 31% in 2013 (Koninklijke Luchtvaart Maatschappij, 2017), amounting to €3.1 billion.

To decrease the fuel costs, aircraft manufacturers focus on designing aircraft with lower fuel burn. Engines are designed to consume less fuel with an increased thrust (Rolls-Royce plc, 2017), while aerodynamics and weight are improved by Boeing (The Boeing Company, 2006), Airbus (Airbus SE, 2017b) or third parties. An operator, like KLM, can only influence operational variables, like the load and its distribution, fuel quantity and route. An airline is thus dependent on a general product and can only customise this product to a small extent.

One of the means to improve fuel consumption is to move the Centre of Gravity (CG) aft (Mongeau & Bès, 2003), while staying within the stability limits (Torenbeek, 1982). Despite the potential savings of shifting the CG aft, combined with the high fuel costs, the result is difficult to quantify. Rough estimations of the potential fuel savings exist (Mongeau & Bès, 2003), (J. Anderson, 2005). However, with statements in the line of "a displacement of the center of gravity of less than 75 cm in a long-range aircraft yields, over a 10,000 km flight, a saving of 4,000kg of fuel" (Mongeau & Bès, 2003), no qualitative conclusions can be drawn. Details on the aircraft type, specific use of the aircraft and configuration are lacking, making replication difficult.

With every flight, an operator can influence the CG position through the load scheme of cargo and baggage. Within KLM, modernisation resulted in the introduction of ALTEA FM and AutoLoad to automate this process. Both are designed to deliver a load scheme that fulfils logistical requirements. These logistical requirements incorporate needs like short connection baggage being placed near the door or quick access during intermediate stops on multi-legged flights. A second theme in ALTEA FM can be selected, which focuses on optimising for the CG, giving the logistical requirements a low priority.

1.1. Problem Introduction

An indication of the rough estimates of the fuel savings due to an aft CG provided by Boeing (Dispatch, 2017) are shown in table 1.1 and give the potential change in fuel consumption. In addition, patents stipulating the relation as a benefit (Lee, Aminpour & Morgenstein, 2003) (Buisson & Moline, 1988), strengthen the practical interest of this relation, but no indication of the savings are provided. Also, the high number and variety of variables influencing the fuel burn are not discussed and make the analysis per flight for KLM difficult. Including operator dependent factors, such as loading approaches and route strategies, decrease the representativeness for an operator of the quantification provided by Original Equipment Manufacturers (OEMs). The lack of detail and means to derive the relation accurately for a specific operator, combined with the increase in fuel prices, show the requirement of such a research. As such, the difficulty to make fuel and load scheme decisions will decrease, which still remains a point of difficulty (Koninklijke Luchtvaart Maatschappij, 2017).

Table 1.1.: Section of CG Fuel Penalty Table (Dispatch, 2017)

ZFWMAC [%]	<16-16.9	17-17.9	18-19.9	20-21.9
Fuel Correction [%]	+1.3	+1.2	+0.9	+0.6
ZFWMAC [%]	29-30.9	31-32.9	33-35.9	>=36
Fuel Correction [%]	+/-0.0	-0.4	-0.5	-0.7

In addition to saving fuel, certain routes are restricted by their Take-off Weight (TOW) (Koninklijke Luchtvaart Maatschappij, 2017). As such, saving fuel can lead to extra passengers or cargo taken on board. In this case, not only fuel is saved, also additional revenue can be generated.

Doing some deeper research, it can be found that the main cause in fuel consumption changes due to a shifted CG is caused by the change in trim drag (Torenbeek, 1982) (see chapter 2 for further details). This relation is discussed in several reports, but only Anderson provides numbers, provided in table 1.2 (D. Anderson, 2006). It immediately becomes clear that no aircraft type is given for the trim drag table. In addition, the figure does not depict the route length and is only considering cruising flight. It does not represent a figure for a specific route, or how to derive this.

Table 1.2.: Trim Drag Change at Cruise (D. Anderson, 2006)

CG Range [%]	14-19	19-26	26-37	37-44
Trim Drag Change [%]	2	1	0	-1

It can be concluded that current literature presents no readily available method to derive a quantification on the CG-fuel consumption relation. Research naming a quantification

of the relation are too generic. In addition, any quantification discussed is either not replicable (D. Anderson, 2006), not detailed (Mongeau & Bès, 2003), or not comparable to the utilisation of KLM their aircraft (J. Anderson, 2005). As such, the need for such a research is further stipulated.

In addition, practical need shows when investigating operators of aircraft. Different operators, but also departments within KLM, have their own methods of accounting for the increase in fuel consumption due to specific variables. Often, these methods are poorly documented. In some cases, the discussed CG location influence is only seen as a beneficial effect, providing the chance of unaccounted fuel savings. The absence of a clear model and literature on the CG-fuel relation results in a sub-optimal situation for aircraft operators like KLM.

The increasing fuel prices (International Air Transport Association, 2017) and accompanying need to increase efficiency within aviation (Jara-Díaz et al., 2012), increases the need to know what the costs of decisions are. The problem found is that due to the absence of detailed research on the CG-fuel consumption relation, decisions related to positioning the CG cannot be performed well.

1.2. Aims and Objectives

With the better understanding of the problem, the goal of this research can be determined. The objective and research questions were derived to determine to what extent this research will be performed. The whole derivation process can be found in Appendix F. Combined with the interest of KLM in a simplified model for practical application and analysis, the research question was defined as:

What is the influence of the Centre of Gravity position on fuel consumption and how can this be modelled to give a simplified model for economic advantage for an airline?

One can see the main research being focused on the development of a fuel prediction program. It is required to be accurate enough compared to flights performed, while including the effects of the CG. The opportunity to perform the research at KLM provides a practical opportunity and access to large amounts of data. The result will be a program not only applicable in practice, but the inclusion of historic flights. These will influence the flight profiles by including regional effects encountered on certain routes.

With the validated, program, the CG can be varied and studied for its effect on the total fuel burn. These results are used to form a simplified model, which can be used by KLM employees, since the main tool will be too complex and time consuming for practical application. As such, dedicated departments can use the tool to see the impact of their CG related work. Due to the simplification, one should consider the decreased accuracy and whether this is acceptable for the intended use.

1.3. Research Outline

Knowing what the goal of this research is, a deeper look will be taken at existing theory and how it will be used in this research. Focus will be put on what variables to include and calculate to get to the fuel consumption of a flight. Also, a look is taken at what the savings are when considering the found theory and some of the sub-questions that were determined at the start of this research.

Chapter 3 will then discuss the theory used to construct the program. Three main parts of the program are defined, consisting of the flight profile generation from data, fuel burn computations and the simplified tool containing the results. Extra focus is put on the effect and implementation of the CG, due to this being the most important subject of this research. Validation and verification of this tool is discussed in the consecutive chapter, finalising the program development. A single aircraft and route will be used from here on in the report, being a Boeing 777-200ER flying between Amsterdam and Tokyo Narita. Discussing the process for each aircraft would result in repetition, and only special cases of other flights and aircraft will be mentioned.

The results obtained with the tool are treated in chapter 5 and their feasibility. Detailed results will be discussed for a number of cases, with the main results being shown for each aircraft type. The conclusion and discussion of these results will be done in chapter 7. Chapter 7 also includes recommendations for the fuel computation tool, while chapter 6 provides recommendations on the loading process and the application of this research. Any additional details on the research deemed not necessary for the report, but were useful or of interest throughout the research, can be found in the appendices.

1.4. Conclusion

Current literature does not provide ready to apply answers to derive a quantification of the fuel saved for KLM by shifting the CG. Therefore, it was decided to develop a model to provide answers on this subject. This model will be the main focus of this report and the coming chapters. Theory is enriched by having insights from the model applied to the practical application of fuel burn when shifting the CG. The conversion of this research and its answers to a quick and easy to use model will be included, such that the results can be applied in practice for KLM.

2. Theoretical Framework

With the objective of this research from chapter 1, research on related theory can be performed more effectively. The most important equations, notable additions and deviations from the standard approach will be discussed here. The Equations of Motion (EOM) will serve as a basis for the model, and their use will be discussed for each phase. The drag is discussed next, due to its presence in the EOM and its importance in this research. After briefly discussing the effect of wind, a look is taken at a theoretical quantification of the fuel savings, as to get an idea of what order of magnitude to expect. The final section focuses on the limits of CG movement.

2.1. Forces, Moments and Accelerations

The equations used throughout the research can be derived using statics and dynamics of a rigid body. To ease the derivation, figures 2.1 and 2.2 are used to see the forces and accelerations. These are a simplification and adjustment to rigid body of the point mass models in figures A.1 and A.2 in Appendix A, of which figure A.1 is a point mass model. The step from rigid body to point mass model is further discussed in 2.3.1. The horizontal tail force was drawn downwards, as this represents its most common direction. Finally, in figure 2.2 the $mV\frac{d\gamma}{dt}$ and $I\ddot{\theta}$ terms are shown for completeness, but will be considered outside the required detail for this research.
One must be warned that figure 2.1 is not to scale. The CG is shifted slightly forward to get a clearer figure. The CG of a Boeing 777 is located between 14% and 44% Zero Fuel Weight CG location expressed as a percent of Mean Aerodynamical Chord (ZFWMAC) (The Boeing Company, 2004). Figure 2.1 does show the relative position of each indicated variable, and enables the derivation of the required functions.

As one can see from the free-body diagram in figure 2.1, the main force counteracting the thrust is the drag. This drag will vary depending on the aircraft design, flight speed, altitude, weight and CG. The focus of this research is the effect of the CG. Looking at figure 2.1 and taking the moments around the CG, the L_h is used to maintain equilibrium. Theoretically moving the CG to the Aerodynamical Center (AC) means L_{wing} causes no moment around the CG. Assuming no change in the aerodynamic moments means only L_h changes to compensate this. In turn, L_h causes drag, establishing the relation between the CG and drag.

A second effect on the total drag of an aircraft can also be derived from the free-body diagram. An increase in L_h due to a forward shifted CG, means a larger downforce.

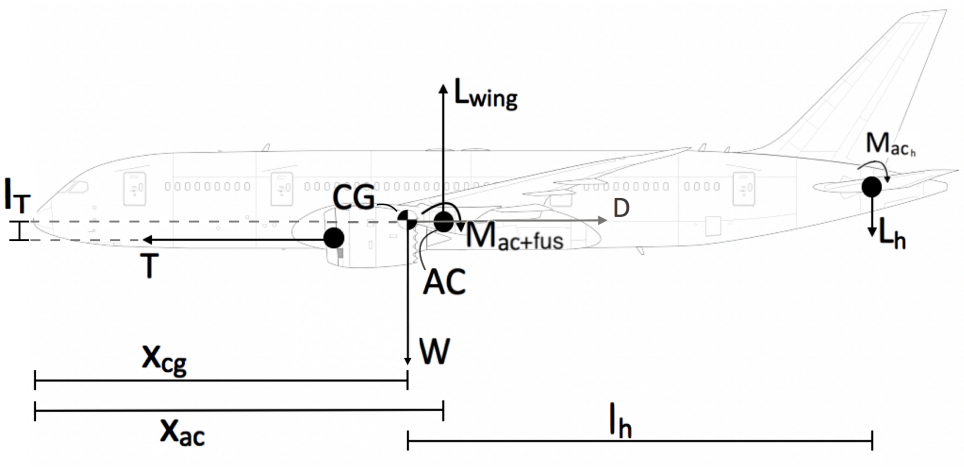

Figure 2.1.: Free-Body Diagram (not to scale), *adapted from Norebbo (2014)*

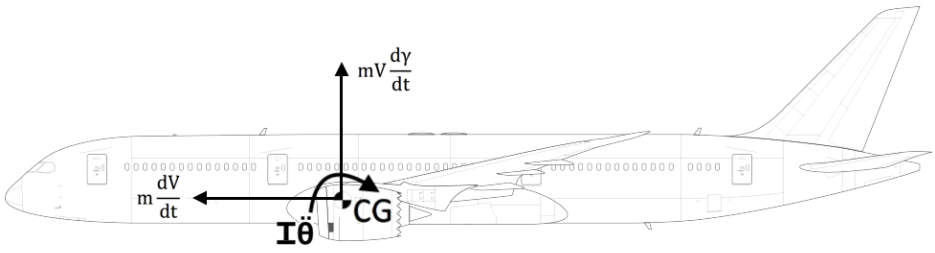

Figure 2.2.: Kinetic Diagram (not to scale), *adapted from Norebbo (2014)*

This requires an increase in lift of the main wing to maintain equilibrium, increasing the drag of the wing. Both the increase in lift and increase in trim drag will cause a higher fuel burn.

The effect of the aerodynamic moment around the horizontal tail is discarded, since the symmetric airfoil results in negligible moment compared to the wing (Torenbeek, 1982). Drag coefficients are provided to compute the total drag under the varying circumstances.

2.2. Equations of Motion

To enable flight related computations, the equations of motion are derived from figures 2.1 and 2.2. The result are equations 2.1, 2.2 and 2.3, where 2.3 was taken around the CG. Use has been made of $\alpha_T = 0$, meaning $cos\alpha_T = 1$. These equations are for symmetric flight and will be referred to for each flight phase.

$$T - D - Wsin\gamma = m\frac{dV}{dt} \tag{2.1}$$

$$L - Wcos\gamma = mV\frac{d\gamma}{dt} \tag{2.2}$$

$$M_{ac+fus} + M_{ac_h} + Tl_T + L_h l_h - L_{wing}(x_{ac} - x_{cg}) = I\ddot{\theta} \tag{2.3}$$

Since no attitude changes are incorporated in this research, $\ddot{\theta}$ is zero. In other words, any rotation of the aircraft around the CG is modelled to be instantaneous, simplifying equation 2.3 to equation 2.4. Note that the moment around the aerodynamic centre of the horizontal tail M_{ac_h} is zero since the horizontal tail has a symmetric airfoil (Torenbeek, 1982).

$$M_{ac+fus} + Tl_T + L_h l_h - L_{wing}(x_{ac} - x_{cg}) = 0 \tag{2.4}$$

To incorporate altitude changes during flight, equation 2.1 is rewritten to equation 2.6, such that the Rate of Climb/Descent (ROCD) can be determined. As an intermediate step, equation 2.5 is added (Ruijgrok, 2009). Their use per flight phase will be discussed in the following parts, with the most important phases discussed first. This will enable the incorporation of the ROCD, being the Rate of Climb (ROC) and Rate of Descent (ROD).

$$(T - D)V = mg\frac{dh}{dt} + mV\frac{dV}{dt} \tag{2.5}$$

$$ROCD = \frac{dh}{dt} = Vsin\gamma = \frac{(T - D)V}{mg}(1 + \frac{V}{g}\frac{dV}{dh})^{-1} \tag{2.6}$$

Cruise
During cruise, the altitude and velocity are constant, simplifying equation 2.1 to $T = D$. As cruising is performed at a constant altitude, no ROCD is present. Equation 2.2 is simplified to $L = W$, since γ is small.

Step Climb
During step climb, the Calibrated Airspeed (CAS) is kept constant, while the altitude changes. Thrust is set to a specified setting, and to maintain the velocity, the rate of climb is varied. Equation 2.6 shows mathematically how the ROCD can be computed. For this research, it was determined to keep the True Airspeed (TAS) constant during step climbs, since data showed changes of at most 5 kts. This simplifies equation 2.6 and 2.1.
A second assumption is related to equation 2.2, stating the lift does not contribute to an acceleration parallel to the flight direction (quasi-rectilinear climb). In other words, the aircraft obtains the altitude change by instantaneously changing its flight direction.

Climb
The next phase considered is the climb to cruising altitude. This consists of an accelerated climb, meaning equation 2.6 is used without any alterations. The lift is, again, not considered contributing to an acceleration, meaning all other equations similar to the step climb.

Descent
As the term ROCD already shows, equation 2.6 and 2.5 can be applied to descent as well. Only difference with climbing is that the ROCD is negative, as is the flight path angle, γ. Thrust is reduced with respect to cruise and climb, as to facilitate the negative ROCD.

Take-off and Landing
The last two phases considered are the take-off and landing, which are very small compared to the whole, long range flight. These phases consist of the section between the first or last waypoint and the acceleration from or deceleration to standstill. Due to their small contribution, the average take-off fuel is used to model the take-off. Any additional effects of take-off (flaps and landing gear) are neglected for the consecutive sections, due to the small contribution and simplification. Landing is treated similarly, neglecting the unique flight conditions encountered due to their small influence on the total fuel burn.

Due to the aircraft either performing a constant CAS or constant Mach climb, the $(1 + \frac{V}{g}\frac{dV}{dh})^{-1}$ term in equation 2.6 is given a second look. Equation 2.7 shows the need, since a constant CAS climb means an accelerating TAS climb. TAS in turn is related to the Mach number using equation 2.8.

$$TAS = CAS\sqrt{\frac{\rho_0}{\rho}} \tag{2.7}$$

$$M = \frac{TAS}{a} \tag{2.8}$$

Using kinetic energy correction discussed by Ruijgrok (2009), equation 2.9 is found for a constant Mach climb in the troposphere. For practicality, the $f(M) = (1 + \frac{V}{g}\frac{dV}{dh})^{-1}$ is used, where $f(M)$ is called the energy share factor (Renteux, 1987). Equation 2.9 also shows the relation between the notation method of Renteux and Ruijgrok.

$$f(M) = (1 + \frac{\gamma R\kappa}{2g_0}M^2)^{-1} = \frac{ROC}{ROC_s} \tag{2.9}$$

Constant CAS climbs require a different equation for $f(M)$. Ruijgrok provides a second function, depicted by equation 2.10 (2009), which uses an instantaneous Mach number. It is applicable in the troposphere (Ruijgrok, 2009). Climbs above the troposphere are frequently at constant Mach, but equation 2.10 can also be applied here.

$$f(M) = (1 + \frac{\gamma M^2}{2}(1 + \frac{R\kappa}{g_0}))^{-1} \tag{2.10}$$

2.3. Drag

As was discussed in 2.2, the drag is the major cause of a higher required thrust, and thus higher fuel consumption. Since this research is focused on the CG, which was determined to be an influence on the trim drag in section 2.1, it will be discussed in more detail. It is followed by a short explanation of its implementation in the total drag.

2.3.1. Centre of Gravity Related Drag

Using figure 2.1 and ignoring any acceleration due to the cruising condition, the relation between the CG and drag can be derived. All forces in x- and y-direction and all moments should be in equilibrium to satisfy the static condition. Considering the moment around the AC, equation 2.11 is obtained.

$$\sum M_{ac} : 0 = M_{ac+fus} - W(x_{ac} - x_{cg}) + Tl_T + l_h L_h \tag{2.11}$$

One can see that shifting the CG aft brings it closer to the AC, thus reducing the moment resulting from the lift force. To counteract this moment, the horizontal tail generates

a downforce. If the moment caused by the lift is smaller, this downforce can also be smaller. Any lift created by an airfoil also generates drag, depicted by equation 2.12 and 2.13, thus establishing the CG drag relation. However, a two term polar does not suffice for conventional aircraft, so a three term polar is used, which is shown in equation 2.14 (Torenbeek, 1982). It introduces C_{L_0} to shift the polar upwards, which is a common occurence for cambered airfoils. In other words, it incorporates the effect of cambered airfoils not having their zero-lift drag and minimum drag at the same value.

$$D = C_D \frac{1}{2} \rho V^2 S \tag{2.12}$$

$$C_D = \frac{C_L^2}{\pi A e} + C_{D_0} \tag{2.13}$$

$$C_D = C_{D_0} + \frac{(C_L - C_{L_0})^2}{\pi A e} \tag{2.14}$$

The drag caused by the horizontal tail is called trim drag (Torenbeek, 1982) and is related to the CG position. To be more precise, equation 2.15 is used to give a more detailed relation. It includes $(\frac{V_h}{V})^2$, the ratio between the free-stream velocity and the velocity encountered by the horizontal tail. This was empirically determined to be 0.85 for conventional tail aircraft (Torenbeek, 1982).

$$D_{trim} = \frac{1}{2} \rho V^2 (\frac{V_h}{V})^2 S_h \frac{C_{L_h}^2}{\pi A_h e} \tag{2.15}$$

If comparing to aircraft under the exact same conditions, only with the aircraft having its CG varied, a parabolic relation can be found between the CG and trim drag. All variables in equation 2.15 stay constant, except for C_{L_h}. C_{L_h} changes, since the CG location changes, as was derived from equation 2.11, thus causing the parabolic relation.

Since the Performance Engineers Manual (PEM) provides a means to determine the change in drag due to a shifted CG, the rigid body model can be altered to a point mass model. All changes in any force or moment due to a shifted CG visible in figure 2.1 are included in this derivation. Using the PEM of the Boeing 777-200ER the lift-drag polar at M=0.8 is obtained. Table 2.1 provides an impression of the variance in the lift-drag polar, resulting in figure 2.3. Figures 4.7a and 4.7b in chapter 4 show the polars obtained with more detailed input if required.

Due to the assumption that the thrust acts parallel to the drag, only in opposite direction, it can be concluded that the required thrust for a constant flight speed is, amongst others dependent on the location of the CG. Therefore, the fuel consumption is related to the CG position.

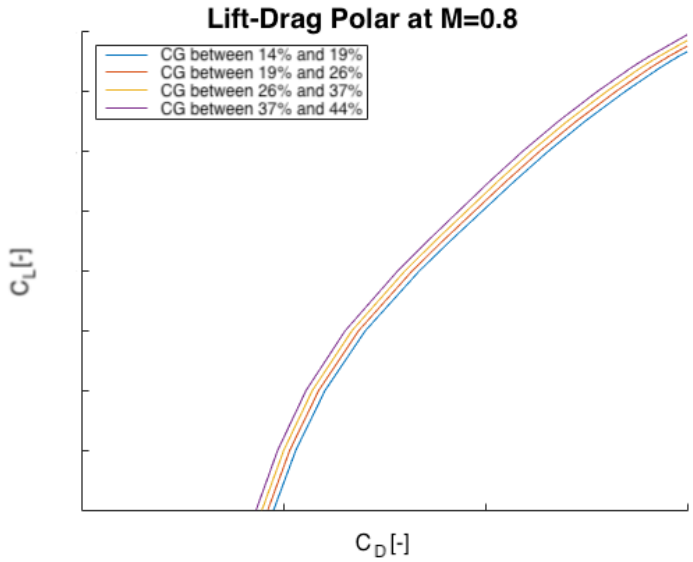

Figure 2.3.: Section of a Lift-Drag Polar at M=0.8 for Varying CG Locations

2.3.2. Total Drag

Despite this research focusing on the CG related drag, it is not sufficient to only include this drag in the model. The main wing will generate lift to keep the aircraft airborne, and once again, the lift also generates drag. The relation between lift and drag for the main wing is also depicted by equation 2.13. An equation similar to equation 2.12 shows how the lift coefficient is determined. It is displayed by equation 2.16, where the lift required is equal to the weight during cruise. The required compensation of an increased trimming (down-) force required by the main wing has been included in lift drag polars, so its consideration is not needed here.

$$L = C_L \frac{1}{2} \rho V^2 S \tag{2.16}$$

The OEM provides the aircraft specific lift-drag polars, which can be used for the discussed purpose. The original values are depicted by the yellow line in figure 2.3, the design case with a CG at 30%.

2.4. Wind

The route flown can be shifted to benefit from weather influences. Despite this determining the route, the aircraft still encounters weather and therefor wind. Wind is the most

prevalent, weather related cause of higher or lower fuel burn (Cheng & Gulding, 2016), depending on the direction. Headwinds will cause a lower ground speed and a longer flight time. One can compare this to swimming in a river, where swimming against the current might look as if the swimmer does not make progress to a bystander.

Any minute spent in the air longer (due to the slower progress from headwind) will mean a higher fuel burn. To include the effects of the wind, the wind contribution in flight direction should be added to the TAS. Cross-wind components were assumed of negligible significance, but they can increase fuel burn.

To obtain a mathematical relation showing the impact of wind, Ruijgrok was consulted (2009). The effect of wind on cruise performance is discussed, which has similar consequences on climb and descent. Due to only considering forces in flight direction and parallel to it, only head and tail wind will be considered in this research. Up and downdrafts or crosswind are not measured by the aircraft, and can therefore not be included. With level and quasi-level flight, equation 2.17 shows the relation between ground speed and flight speed, with headwinds being negative (Ruijgrok, 2009).

$$V_g = V + V_w \tag{2.17}$$

The relation in equation 2.17 can be used directly, but equation 2.19 can be used to get an impression of the impact of wind on the range (Ruijgrok, 2009). In a similar fashion as will be done in section 2.5, the Breguet range equation can be rewritten to calculate the change in fuel needed to compensate the wind. This is related to the endurance (E), which determines the time that can be spent in the air. This will be constant if the flight is performed identically, with any wind influencing the total range. In short, any headwind will have a negative impact on the total range. If the same range needs to be achieved, the weight ratio needs to be adjusted, meaning more fuel is required.

$$R = \int_{W_2}^{W_1} \frac{V_g}{F} dW = \int_{W_2}^{W_1} \frac{V}{F} dW + \int_{W_{end}}^{W_{init}} V_W \frac{dW}{F} \tag{2.18}$$

$$R = R_{V_W=0} + V_W E \tag{2.19}$$

2.5. Theoretical Gain

As a means to establish the theoretical fuel savings, the range equation derived by Breguet is considered. To do this for a constant Mach and constant altitude flight, Peckham was referenced (1974). To compute the range, equations 2.20 to 2.22 are used. Together, they form equation 2.23. Equation 2.23 is applicable to constant airspeed flights, at a constant angle of attack. Due to the small flight path angle γ, thrust is set equal to drag and lift equal to weight.

$$R = \int_{W_{end}}^{W_{init}} \frac{V}{F} dW \tag{2.20}$$

$$F = c_T T \tag{2.21}$$

$$T = D = \frac{C_D}{C_L} W \tag{2.22}$$

$$R = \int_{W_{init}}^{W_{end}} \frac{V}{c_T} \frac{C_L}{C_D} \frac{dW}{W} \tag{2.23}$$

Noting relations 2.24 and 2.25, along with the general equations to make a force dimensionless shown in equation 2.12, equation 2.26 is obtained from equation 2.23.

$$\frac{D}{L} = \frac{C_D}{C_L} = \frac{C_{D_0}}{C_L} + \frac{kC_L}{\pi A} \tag{2.24}$$

$$k = \frac{C_L}{e} \tag{2.25}$$

$$\frac{C_D}{C_L} = \frac{\frac{1}{2}\rho V^2 S C_{D_0}}{W} + \frac{kW}{\frac{1}{2}\rho V^2 \pi A S} \tag{2.26}$$

For a constant Mach flight in the stratosphere, the speed will be constant too. To achieve this form of cruising, the angle of attack should be decreased during the flight, since the aircraft becomes lighter. The lighter aircraft requires less lift, but also less thrust due to lower drag. Therefore, thrust should be decreased steadily during the cruise. This has to be kept in mind when evaluating equation 2.28. Note that $q = \frac{1}{2}\rho V^2$ has been introduced to reduce complexity.

$$R = \int_{W_{end}}^{W_{init}} \frac{V}{C_T q S C_{D_0}} \frac{dW}{1 + \frac{kW^2}{\pi A q^2 S^2 C_{D_0}}} \tag{2.27}$$

$$R = \frac{V}{c_T} \sqrt{\frac{\pi A}{k C_{D_0}}} [tan^{-1}(\frac{W_{init}}{qS} \sqrt{\frac{k}{\pi A C_{D_0}}}) - tan^{-1}(\frac{W_{end}}{qS} \sqrt{\frac{k}{\pi A C_{D_0}}})] \tag{2.28}$$

To simplify equation 2.28, equations 2.29 and 2.30 are introduced. Together, equation 2.32 is obtained.

$$C_{L_{mindrag}} = \sqrt{\frac{\pi A C_{D_0}}{k}} \tag{2.29}$$

$$(\frac{L}{D})_{max} = \frac{1}{2}\sqrt{\frac{\pi A}{k C_{D_0}}} \tag{2.30}$$

$$R = 2\frac{V}{c_T}(\frac{L}{D})_{max}[tan^{-1}(\frac{C_{L_{init}}}{C_{L_{mindrag}}}) - tan^{-1}(\frac{C_{L_{end}}}{C_{L_{mindrag}}})] \tag{2.31}$$

$$R = 2\frac{V}{c_T}(\frac{L}{D})_{max} tan^{-1}(\frac{C_{L_{init}} - C_{L_{end}}}{C_{L_{mindrag}} + \frac{C_{L_1} C_{L_2}}{C_{L_{mindrag}}}}) \tag{2.32}$$

Since the initial Mach number and altitude are equal to their end values, equations 2.33 to 2.38 can be used to further rewrite equation 2.32. The result is equation 2.38, which calculates the range for a constant altitude and constant velocity cruise.

$$C_{L_{end}} = C_{L_{init}}(1 - \frac{W_{end}}{W_{init}}) \tag{2.33}$$

$$C_{L_{init}} - C_{L_{end}} = C_{L_{init}}\frac{W_{end}}{W_{init}} \tag{2.34}$$

$$\frac{C_{L_{end}}}{C_{L_{init}}} = 1 - \frac{W_{end}}{W_{init}} \tag{2.35}$$

$$m^2 = \frac{V^2}{V^2_{mindrag}} = \frac{C_{Lmindrag}}{C_L} \tag{2.36}$$

$$\begin{aligned} \frac{(\frac{L}{D})_{max}}{\frac{L}{D}} = \frac{D}{D_{min}} &= \frac{1}{2}(\frac{C_{L_{mindrag}}}{C_L} + \frac{C_L}{C_{L_{mindrag}}}) \\ &= \frac{1}{2}[(\frac{V}{V_{mindrag}})^2 + (\frac{V_{mindrag}}{V})^2] \end{aligned} \tag{2.37}$$

$$R = \frac{V}{c_T}(\frac{L}{D})_{init}(\frac{C_{L_{mindrag}}}{C_{L_{init}}} + \frac{C_{L_{init}}}{C_{L_{mindrag}}})tan^{-1}(\frac{\frac{W_{end}}{W_{init}}}{\frac{C_{L_{mindrag}}}{C_{L_{init}}} + (C_{L_{init}}\frac{1-\frac{W_{end}}{W_{init}}}{C_{L_{mindrag}}})}) \tag{2.38}$$

Having derived the range equation for a constant velocity and constant altitude flight, it can be used to determine the effect of a change in drag. To do this, two flights are considered, performed with the same aircraft and with the same flight profile. As such, the starting weights W_1, velocity V, specific fuel consumption c_T, initial lift coefficient $C_{L_{init}}$ and lift coefficient for minimal drag $C_{Lmindrag}$ are equal for both cases. Due to the difference in lift to drag ratio $\frac{L}{D}$ the ending weight W_{end} will differ.

Starting with the reference flight, a lift to drag ratio was obtainable from the PEM. A Mach number of 0.8 is used, giving a $\frac{C_L}{C_D}$ of 14.84. This is at the design CG of 30%, which

will be different for a shifted CG. Using the same graph, a lift coefficient at minimal drag of 0.13 is obtained.
Obtaining the initial lift coefficient is dependent on flight characteristics, so a flight from Amsterdam to Tokyo was referenced. An altitude of 33000ft was chosen along with a Mach number of about 0.8 and a TOW of 306300kg. Since fuel has been burned to reach the altitude, the burned fuel is subtracted, resulting in an updated weight of 291900kg at the start of the cruise section. The weight at the end of the cruise section is determined to be roughly 262950kg, since 28950kg is burned over the considered section.

For the second flight, the lift to drag ratio needs to be updated due to the shifted CG. This is done with the aid of the PEM. Table 2.1 is extracted to specify the change in drag coefficient due to a change in trim drag at given CG locations (The Boeing Company, 2004). Shifting the CG to the 41% to 44% bracket, a $\Delta C_{D,trim}$ of -1% is found, which is applied to the get the new, more efficient $\frac{C_L}{C_D}$ of 14.99.

Table 2.1.: Indication of Provided CG Trim Drag Coefficient Change

CG Range	$\Delta C_D Trim$
14% to 21%	+2%
21% to 29%	+1%
29% to 41%	0%
41% to 44%	-1%

With the determined variable values, equation 2.38 can be filled in for the two flights considered. The original flight is designated as 1, while the flight with the shifted CG is designated with a 2. This results in equation 2.39, where V, c_T and $\frac{C_{L_{mindrag}}}{C_{L_{init}}} + \frac{C_{L_{init}}}{C_{L_{mindrag}}}$ have already been omitted due to cancelling out. Note that obtaining $C_{L_{init}}$ is done through equation 2.16, International Standard Atmosphere (ISA) conditions and using a wing area of $428m^2$ from the PEM, giving a value of 0.46.

$$\begin{aligned}(\frac{L}{D})_{init1} tan^{-1}(\frac{\frac{W_{end1}}{W_{init}}}{\frac{C_{L_{mindrag}}}{C_{L_{init}}} + (C_{L_{init}} \frac{1-\frac{W_{end1}}{W_{init}}}{C_{L_{mindrag}}})}) \\ = (\frac{L}{D})_{init2} tan^{-1}(\frac{\frac{W_{end2}}{W_{init}}}{\frac{C_{L_{mindrag}}}{C_{L_{init}}} + (C_{L_{init}} \frac{1-\frac{W_{end2}}{W_{init}}}{C_{L_{mindrag}}})})\end{aligned} \tag{2.39}$$

Solving equation 2.39 one can see that an ending weight of 2576800N is obtained, or 262670kg. This means the aircraft is 259kg heavier than the reference flight with the CG at the design value of 30%. This is 287kg of fuel that has not been used and is therefore still in the aircraft. Since this section is about 3200km long, this represents about 1/3 of the total length. Assuming there are 3 cruising altitudes in the data, a

saving of 837kg is found, or 1.01% over the whole flight. This is excluding any climb and descent, which are also influenced by the shifted CG. Also, due to the flight being lighter, the aircraft will be able to climb to a higher altitude earlier, resulting in a more efficient flight. As such, this rough theoretical calculation is used to provide a theoretical saving potential serving as an indication.

2.6. Limitations

Until now, it seems shifting the CG aft as far as possible will be the most ideal situation in terms of fuel burn. However, three limitations, derivable from theory, come into play. First one is the risk of tail tipping, the second is due to the stability of the aircraft. The last limitation is related to a forward CG, and encompasses the controllability of the aircraft. Any practical or logistical limitations, like the absence of cooling facilities in the aft section, will not be treated in this section, but are limitations that should be kept in mind.

Tail Tipping

Tail tipping occurs on the ground when the CG moves aft of the main gear, causing the aircraft to tip aft due to the imbalance. This can happen during loading, especially when loading the aft section first. According to Torenbeek (1982), a diagram can be made to represent the shift in the CG for varying loading sequences. An indication is given in figure 2.4 for twin engine, fuselage mounted aircraft. For four engine aircraft, a similar figure can be used, while fuselage mounted engines are not considered, since KLM no longer operates these.

Figure 2.4 shows that the fuel shifts the CG forward. This confirms the claim of KLM that the CG moves aft during the flight due to the burning of fuel.

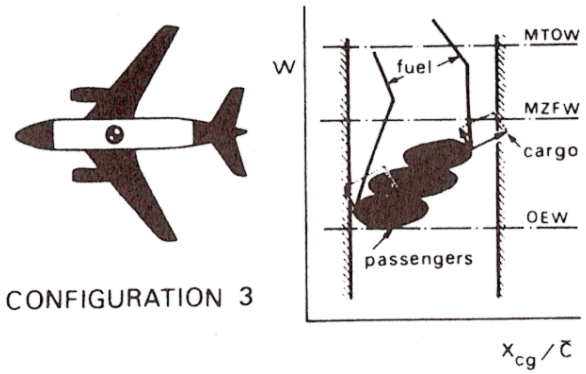

Figure 2.4.: Loading Diagram (Torenbeek, 1982)

When determining the order of loading, tail tipping is taken into consideration to avoid injuries and damaging the aircraft. This is unwanted, and measures are present to give a warning, depending on the aircraft type (Koninklijke Luchtvaart Maatschappij, 2017). A tail tip is also possible when fuel is present in the aft tanks. Figure 2.4 shows a dent in the line representing the fuel. According to KLM, this dent, caused by the wing tanks pulling the CG aft, can pull it aft of the rear limit. During loading, the presence of fuel in the tanks is incorporated to prevent this from happening. Especially when landing with large quantities of fuel are critical.

Stability

Stability is, contrary to tail tipping, of a bigger issue. OEMs set limits for the CG, preventing the aircraft from becoming unstable. If the CG moves behind the so-called Neutral Point (NP), the aircraft will no longer stabilise itself after a perturbation. Figure A.2 in appendix A shows how the moment equilibrium used to derive this and following relations in more detail. One can see that the increase in lift due to an increase in angle of attack α results in a nose-down moment, stabilising the aircraft.

A Static Margin (SM) is introduced, expressing the distance between these two points, normalised with respect to the Mean Aerodynamic Chord (MAC). It defines the minimal distance the CG should be in front of the NP, enabling pitching requirements placed on the aircraft (Raymer, 1992). A mathematical relation defining the stability limitation related to the aftmost CG can be found in equation 2.40. The SM is defined in equation 2.41.

$$\bar{x}_{CG} = \bar{x}_{ac} + \frac{C_{L\alpha_h}}{C_{L\alpha_{A-h}}}(1 - \frac{d\epsilon}{d\alpha})\frac{S_h l_h}{S\bar{c}}(\frac{V_h}{V})^2 - S.M. \tag{2.40}$$

$$S.M. = \bar{x}_{CG} - \bar{x}_{np} \tag{2.41}$$

The NP is defined as the location where no resultant moment is present when a perturbation is acting on the aircraft. The perturbation causes a resultant force which acts through the NP. In equation 2.40 it is normalised with respect to the MAC, just like the CG location. Equation 2.40 only takes the contribution of the wing and tail into account.

Equation 2.40 shows how the design related terms ($\frac{S_h l_h}{S\bar{c}}(\frac{V_h}{V})^2$) are dependent on the CG location. Referring to equation 2.15, one can see how these terms in turn influence the trim drag. This shows the relation between the aft CG location being more efficient, while it is limited by the stability.

Modern technology does enable the SM to be smaller or negative, since continuous interaction by a flight computer can be used to maintain the stability artificially. This is known as relaxed static stability (Raymer, 1992). Despite this promising technology,

which means the aft CG limit is shifted further aft, it does not mean the CG can move aft infinitely. The application of relaxed static stability is something that is linked to the aircraft design, thus requiring the OEM to implement this if desired. An operator like KLM cannot implement this technology without the agreement of the OEM.

Controllability

Next to maintaining stability, the aircraft should be able to perform a rotation during take-off, a 2.5g pull-up manoeuvre and the landing flare. This includes the change in moment due to the extension of flaps. The limit in the CG location is found using equation 2.42, only considering the wing and tail contribution. With this equation, the defined foreword limit of the CG provided.

$$\bar{x}_{CG} = \bar{x}_{ac} - \frac{C_{m_{ac}}}{C_{L_{A-h}}} + \frac{C_{L_h}}{C_{L_{A-h}}} \frac{S_h l_h}{X \bar{c}} (\frac{V_h}{V})^2 \tag{2.42}$$

2.7. Conclusion

With the relation between the CG and trim drag derived, it is known what parts of the drag and flight variables need inclusion in the model. Due to fuel being burned, the CG location throughout the flight needs to be determined. This will provide accurate drag computations in terms of trim drag.

Using the Breguet range equation, rewritten for level flight at constant Mach number, it was derived that for a 9300km flight, roughly 780kg of fuel is saved when the trim drag coefficient decreases by 1%. Despite this benefit, the limitations to CG shift will influence the achievability of this trim drag reduction. Such limits come into play when loading the aircraft and, most importantly, when satisfying controllability and stability of the aircraft.

The theoretical framework provides an extensive overview of all aspects influenced by the CG. Partly, it serves as input for the development of a fuel burn computing tool. The knowledge of this chapter will be used in the following chapters to develop the modules and obtain the research results.

3. Methodology

With the theoretical knowledge, briefly discussed in the previous chapter and in more depth in appendix A, the method to perform this research can be set out. It was chosen to have a numeric calculation of the fuel usage, as the data provided by KLM and the PEM and decreasing the complexity made this method a good match.

This chapter and research has its main focus on two sections, as depicted in figure 3.1. First, the input variables for the fuel computation model will be discussed, which is done in the flight profile module. It will use flight data to develop a standard or average flight profile per destination and aircraft type. This module in turn serves as the input of the fuel burn calculation module. Finally, a third, less intensive module will be discussed, which will consist of the final deliverable for KLM.
Note that figure 3.1 considers the two modules for a single combination of origin-destination, aircraft type and the season. This was done to represent a single flight and the variables that can vary, while also reducing complexity. More detail will follow in the next sections.

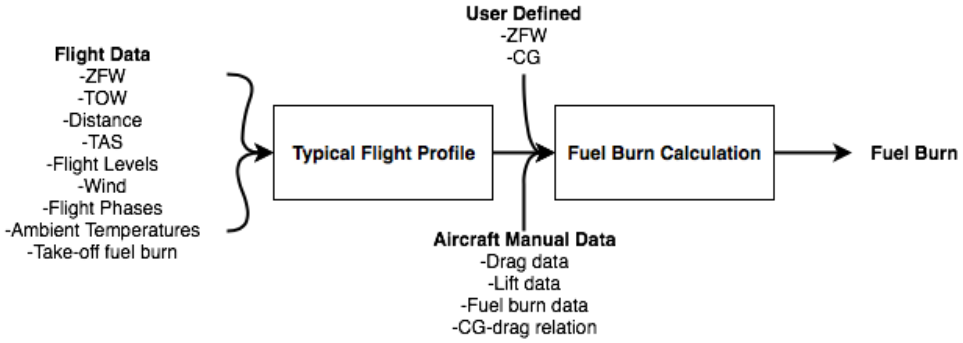

Figure 3.1.: General Approach of Research Tool

3.1. Flight Data Module

Due to this research taking place at KLM, flight data is available for detailed use. This enables the tool described in 3.2.3 to analyse the relation more realistically. Practical results can be achieved by incorporating this data in the fuel computation model, which

in turn distinguishes this research from theory. This section describes how the data was used to derive a standard flight profile per destination and aircraft type.

Two sets of data were considered; data varying throughout the flight and initial, constant variables. Both are variables, however the varying variables change between waypoints, whereas initial variables only differ between flights, hence calling them initial, constant variables. These constant or initial variables will have an influence on the rest of the flight, as the TOW or ZFWMAC show.

The varying variables are mostly difficult or tedious to model, of which weather and routing are two examples, since both change unpredictably between waypoints. These varying variables are averaged over all data. All data is processed in such a way that they serve as input for the fuel calculation module discussed in 3.2.

The discussed method was chosen since it enabled the incorporation of regional effects. For example, if a region along a route provides heavy headwind, and it cannot be evaded due to regulations, the effects are incorporated in the average flight profile. Another example can be periodic regulations, where an airspace can be closed during weekends. To prevent diverted flights influencing the average, any flight not originating or ending in Amsterdam, or not flown more frequent than two times per year, will be discarded. This also results in flights with intermediate stops being discarded. These are often short legs, and are assumed to have little fuel savings. With this approach, the model takes these effects into account when producing a standard route.

All flights have been split into summer and winter. This is done due to the weather characteristics being significantly different during these seasons (Dispatch, 2017). The winter season is defined from November 1^{st} to April 1^{st}.

3.1.1. Initial, Constant Variables

As defined, initial, constant variables are variables which occur only once throughout a flight. They are the first values used by the model, and represent the state of the aircraft before take-off and therefore stay constant during the flight. As such, they are averaged to get an impression of their average value, the results of which are shown for winter in table 3.1. Examples of this are the Zero-Fuel Weight (ZFW) and the ZFWMAC per origin-destination and aircraft type combination. The ZFWMAC will be used to calculate the fuel burn, as to facilitate the potential gains of a shifted ZFWMAC.

Table 3.1.: AMS-NRT Initial, Constant Variables Indication December 2017

Average ZFWMAC [%]	**Average ZFW** [kg]	**Average TOW** [kg]	**ZFW-TOW Ratio** [-]	**Average Take-off Fuel**
28.9	212456	302545	0.424	1598

The ZFW and TOW are treated similarly, but are used to determine per route what the average amount of fuel on board. As such, the user will be able to specify a ZFW, and the program determines the typical amount of fuel available. This was done since at the moment of determining the loading order, the required fuel is not planned yet. Additionally, this method enables the reduction of a variable in the simplified model, being the TOW. A final benefit is the ability to include extra fuel taken on board. At certain outstations, if the price is low enough, a flight crew can take extra fuel since this is cheaper, despite having to take it back to Amsterdam.

The required fuel for a given flight was assumed to have negligible variance under ideal conditions. The CG location is assumed to not be accounted for, with the only large variance in fuel loaded being attributed to the weather by dispatch. These effects are incorporated in the average ZFW-TOW factor, with the number of weather occurrences will influence the average fuel factor.

Next to the averages, the minimal and maximal values of the ZFWMAC and ZFW within the data are obtained per route. The minimums are rounded downward and the maximums upward. By doing so, a range within which the ZFWMAC and ZFW occur is obtained, providing an impression of the performance of the route. This method also enables the inclusion of practical limits. With the large amount of data, if a practical limit constrains the ZFWMAC or ZFW, the chance of it occurring is significant. Thus, if a flight requires the full use of the fuel tank volume, causing the CG to shift outside of the limits, it is assumed occur within the provided data. By having a warning presented to the user if the ZFWMAC is below the minimum or above the maximum, a practical limit of the ZFWMAC is included.

3.1.2. Flight Varying Variables

With the initial, constant variables discussed, a closer look is taken at the flight varying variables within the flight data. These variables are logged throughout a flight and gathered in a file by KLM. This data is sorted according to flight date, flight number, actual flight duration and actual distance. This results in a chronological logging order of the data, with the separation of multiple flights during a day on the route. An example flight is given in table 3.2, showing the condensed flight profile of AMS-NRT performed on December 1^{st}. It consists of the first and last logged data of the flight (therefore climb and descent phases), a cruising section, a climb at cruising altitude and the last cruise data point. It also shows a faulty data point, which shows zero values for certain variables, its preceding and consecutive data.

As said, the provided data includes logging errors resulting in empty fields or zero entries. These rows with an empty field are checked with the actual fuel burn, actual duration and actual distance. It was found that if an aircraft deviates from the planned route (and therefore doesn't encounter a planned waypoint), it will not log these three variables. If these three are not missing, linear interpolation is performed, based on the distance

Table 3.2.: AMS-NRT Condensed Flight Data Indication December 2017

Normalised Location [-]	**Flight Distance** [nm]	**Ambient Temperature** [^oC]	**TAS** [kts]	**Wind** [kts]	**Flight Level** [-]	**Flight Phase** [-]
0	0	5	108	-6	-1	Climb
0.022	110	-53	420	72	310	Cruise
0.159	820	-54	480	13	330	Climb
0.915	4710	-51	500	-17	370	Cruise
0.995	5120	-5	275	6	75	Descent
0.998	5140	0	0	0	0	Descent
1	5150	0	165	-14	0	Descent
0.998	*5150*	*-1.3*	*194*	*-9*	*21*	*Descent*

between two measuring points, to enter a value. Table 3.2 shows the updated values for the considered flight in the last row, in italics.

The final preparation step is to add phase designators to each measuring point, as shown in the leftmost column of table 3.2. These are based on the Flight Level (FL) of the current and the next way-point. These will aid in determining the upcoming flight phase (see chapter 3.2.3) and what module to run. It was decided to add these designators to the data, since it aids in troubleshooting and understanding of the data and results.

Processing

With the preparations finalised, the process of creating an average or typical flight profile is initiated. The distance from the origin of each waypoint is normalised with respect to the total distance, per flight. The average number of waypoints during take-off and climb, cruise and descent and landing are determined respectively, along with their normalised locations of occurrence. Example data is given in table 3.3, showing average climb, cruise and descent distance and waypoint numbers. Additionally, the percentage of the section with respect to the total flight is given behind each distance. These percentages give an indication of the normalised locations where the flight phase changes.

The average, normalised distance from the origin of each waypoint is determined. These normalised locations represent the location of the waypoints encountered during an average/typical flight. They are visible in the second row of table 3.4. Using spline interpolation, the flight variables can be determined at these normalised waypoint locations. By doing so, the average value of each required flight variable can be determined for each average waypoint. The climb to cruise and descent after cruise are treated separate from the total flight, since they have a large number of waypoints in a small amount of time. The benefit of doing this is that any local, recurring flight conditions are incorporated in more detail. As an example, during an introduction to dispatch of KLM, the diversion

Table 3.3.: AMS-NRT Winter Phase Averages Indication

Average Climb Way-points [-]	**Average Climb Distance** [nm]	**Average Cruise Way-points** [-]	**Average Cruise Distance** [nm]	**Average Descent Way-points** [-]	**Average Descent Distance** [nm]
9	183 *(3.5%)*	72	4700 *(90.9%)*	23	288 *(5.6%)*

and weather influences were presented for a certain route. The dispatcher is prompted this information to take into consideration when planning a flight route (Dispatch, 2017). These are dependent on the flight loading and weather conditions, and these effects are included in the averages.

Table 3.4.: AMS-NRT Winter Condensed Standard Flight Indication

Waypoint Number [-]	1	12	29	83	103
Normalised Location [-]	0	0.035	0.259	0.944	1
Distance [nm]	0	180	1310	4880	5170
Temperature $[^oC]$	7	-53	-57	-50	3
Mach [-]	0.195	0.84	0.84	0.84	0.30
TAS [kts]	130	485	485	485	195
Wind [kts]	-8.9	9.6	21.1	39.9	-9.5
Flight Level [-]	0	330	330	370	0
Phase [nm]	Climb	Cruise	Climb	Descent	Descent

The decision to use splines is based on the ability of splines to incorporate gradual changes. Linear interpolation will not have a smooth transition in variables between two measuring points. This can be seen in figure 3.2, where Tokyo to Amsterdam was used since it provided a clear example. One can see that all data points are gradually connected, without instantaneous heading changes at every waypoint.
Despite this benefit of splines, splines can also result in oscillating behaviour when two points are located near each other. This effect is accounted for and prevented by comparing linear and spline interpolation. Depending on the variable considered, a deviation of 10% to 50% is set as the deviation limit.

Finally, due to operational reasons, it was decided to include the Mach number in the flight varying variables and convert it to TAS. Section 3.2.1 mentioned that certain routes require a higher flight speed to reduce flying time and crew costs. Also, theoretically, flight speed restrictions can be enforced in certain regions. These two effects will be

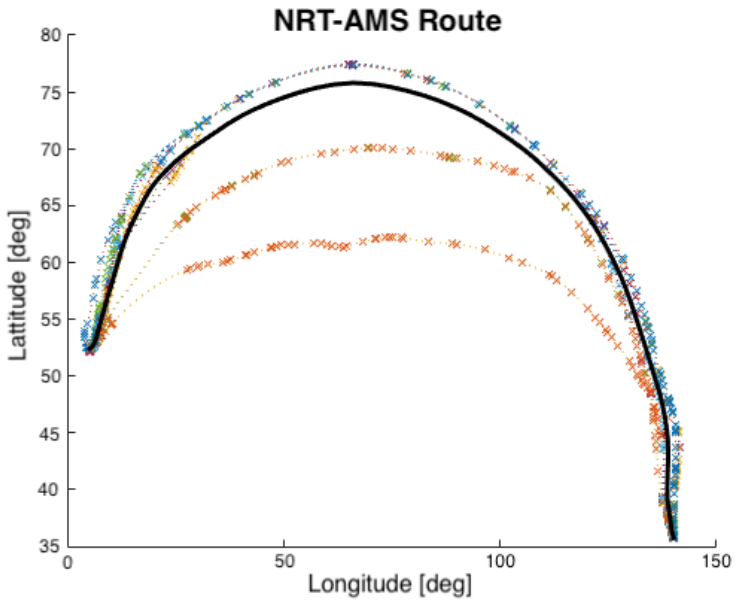

Figure 3.2.: NRT-AMS Routes and Average December 2017

incorporated in an average, since this deviates from ideal flight speeds mentioned in the manufacturer handbooks like the PEM. Resulting averaging of the required parameters can be found in table 3.4. A climb phase, cruise, step climb and descent are shown, with the final data point during landing. These were chosen, since they represent all considered flight phases. A warning should be given for the FL during cruise and step climb, since it represents the rounded average. The actual flight level is based on the weight of the aircraft, but is not considered in this table to display the averaging.

All variables are written to a structure, depicting the origin and destination for the considered aircraft. This matrix consists of all required flight profile data for fuel computation. A second structure contains the initial, constant variables required for the fuel computation.

3.2. Fuel Burn Module

With the input data for the model defined, a look is taken at the module that will calculate the fuel burn. The dependence, per origin-destination, aircraft and season, is shown in figure 3.1. To ease validation, the typical flight profile output is modelled the same way as the actual data provided by KLM, with the fuel burn module designed to have this as input. Aircraft specific data is extracted from dedicated manuals. The user will have to define the ZFW and ZFWMAC, as well as the aircraft type, season and origin-destination combination. These last three variables are not shown in figure 3.1,

as to reduce the figure size.
Numerical methods discussed by Anderson (2005) and Ruijgrok (2009) are used throughout this research, where the Base of Aircraft Data (BADA) user manual (2014) aided in the order of application.

3.2.1. Aircraft Design Data

Before calculations can be performed, input data needs to be obtained, other than the flight data discussed in section 3.1 and user defined inputs. As depicted in figure 3.1, aircraft specific data is needed, which is obtained from the PEM and Aircraft Flight Manual (AFM) for Boeing aircraft. The PEM is provided upon first delivery of the aircraft type to the operator. It provides the operator a means to do performance related computations for the considered aircraft. These manuals provide plots that can be used for each flight for the considered aircraft (The Boeing Company, 2004), (The Boeing Company, 2010). Figure 3.3 gives the generalised thrust curve as provided, which is a typical plot used for the fuel computations.

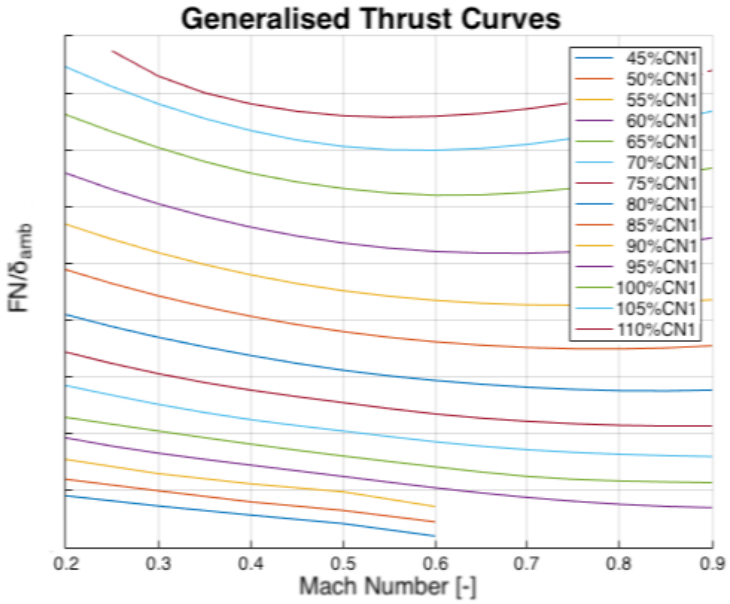

Figure 3.3.: Generalised Thrust Curve

The data is, according to Boeing, based on flight tests and calculations (Koninklijke Luchtvaart Maatschappij and The Boeing Company, 2018). Directly measurable data is obtained from testing, while indirect data, like the optimal cruising altitude, was computed. A second means to derive the origin is provided, being the shape of the provided figures in the manuals. Smooth figures are computations (based on test data), while figures that are not smooth are test based. This is also applicable for Airbus aircraft.

As an example, figure 3.3 is taken, since it is test data based with small computational adjustment to obtain the provided figure (Koninklijke Luchtvaart Maatschappij and The Boeing Company, 2018). It can be seen that at low thrust settings, between Mach 0.5 and 0.6, the lines deviate from the general trend. At higher thrust settings, this also shows, only hardly visible. Inspecting other sections of the plot also show some deviations. Because of this, one can see figure 3.3 is test data based, which was confirmed by Boeing (Koninklijke Luchtvaart Maatschappij and The Boeing Company, 2018).

An exception on the fact that the manuals can be used for each flight is the cruising Mach number, despite being provided in the manuals. As discussed in 3.1.2, these are not always followed due to various reasons. Reducing delays or the crew number due to shorter flight times are two of these reasons. Excluding the Mach number from the manual based inputs enables the effects of recurring delays or cost cutting measures on certain legs.

3.2.2. Airbus Data

Despite this report discussing the methodology of the Boeing 777-200ER, which follows the approach of Boeing aircraft, Airbus aircraft are included in the research. Airbus does not provide a PEM, but has Performance Engineers Program (PEP). Within this, the In Flight Performance (IFP) and Fuel Temperature Prediction (FTP) are used. By entering the flight speed and CG location, the lift drag polars can be determined. Varying these will give the polars at specified inputs, enabling interpolation. Due to the weight being entered, the program is also able to determine the drag, which can be used for validation.

To obtain the conversion of thrust to fuel consumption, FTP comes in. For given thrust settings, the fuel flow can be extracted. The thrust setting and thrust delivered data is also extracted, enabling thrust to fuel flow conversion. This data is used similarly to the Boeing data, and only one major alteration is required to the methodology, being the k-factor discussed in section 3.2.5.

3.2.3. Fuel Burn

Having the input for the fuel burn model available, the first step is to derive ISA condition related values. These results are compared to the input variables, as to determine a temperature offset for each waypoint.

A second step is to determine the TOW. As discussed in section 3.1.1, the average multiplication factor of the ZFW (a user input) is used to derive the the TOW. This weight serves as the initial weight of the flight. Using the theory discussed in sections 2.2 and 2.3, combined with plots in the PEM describing the conversion of the thrust to

the fuel flow, the fuel flow is obtained. Knowing the duration of the section, derivable from the wind, flight speed and distance, the fuel burn per section follows.

Since the average weight is used to determine the drag per section, one can see an iterative process occurs. The average weight is dependent on the fuel burn of the section, which in turn is dependent on the average weight. As such, the average weight is initially set to the starting weight of the section. The resulting fuel burn is used to update the final weight and consecutively the average weight, until the iterations result in a change of less than 1% between the old and new average weight. The entire process is depicted by the simplified diagram in figure 3.4. For simplification, not all relations are depicted, and no details for different phases are shown.

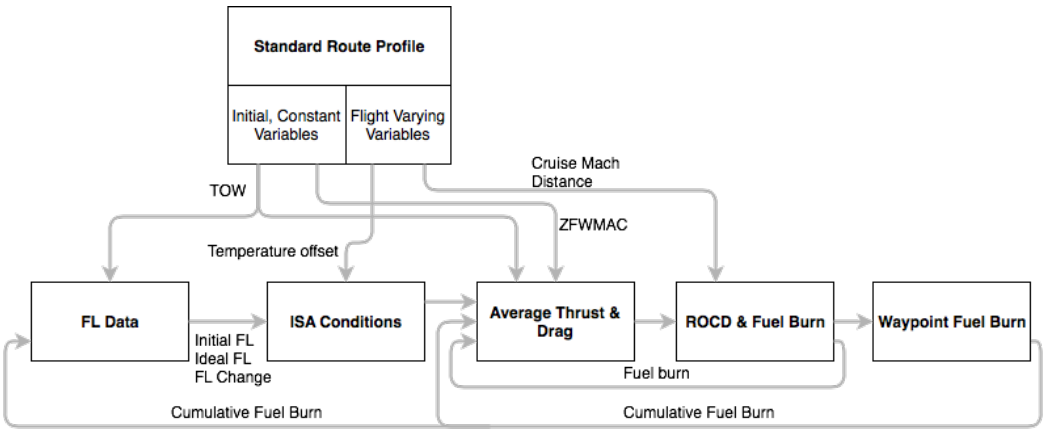

Figure 3.4.: Simplified Fuel Burn Diagram

Within each iteration, the tool calculates the drag based on the flight speed, altitude, and weight using equations discussed in chapter A and lift and drag polars from the PEM. These are obtained from flight data and manuals, as depicted in figure 3.1. Spline interpolation is used if required, since it provides smoother, more gradual changes than linear interpolation. Depending on the flight phase, different computations are needed. These computations are based on equation 2.1, discussed in chapter 2. The method to determine the fuel used per section and its phase is discussed briefly per flight phase.

Cruise
During cruise phase, equation 2.1 states only drag is determining the required thrust, assuming no acceleration is taking place. No acceleration or altitude changes are performed. Thus, the thrust required is obtained, from which the Thrust Specific Fuel Consumption (TSFC) plots in the PEM are used to determine the fuel flow. Using the distance of the section, wind encountered and the velocity, the fuel burn for the section is derived.

Step Climb
As discussed in chapter 2, during step climb the aircraft maintains its flight speed. The thrust is set to a specific setting, being 95%CN1 for flights below FL200 and 100%CN1

above (EUROCONTROL, 2009) (Airbus SE, 2013). Using the PEM, the amount thrust produced for that setting and under the considered flight conditions is determined. With this produced thrust, the fuel flow is determined from the dedicated PEM tables.
By using equation 2.6, the Rate of Climb (ROC) is determined. The change in altitude, the ROC, flight speed and ground speed are used to determine the time and distance needed to perform the step climb. Once the climb reaches its final altitude, cruising conditions are maintained for the duration of the section. The total fuel consumption is equal to the sum of the climb fuel burn and the cruise fuel burn.
Note that no increase of lift to aid in the altitude change is considered to simplify calculations. Therefore, the altitude change is purely achieved through the pitching up of the nose, creating an upward component of the velocity with respect to the earth surface.

Climb
Climb is considered an expansion of the step climb. Next to the change in altitude, the TAS increases. The TAS was chosen since the flight data log the TAS and not the CAS. As such, equation 2.6 has its $\frac{dV}{dh}$ term as nonzero, resulting in equation 2.5 being used. The steps taken to derive the fuel burn and ROC are the same as for the step climb module. As such, the modules have the same basis.
Expanding the basis, the accelerations are incorporated by substituting the $(1+\frac{V}{g}\frac{dV}{dh})^{-1}$ with an energy share factor discussed at the end of section 2.2. By using this factor, part of the thrust of the engines is used for acceleration, with the rest being used for the altitude change and the drag. The same thrust settings are maintained as during step climb, meaning lower ROCs can be expected during accelerated climb. Due to the same concept as during step climb, the computed ROC is used to determine the amount of time the aircraft will cruise after climbing. The total fuel burn is derived from this.
Again, no lift contribution to the altitude change is considered. To facilitate a speed increase, the altitude change will progress more slowly compared to a constant speed climb under the same conditions. This leaves some thrust to achieve the acceleration, which is modelled to only change due to the thrust or drag.

Descent
As stated in chapter 2, descent is seen as a special case of the climbing module. A negative ROC is encountered due to a negative flight path angle (γ). The ROD is determined via the altitude change between the considered waypoints, in combination with the duration of this section. Based on this continuous descent throughout the section, the ROD is used to determine the thrust required. The thrust, again, is used to determine the fuel flow and fuel consumed for the section. If the thrust is smaller than the fuel flow curves allow, idle thrust is used, with the corresponding chart provided in the PEM.
The second effect that can occur is a deceleration. This was incorporated by using the first law of Newton ($F = ma$). A cruising flight at the average flight level was considered. Comparing with the same cruising flight, only applying Newton's law, shows the difference in fuel consumption due to deceleration. This difference was subtracted from the fuel use of the descending flight. The decision of this method is further discussed in section 4.2.

Due to flap extensions and landing gear required for landing (The Boeing Company, 2010), more thrust is required, increasing fuel burn. Since descent using flaps is considerably shorter than cruise for long haul flights (Roberson & Johns, 2008), this effect is not included.
Finally, as with climbing, the altitude change is modelled to not depend on a change in lift. The same applies to the drag, which together with the thrust results in a change in velocity.

Take-off
Due to the large acceleration during take-off, which does not make use of the defined thrust settings, it is more difficult to model. Adding the effect of flaps and landing gear would make the model more complex, while take-off only consists of a very small part of the whole flight (Roberson & Johns, 2008). As such, the average fuel burn between the first two waypoints is used for the considered aircraft on the considered route.

3.2.4. Drag Coefficient Details

With the method to derive the fuel flow per established flight phase, it arises that the drag needs to be considered in more detail. As discussed in section 2.3, the CG influences the trim drag, explaining the separate discussion of the drag coefficients. Once the derivation of the drag coefficient is established, the CG implementation is considered.

The total drag is derived using lift-drag polars provided by the PEM of the respective aircraft and the conversion of the drag coefficient to drag discussed in section 2.3. The weight is dependent on the TOW and cumulative fuel burn, discussed in section 3.1.1. In addition, Boeing provides additions to the lift-drag polars, which proved to be more accurate (The Boeing Company, 2004) than using purely this relation. Effects like aeroelasticity are considered due to their influence on the drag coefficient (Miller, 2010). This method resulted in smaller differences between the calculations and the general drag polar within the PEM, which is further discussed in chapter 4, although it considers the resulting fuel burn and not the drag.

Next to the aeroelastic adjustment, Boeing also addresses the difference in actual and reference change in drag due to the Reynolds number. This consists of using equation 3.1, where $Re/Ft/Mach$ is found using equation 3.2 (The Boeing Company, 2004).

$$\Delta C_{D_{Re}} = -0.004529 log(\frac{(Re/Ft/Mach)_{ACT}}{(Re/Ft/Mach)_{REF}}) \tag{3.1}$$

$$Re/Ft/Mach = 5.1338(\frac{\delta(\theta + 0.38312)}{\theta^2})10^6/Ft \tag{3.2}$$

The result of equation 3.1 should be subtracted from the drag coefficient found in the drag polars (discussed in 3.2.3). After doing so, the multiplication factor for the aeroelastic drag should be used.

3.2.5. Centre of Gravity Implementation

Using the initial tool, an estimate of the fuel can be made. This tool is then expanded to incorporate the effects of the CG, as to enable the research of its effects. This implementation is treated separately from the drag coefficient section, due to the amount of additional work and being the subject of most interest for this research. In addition to the need for the research, it also ads details to the fuel computation resulting in higher accuracy, which is favourable. For Boeing aircraft a k-factor is provided (The Boeing Company, 2004) to implement CG effects, while Airbus enables the extraction of CG varying lift-drag polars through the PEP. Boeing describes the derivation and implementation of this k-factor as follows (The Boeing Company, 2018):

- With initial tank quantities lookup tank body station, repeat for flight tank quantities
- ZFW=W-(sum of intial tank quantities)
- Initial moment=initial fuel*tank body station
- ZFWCGBS=(TOW*GWCGBS-Sum of initial moments)/ZFW
- ZFWCGMAC=((ZFWCGBS-LEMAC)/MAC)*100
- WTCGBS=(ZFW*ZFWCGBS+Sum of flight moments)/W
- WTCGMAC=((WTCGBS-LEMAC)/MAC)*100
- With M and C_L lookup $\Delta Cd_{Trim@ReferenceC.G.}$
- With WTCGMAC lookup K_{trim}
- $\Delta Cd_{Trim@Cond} = \Delta Cd_{Trim@ReferenceC.G.} * K_{trim}$
- $Cd_{corr} = Cd - \Delta Cd_{Trim@Cond}$

Especially the last four steps are of interest, since the first steps comprise the establishment of the standard CG location (The Boeing Company, 2018). WTCGMAC represents the location of the CG with respect to the MAC. This varies throughout the flight, since the fuel burn influences the aircraft weight and CG (Torenbeek, 1982). These steps are used to determine the drag coefficient at given CG locations, which is used to compute the overall drag.

Fuel Vector

As mentioned and visible in figure 2.4, the burning of fuel causes the CG to move throughout the flight (Torenbeek, 1982). To account for this, a so-called fuel vector has been investigated. ALTEA FM has the ability to display this for an aircraft, but does not provide the means to derive this. In addition, ALTEA FM is a tool available for any airline, thus general assumptions apply to the fuel vector. Finally, ALTEA FM

derives the fuel vector based on the design CG location and does not account for any deviations in ZFWMAC, being the CG location at ZFW expressed as percentage of the total MAC.

Due to this, KLM has conducted their own investigation into the matter, with data from the OEM. Resulting are plots and functions providing the percent shift of the CG with respect to its location at ZFW, as a function of the cumulative amount of fuel burnt. Equations 3.3 and 3.4 are the result of this investigation and are applied to the model to get an actual location of the CG at each waypoint (Koninklijke Luchtvaart Maatschappij, 2011). Note that K and C are unnamed, aircraft dependent constants and are provided by KLM. K is used to ensure the index equals zero at zero fuel, where C is used to convert the moment values to index values. For Airbus aircraft, K had to be obtained manually, through this knowledge, since K was not provided.

$$I = \frac{W(BalanceArm - ReferenceArm)}{C} + K \tag{3.3}$$

$$\%MAC/RC = \frac{\frac{C(I-K)}{W} + ReferenceArm - LEMACorLERC}{\frac{MACorRC}{100}} \tag{3.4}$$

In equation 3.3 the Balance Arm is the horizontal distance of the horizontal tail H-arm. The Reference Arm is the selected, fixed balance arm around which all index values are calculated. MAC/RC is the length of the MAC/Reference Chord. Finally, the LEMAC or LERC is the horizontal distance in length units from the reference datum to the location of the leading edge of the MAC/RC (Koninklijke Luchtvaart Maatschappij, 2011).

Applying the CG location determination method, one can see the dependence on the fuel consumption. Recalling from section 3.2.3, the fuel burn is determined through iterations. The same applies to the CG, with the average between two waypoints being used over the whole section. The initial guess of the CG location is based on the end weight, which is also guessed for the initial loop.

A330 Trim Tank

The benefit of aft CG of aircraft is also known to OEMs, with Airbus implementing a trim tank in their aircraft. It is used to shift the CG aft with fuel (Airbus SE, 2017a) (Airbus SE, 2013). This raised questions considering its effect, which was investigated.

In the Flight Crew Operating Manual (FCOM), Airbus provides the working principle of the trim tank. In short, fuel will be moved to or from the trim tank to move the CG to a certain target. When climbing through FL255, the system can initiate a rearward fuel transfer. This is only done if the CG differs more than 0.5 percentage points from

the target. Similarly, due to fuel burn the CG will shift forward during flight, generally aft. If the CG is more than 0.5 percentage points from the target, fuel can be pumped out of the trim tank to the forward located tanks. To determine the target, the FCOM provides a plot, depicting the fuel vector discussed in section 3.2.5, but applied to the target. The system ensures that even with a failure preventing the trim tank to be emptied, the CG will be at most 2 percentage points in front of the aft CG limit. It can therefore happen that due to an aft CG, the fuel tank will not fill, despite the CG not being very close to the aft limit.

To research the effect of this system, a small alteration was made to the fuel vector. Using the FCOM and AFM, the alterations to the input values or the fuel vector derivation was obtained. For simplification, the trim tank can only be used completely full, or empty. If the fuel vector exceeds the maximum CG value minus 2 percentage points, the program would run with an empty trim tank.

3.3. Simplified Model

Due to the size and complexity of the developed model, it is difficult to implement this within KLM. Therefore, a simplified module is added, in which an employee can quickly determine the effects of shifting the CG aft per flight. This was determined as a deliverable in chapter 1 and is a driving requirement for KLM.

With the simplified tool, motivation for aft CG effort is expected to increase and managerial decisions will be simplified. The dependence of the simplified model, within the whole research is depicted in figure 3.5. It resembles figure 3.1 and shows the dependence of the simplified tool on the extensive computations, but as a quick overview.

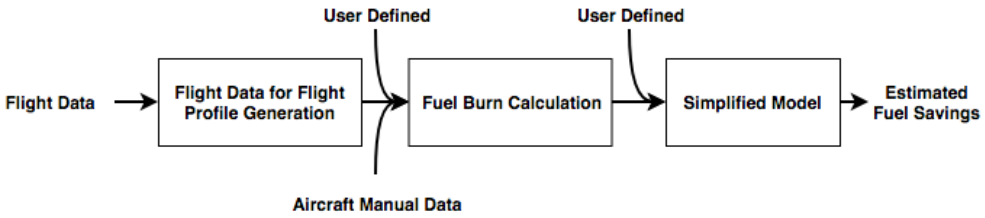

Figure 3.5.: Simple Structure of the Whole Research

To determine what variables load-controllers have available, a work shift has been joined. It was determined that the load-controllers have knowledge of the aircraft type, destination and ZFW. When determining the load plan of cargo, the location of the CG at ZFW, the ZFWMAC, is determined. Therefore, these four variables are determined as the input for the simplified tool. Due to the difference in routing and flying conditions between summer and winter, a fifth variable was added, namely the season. The use of Excel was chosen, as its wide knowledge and availability simplifies the use by employees.

The main (complex) tool, consisting of the first two modules, will be used to simulate average flights per destination, where the Zero Fuel Weight CG location expressed as a percent of Mean Aerodynamical Chord (ZFWMAC) is varied between the most forward and aft ZFWMAC allowed. The average ZFWMAC is a third considered situation, as it will result in an accurate calculation of this situation being available in the simplified tool. A final point is chosen between the average and aft most ZFWMAC, since added accuracy between these points was deemed necessary under the assumption that the ZFWMAC will improve after introducing this tool.

In a similar fashion, varying the ZFW between the Operating Empty Weight (OEW) and Maximum Zero-Fuel Weight (MZFW) for every previously defined ZFWMAC will provide fuel burn results for the chosen situation. By doing so, the whole allowable range of ZFWMACs and ZFWs is analysed, providing high flexibility of the analysis. Again, the average ZFW for each considered route, season and aircraft set is considered as a third data point. Two more ZFW values are evaluated, which are located evenly between the average ZFW and MZFW. This was done under the assumption that the slot restrictions at Schiphol (Royal Schiphol Group, 2018) and increasing demand (Koninklijke Luchtvaart Maatschappij, 2017) will cause an increase in ZFWs per flight. Added accuracy at higher than average ZFW is thus preferred.

The ZFW and ZFWMAC inputs are evaluated per origin-destination, aircraft type and season set. Figure 3.6 shows a more detailed structure of the simplified module, with the input variables from the complex tool and the user defined input. The results for the ZFW and ZFWMAC serve as input for the simplified module.

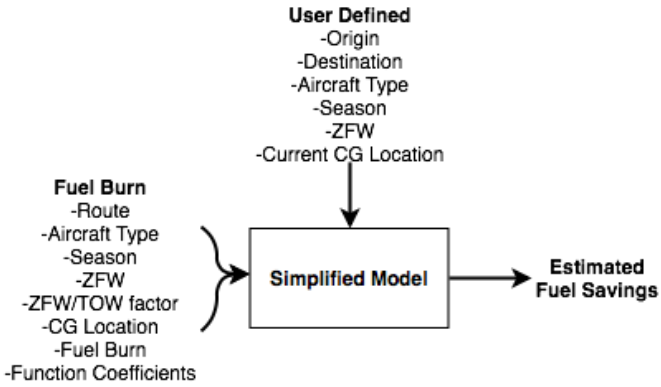

Figure 3.6.: Structure of the Simplified Model

With these inputs and outputs being written to Excel, a database is created for KLM. However, the complex tool writes one more result to the simplified tool, as can be seen in figure 3.6. The function coefficients depict the coefficients of the three dimensional, nearest fit of the ZFW, ZFWMAC and fuel burn relation. They are found by minimising the root mean square error while varying the coefficients. These coefficients result in the lowest root mean square error for the input data points and enable the replication of the function in Excel. By doing so, the expected fuel burn can be replicated for each ZFW

and ZFWMAC input necessary.

A second functionality of the Excel file is to provide a ranking of the routes with the highest potential for fuel savings. This is achieved by taking the average ZFWMAC and ZFW for each set and the logged fuel burn. By changing the ZFWMAC by 5 percentage points, the potential savings are determined. The highest savings are provided to the user.

3.4. Assumptions

Since the goal is to develop a model to calculate the fuel consumption for a flight, assumptions were made. These simplified the modules in the model to an extent that will enable the development in the given time. These assumptions were mentioned throughout the previous sections and are summarised in this section to give a better overview.

- Cruise angle of attack is small and can be rounded to zero
- Drag acts opposite and parallel to the flight direction
- Thrust acts parallel to the flight direction
- The lift only counteracts the weight; it does not contribute to an acceleration parallel to flight direction
- $\frac{d\gamma}{dt} = 0$, meaning all flight path angle changes are instantaneous
- No bank or sideslip is present due to crosswind
- Only the horizontal tail is used to control the moment equilibrium around the CG
- Wind is assumed to vary smoothly between way-points
- Long haul flights spend small amounts of fuel on take-off and landing (Roberson & Johns, 2008) compared to the whole flight, thus inaccuracies in take-off and landing fuel have small impact on the total
- High lift devices are not considered due to its short use compared to the whole flight (Roberson & Johns, 2008)
- The landing gear drag is not considered due to its short use (Roberson & Johns, 2008)
- Systems requiring fuel, but not directly contributing to the flight, like the Auxiliary Power Unit (APU) have negligible impact

3.5. Conclusion

By splitting the research into three parts, being the flight profile, fuel burn and simplified modules, a clearer structure for the tool was created. Firstly, flight data was used to create a standard or average flight by normalising the route. Through spline interpolation this was averaged at average waypoint locations.

Consecutively, resulting flight profile is used to calculate the fuel burn per waypoint. PEM and PEP data was used to determine the CG related drag, total drag, thrust and fuel consumption required to compute the fuel burn.

Finally, the results are used to determine a mathematical relation between the fuel consumption, ZFWMAC and ZFW. The coefficients of the function are saved to the third module, which will serve as a simplified tool to derive the results. The user can then specify the aircraft type, origin, destination, season, ZFW and ZFWMAC. The module will then return the expected savings if the ZFWMAC is shifted by a given amount. As such, this research can quickly be applied to practical issues.

4. Validation and Verification

With the methodology determined to develop the model, the actual construction took place. To ensure the model was built correctly and provides realistic answers, validation was performed. This chapter will discuss the development progress of the tool and how the accuracy of the tool was obtained. The order of discussion of each subject depicts the chronological order of development, which may aid in the thinking process of certain decisions. Some smaller validation steps are not discussed, to reduce size and due to the dependencies of more major validation steps. At the end of this chapter, verification is discussed to ensure the right tool has been developed.
Please note that despite discussing the return flight from Amsterdam to Tokyo Narita for the Boeing 777-200ER, the same steps have been performed for other routes and aircraft. This is not discussed since it mainly consists of repetition work or singular, minor errors. The same applies to the month, only December 2017 is considered, preventing too much data being shown in the plots and maintaining clarity. This specific route proved to contain a constant outbound flight, with the return flight having more variance. This way, both a flight without outliers in the route, and with outliers are provided for validation.

4.1. Flight Data Module

As discussed in section 3.1, two types of variables are considered; variables varying between each waypoint and variables at the beginning of each flight. This second group consists of averages obtained from the data, and require a simple comparison between the result and the input. Considering the Maximum Take-off Weight (MTOW), OEW and CG ranges provided by the OEM (The Boeing Company, 2004), checks were performed to ensure these input and output values are within expected values. Nothing unexpected was found during the validation process of these averages, except for destinations with a small number of flights. Aircraft changes or occasional events like the Olympics are the cause, and are seen as unrepresentative, since they can cause deviations in the ZFW and ZFWMAC. As such, if two or less flights per season were available for the aircraft type, the considered route was discarded.

4.1.1. Flight Varying Variables

Route

With the flight varying variables consisting of weather, Air Traffic Control (ATC) related and flight state related variables, these will have to be looked at more carefully. First, the typical route was constructed from flight data using the logged longitude and latitude. The result of which can be seen in figure 4.1. The thicker black line represents the average, while the crosses represent measuring points. A dotted line shows the path between the measuring points, which is obtained using spline interpolation.

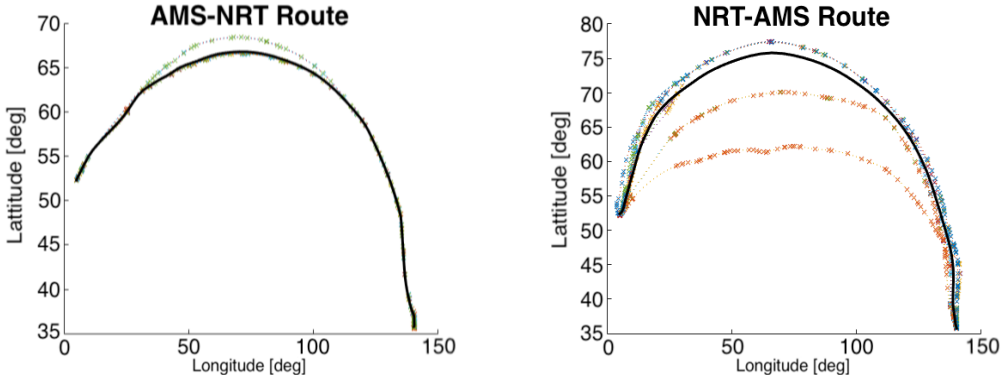

(a) AMS-NRT Route Averaging (b) NRT-AMS Route Averaging

Figure 4.1.: Actual and Averaged Route, Outliers Removed

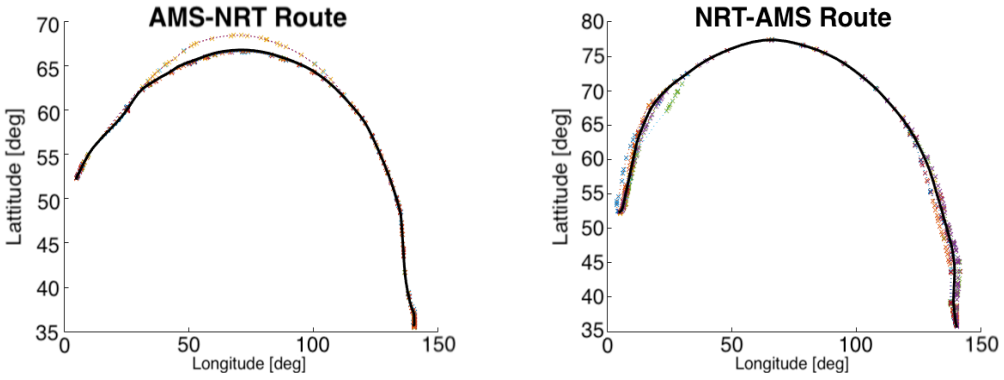

(a) AMS-NRT Route, Outliers Removed (b) NRT-AMS Route, Outliers Removed

Figure 4.2.: Actual and Averaged Route

Despite the longitude and latitude not being used for fuel calculations, their routes can encounter deviating flight conditions. Deviations in routing are visible in figure 4.1b, which shows two flights deviating significantly from the others. Due to this, it was

decided to add a function to check for these outliers. This is achieved by finding the closest matching longitude at a 1/4, 1/2 and 3/4 of the normalised distance. For each flight, the corresponding latitude is obtained. If the longitude-latitude combination has a latitude that is more than 3 times the mean absolute deviation, it is considered an outlier and removed.

The resulting routes are used as input and the corresponding standard route can be found in figures 4.2a and 4.2b. As mentioned in the introduction of this chapter, the outbound flight shows no change, but the return to Amsterdam does. Due to this, the following sections will consider the return flight, from Tokyo Narita (NRT) to Amsterdam Schiphol (AMS) to include the outlier processing during validation, unless mentioned otherwise.

TAS

Next is the TAS, which is related to the Mach number and air density. It can be higher on certain routes or within certain regions. Therefore, it was decided to model it as an input, extracted from flight data, which would incorporate frequent, regional speed changes if needed. Figure 4.3 shows the average TAS throughout a standard flight. It is expected that the TAS stays constant during the cruise, increases at the beginning of the flight, increases during step climb and decreases at the end. This is validated, but one can see that once the cruising altitude is reached, the TAS decreases slightly. Using the data from KLM, it is determined that this decrease is due to initiated step climbs affecting the average, since the climbing Mach number is lower. Each individual step climb is initiated at different distances from the origin. Due to the lower Mach number, the TAS is lower. Since many step climbs are performed in the data, especially between 1000nm and 3000nm, it explains the decrease in average TAS.

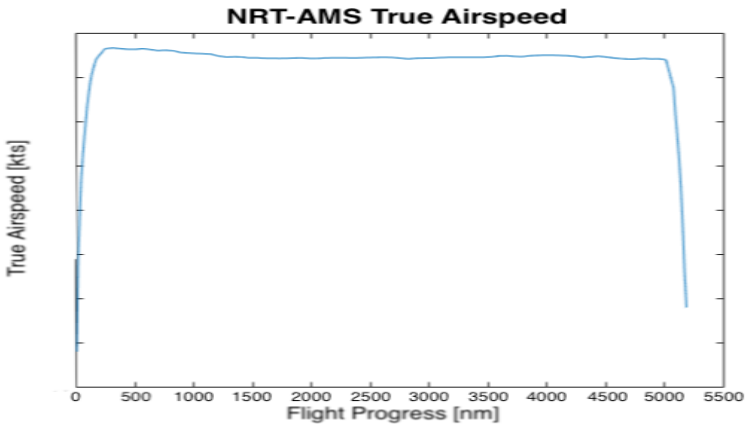

Figure 4.3.: Averaged True Airspeed, Outliers Removed

Wind

Due to the wind being a major reason for choosing a route, it is included in the model. Due to the difficulty to model it, averages were taken and these had to be validated. The average wind encountered from Amsterdam to Tokyo and its return can be found in figures 4.4a and 4.4b. Due to the difficulty of determining if the result is realistic and the addition of the input data in the plot creating a chaos, validation is done using reasoning.

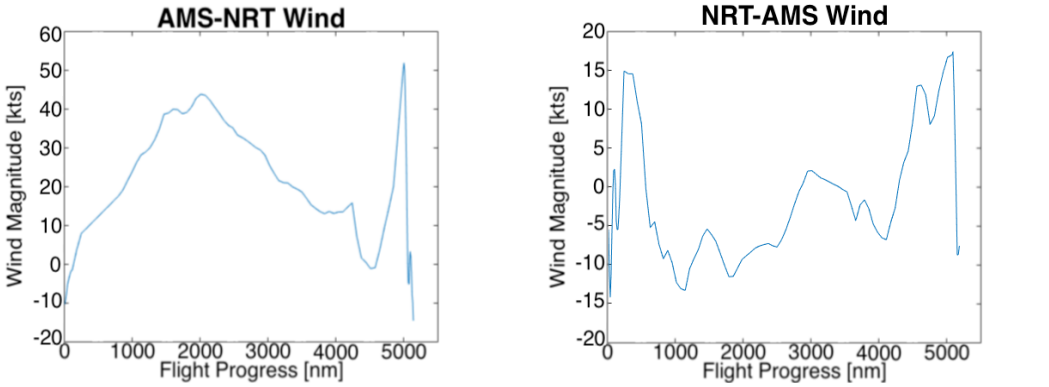

(a) AMS-NRT Wind, Outliers Removed (b) NRT-AMS Wind, Outliers Removed

Figure 4.4.: Average Wind Results

Tailwinds are favoured, since they increase the ground speed and therefore reduce flight time. Only exception to this are the take-off and landing, where headwinds reduce the take-off and landing distance (The Boeing Company, 2010).
Taking into account the prevailing stratospheric winds, flights heading east will encounter tailwind. Vice versa, flights heading west encounter headwinds (G. B. Chatterji, 2011). Figure 4.4b shows predominantly negative values, which means headwinds. This flight, from Tokyo to Amsterdam is in western direction, and thus is as expected. As a double check, figure 4.4a shows the outbound flight. Here, the wind is mainly positive, meaning tailwinds, which is also as expected. A third validation is done by looking at take-off and landing, which in both plots have negative results, meaning headwinds. Therefore, the module was deemed validated.

Flight Level

The last variable considered that changes between waypoints is the flight level. It is slightly different to previous variables, since it has been modelled to be dependent on the actual weight of the aircraft. As such, it has been adjusted to no longer be an input.

For validation, the flight levels during cruise have been taken from the average of flights

that had a TOW close to the average TOW. The result is depicted by the blue line in figure 4.5. It approaches a linear climb, which would be ideal, but is obtained due to each flight initiating the step climb at a different distance.

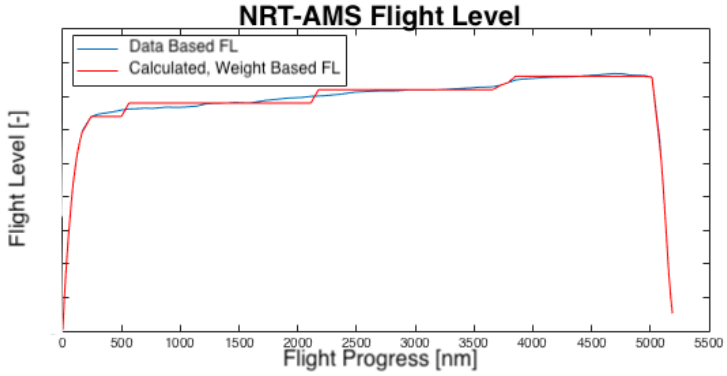

Figure 4.5.: NRT-AMS Flight Levels, Outliers Removed

Using the same flights, the average fuel burn during cruise is determined and used to update the current weight. Based on this weight, the ideal FL is computed and rounded to the nearest FL allowed for the flight direction. This result is depicted in red in figure 4.5. Comparing concludes that the computed, weight based flight levels, were near the average flight levels. Therefore, no further adjustments were deemed necessary.

4.1.2. Initial, Constant Variables

Discussion of the validation of initial, constant variables was not considered necessary. However, during validation discussed in section 4.1.1, it was discovered that one occurrence required extra attention. So-called "wind days" occur when the wind is too strong to open the cargo hold. As such, the aircraft cannot be loaded with the planned load. This causes the logged ZFW and TOW to be lower than planned. As such, fuel burn is about 15% lower than expected, depending on the destination. To reduce the impact of this, the actual fuel burn is compared with the planned fuel burn. If this deviates more than 10%, the day will be discarded.

4.1.3. Aircraft Manual Data

The last inputs considered are the inputs from the PEM and AFM. All data extracted from these manuals were entered manually. As a validation step, all the data was plotted to check if the plots were the same as in the manuals. Any errors were corrected, such that the plots were valid for use in the model. An example has already been shown in figure 3.3 in section 3.2.1.

4.2. Fuel Burn Module

With all inputs being validated, the first steps in the validation and development process of the fuel burn module were taken. Following sections will discuss the four flight phases considered; climb, cruise, step climb and descent. The order of discussion of these phases shows the chronology of development and their importance.

The validation has been performed by entering the actual flight data in the fuel computation module. The resulting fuel burn per waypoint, the actual fuel burn and the accuracy of the calculation are then derived. These results, per numbered waypoint, can be found in appendix B. To visualise these results, the cumulative fuel burn is plotted versus the distance in figure 4.6.

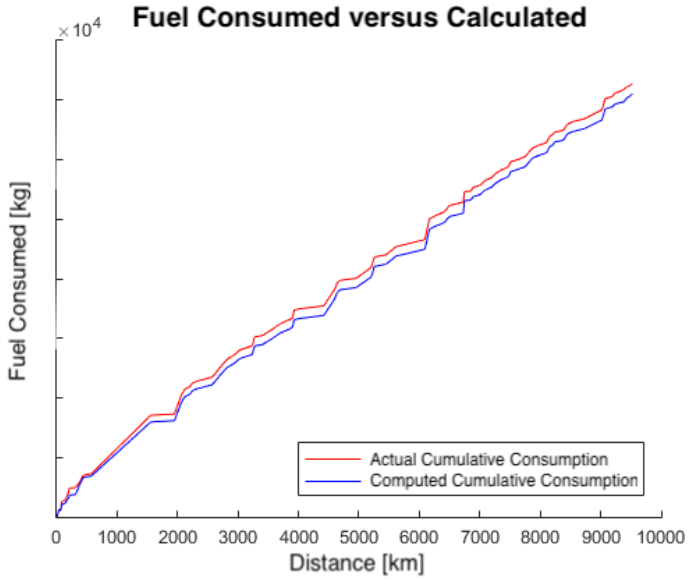

Figure 4.6.: NRT-AMS Fuel Validation

The following sections only show and discuss the corresponding flight phase in appendix B. The fuel burn module validation is finalised with the discussion of the whole, computed flight fuel burn with respect to the data for a whole month, followed by validation of the standardised flight.

4.2.1. Cruise

Due to long haul flights consisting primarily of cruising, this is seen as most important. It was decided not to display an extraction of the cruise data from appendix B, since cruise consists of 65 lines. This would become too big for this section, so instead one should refer to appendix B. This fact shows the validity of the reference and application

of assumptions stating the climb and descent fuel are insignificant compared to cruise fuel (Roberson & Johns, 2008).

Considering the comparison of calculated and actual fuel burn, the calculation is roughly between 95% and 103% of the actual fuel burn. Exceptions are waypoints 13, 51 and 53, with waypoints 87, 91 and 92 ignored since they mean a holding of altitude during descending, meaning flaps and gear can be extended. Waypoint 53 is deviating percentage wise, but considering the small fuel burn quantity, one can conclude that this is insignificant. Waypoints 13 and 51 are left, but one can see that the preceding waypoint is a climb phase. The differences are therefore attributed to this, where it is assumed that after a climb, the aircraft will have to stabilise. One can think of accelerating to the cruising Mach number, which is higher than the climbing Mach number. This acceleration is not considered, and will cause the differences. Therefore, no adjustments are required to the cruise module.

Please note that despite only discussing validation of the fuel burn, also intermediate results have been validated. Since the fuel burn is dependent on these intermediate results, discussing the validation of the fuel burn is considered sufficient. As intermediate results, one can think of the drag of the aircraft or the fuel flow per minute, which is compared to standard values given by the OEM (The Boeing Company, 2004).

4.2.2. Step Climb

With the cruise phase validated, a look was taken at the step climb. This is a constant Mach climb during cruise, with a thrust setting of 95%CN1. Since it occurs during cruise, it translates to all climb phases in appendix B which have a cruise designation before and after the climb. The result can be found in table 4.1.

Table 4.1.: Step Climb Fuel Validation Indication

Waypoint [-]	**Flight Level** [-]	**TAS** [m/s]	**Phase** [-]	**Actual Fuel** [kg]	**Computed Fuel** [kg]	**Accuracy** [-]
11	310	490	Climb	61	59	0.96
12	325	490	Climb	1118	1909	1.71
15	330	480	Climb	239	233	0.98
50	350	480	Climb	648	639	0.99
69	370	490	Climb	391	379	0.97
70	375	490	Climb	465	529	1.14
71	385	490	Climb	282	324	1.15

Inspection shows that the step climb has an accuracy close to 100%. Only waypoints 12, 70 and 71 deviate from this accuracy. Inspecting waypoints 11 to 13, one can see that the climb has a decreasing TAS. In other words, kinetic energy is converted to potential

energy, reducing the thrust and thus fuel flow. Despite this, 800kg difference for a total of 1900kg of fuel is significant. The exact cause was not determined, but doing the same analysis for other flights showed no similar differences. As such, it is assumed that the cause is an input error. Also, 800kg of fuel is only 1% compared to the total flight fuel, and is therefore insignificant when considering the overall underestimation of fuel consumption.

Waypoints 70 and 71 are determined to have a different cause, being the slower climb than used during calculations. One can see that it takes 3 waypoints with a total of roughly 1200kg of fuel to climb from FL 370 to FL 390. This means a slow climb, thus requiring less thrust. The reason for this is unknown, but it results in the model calculating the climb with a staircase shape. It climbs at a certain ROC until it reaches the FL of the next waypoint. From this moment, it considers cruising until the waypoint is reached. After this, it undergoes the same process. The actual flight is most likely to have a continuous climb. As such, the computed fuel is an overestimate, with roughly 100kg of fuel overestimated. This comes down to roughly 0.1% of the total fuel and is therefore insignificant. Inspecting other flights, the same, insignificant deviations exist, but are of no concern. As such, the step climb calculations are considered validated.

4.2.3. Climb

The climb phase is an addition to the step climb module. This module was adjusted to incorporate the effects of acceleration in flight direction using the energy share factor discussed in section 3.2.3. Initially, the energy share factor was set constant and equal to 0.3 for simplicity reasons. This proved to give low ROC values, and was therefore adjusted to be a function provided by Ruijgrok, which is discussed in section 3.2.3.

Despite the improved ROC due to changing the energy share factor, the thrust setting of 95%CN1 proved to be too high at lower altitudes, resulting in unrealistic fuel burn projections during accelerating TAS climbs. As such, it was decided that below FL 200, constant TAS climbs will have a thrust setting of 85%CN1. By doing this, ROCs of around 2500 ft/min were obtained, which is as expected (The Boeing Company, 2010). With these adjustments, the results in table 4.2 are obtained, which is an extract of appendix B. Interesting to see is that at the end of climb, no acceleration is performed, since the cruising TAS has been reached. This corresponds with the assumption made in section 3.2.3 stating acceleration does not take place during cruise.

Note that the climb module performs a climb computation which can also be considered a step climb. At waypoint 8 the TAS is identical to the next waypoint and stays constant (allowing maximum 2.5% variance), while the flight level is equal to 300, which can be a cruising altitude. The 2.5% variance has been chosen based on analysis of the data. All TAS stays within 2.5% when climbing between cruise sections. It proved a valid assumption, since the results for step climb were accurate enough, and was therefore applied as to determine if the TAS was constant or not during climb.

Table 4.2.: Climb Fuel Validation Indication

Waypoint [-]	**Flight Level** [-]	**TAS** [m/s]	**Phase** [-]	**Actual Fuel** [kg]	**Computed Fuel** [kg]	**Accuracy** [-]
1	0	115	Climb	-	-	-
2	20	205	Climb	525	806	1.53
3	60	280	Climb	734	359	0.49
4	80	300	Climb	249	183	0.74
5	170	405	Climb	1388	992	0.72
6	190	420	Climb	200	181	0.90
7	260	460	Climb	1161	800	0.69
8	300	485	Climb	395	407	1.03

Continuing the analysis, the accuracy of the fuel computations, one can see that the very first fuel computation is overestimated significantly. This is due to the first fuel burn computation based on the average of all flights on the considered route. This was done since take-off is too time consuming to model for this research, and is only a very small proportion of the total flight (Roberson & Johns, 2008). Comparing the actual fuel burn of other flights shows the figure is within reason, and requires no further alteration. The effects of take-off are also visible in the fuel burn accuracy for the consecutive waypoints.

As such, only waypoint 7 is of interest for further validation. The module shows an underestimate for this waypoint. Despite the average calculation of an increasing TAS climb (but these can be constant CAS) being close to real life figures, it is out of proportion for this instance. Looking at other data shows, as was just mentioned, that the overall accuracy of the accelerating climb module is accurate. As the same goes for a constant TAS climb, as point 8 shows, the climb module was determined to be validated, with waypoint 7 being a singular occurrence.

4.2.4. Descent

The final module to require validation is the descent module. At first, this was modelled to use idle thrust, calculate the ROD with the energy share factor and determine how long it takes to reach the new FL and TAS. Once the new FL and TAS has been reached, this would be maintained until the waypoint is reached. This, however, resulted in fuel burn calculations not corresponding to the actual fuel burn.

The second method used a constant, predetermined ROD, combining with the energy share factor to determine how much thrust is needed to achieve this ROD. Once the FL and TAS of the next waypoint have been reached, these would be maintained to calculate fuel burn of this second part. This also failed to simulate the fuel burn accurately.

Due to the two failed attempts, contact was made with a KLM pilot. The conversation learned that descent can vary significantly. Sometimes spoilers are used to expedite descent, since idle thrust is not sufficient. At other moments a slow descent can be initiated, depending on ATC assignments. Also, at times, altitude can be maintained between waypoints, only to descend for a small duration between the points. Due to the difficulty to model this, it was decided to assume a constant descend between two waypoints.

To incorporate the effect of changing TAS, the first law of Newton ($F = ma$) was applied. Due to the need of incorporating two thrust changes, one to enable descent without gaining speed and the other to enable a speed change, first the thrust to satisfy the ROD was determined. This was followed by determining the thrust needed, via Newton, to facilitate the speed change. The corresponding fuel burn was compared to the fuel burn under the same conditions, but when maintaining the same speed. The difference in fuel burn, due to decelerating, was subtracted from the fuel burn computed for the descent. This method was chosen due to the reduced complexity. The resulting fuel burn results and validation data can be found in table 4.3, which is, once again, extracted from appendix B.

Table 4.3.: Descent Fuel Validation Indication

Waypoint [-]	**Flight Level** [-]	**TAS** [m/s]	**Phase** [-]	**Actual Fuel** [kg]	**Computed Fuel** [kg]	**Accuracy** [-]
77	390	480	Descent	376	355	1.00
78	340	480	Descent	756	577	0.76
79	300	465	Descent	174	158	0.91
80	250	430	Descent	243	148	0.61
81	220	400	Descent	149	25	0.17
82	180	400	Descent	149	300	2.01
83	160	390	Descent	194	213	1.09
84	150	385	Descent	53	119	2.23
85	130	375	Descent	171	171	1.00
86	120	370	Descent	58	128	2.21
88	100	310	Descent	208	278	1.34
89	80	270	Descent	95	80	0.84
90	70	260	Descent	12	78	6.35
93	60	240	Descent	0	46	∞

As was mentioned, descent is difficult to model. Looking at the results, one can see that the accuracy indeed is often not close to 100%. Often, waypoints are close to each other, resulting in fuel calculations being overestimates of the actual fuel burn. The cause lies in the aircraft encountering multiple waypoints in the same minute, meaning a time difference of 0 minutes. If this is encountered, the tool will assume a duration of

1 minute, which means 128kg of fuel computed versus 58kg used. As such, the accuracy of waypoints 82, 84, 86, 88, 89 and 93 can be ignored. The same reasoning applies to logging 1 minute when in fact it took 10 seconds, as waypoints 80, 81, 82 and 90 show.

The remaining waypoints do show a reasonable accuracy, with most deviations being attributed to effects discussed, such as expedited descent using spoilers and then maintaining altitude or flaps and landing gear extension. This leaves no waypoint with good accuracy, so the whole descent is considered for validation. 2592kg of fuel is used on the actual flight, with 2654kg of fuel calculated. This means a 102.40% accuracy, a slight overestimation. Doing similar analysis for other flights results in similar figures, with the accuracy varying between roughly 95% and 106%. Considering the magnitude of the total fuel consumption and the descent consumption, 78128kg and 2654kg respectively, shows the descent fuel consumption is small (3.4%) compared to the cruise. Therefore the descent model is sufficient for this research.

4.2.5. CG Effects

Despite the model discussed until now including the CG effects, it will be treated separately in this section. This due to the focus of the research being on this subject. The lift-drag polar for different CG locations is obtained using OEM provided manuals. To validate the computations, the lift-drag polar at M=0.80 and M=0.85 are plotted in figures 4.7a and 4.7b. These Mach numbers were chosen since the typical cruise speed lies within this range.

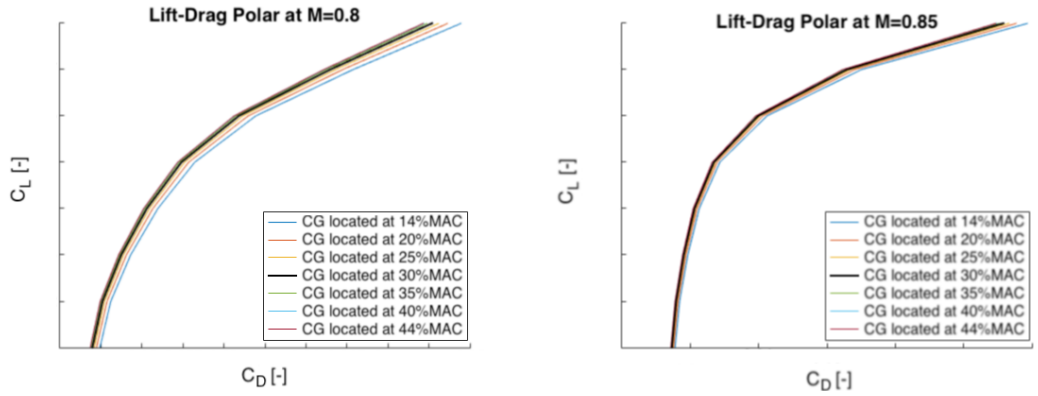

(a) M=0.8 with Varying CG

(b) M=0.85 with Varying CG

Figure 4.7.: C_L-C_D Polars

The design location of the CG for the 777-200ER, the aircraft considered, is at 30%. This is depicted by the thicker, black line in both figures. The PEM provides the same plots under various flap settings, and combined with the high speed lift-drag polar, can

be used for a rough comparison. This shows similar behaviour of the plots. Both show similarity in the aft CG having a lower drag, but the gain in drag reduction is bigger when starting at forward CGs. This matches theory discussed in chapter 2 and appendix A, showing a parabolic relation between drag and lift coefficient. Also the original drag polar in the PEM has the same shape and values as the polar in figures 4.7a and 4.7b with the CG at 30%. Finally, considering table 4.4 as indication, the similarities result in this implementation being validated.

Table 4.4.: Section of CG Fuel Penalty Table (Dispatch, 2017)

ZFWMAC [%]	<16-16.9	17-17.9	18-19.9	20-21.9
Fuel Correction [%]	+1.3	+1.2	+0.9	+0.6
ZFWMAC [%]	29-30.9	31-32.9	33-35.9	>=36
Fuel Correction [%]	+/-0.0	-0.4	-0.5	-0.7

Fuel Vector

A second step to consider is the movement of the CG during flight. Since fuel is burned, the CG moves aft during flight (Torenbeek, 1982). This effect is displayed by fuel vector plots, available within KLM. A fuel vector plot for the 777-300ER provided by KLM, seen in figure 4.8a, has been added for illustration. With this, the movement of the CG will be updated, resulting in more accurate CG related drag computations. Since KLM only has a plot readily available for the an aircraft different than the Boeing 777-200ER, this aircraft will be considered for the validation of the fuel vector. The method of derivation is the same for all other aircraft. Both the validation and computed plots can be found in figures 4.8a and 4.8b respectively. The resemblance is clear, with the minor differences being attributed to the difference in ZFW used in the validation data and fuel quantity. Therefore, no adjustments are needed, leaving the fuel vector validated.

Interesting note is that in rare cases, with a ZFWMAC very forward, the CG will actually be slightly aft when taking the maximum fuel quantity. In this exception, the CG will move aft during flight, but can end up in front of the CG location at take-off.

Based on figure 4.8b, the effect of the ZFWMAC discussed in section 3.1.1 are visualised. When the ZFWMAC is at 44%, adding fuel can result in an out of trim situation. The CG can move behind 44%. This shows there are practical limits which determine the range of the ZFWMAC. It proved difficult to obtain these limits from flight data, and was therefore not further investigated. With the average ZFWMACs lying more than 10 percent points in front of the aft limit and the ZFWMAC not expected to improve more than 5 percentage points, it is considered outside the scope of this research.

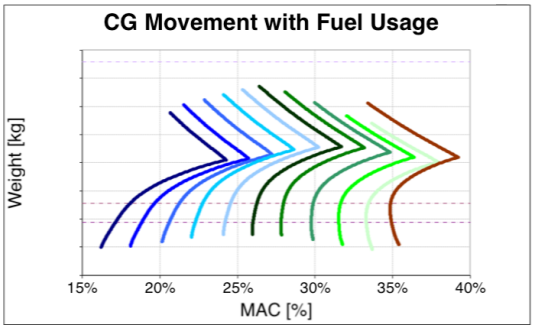

(a) Provided Fuel Vector. *Courtesy KLM*

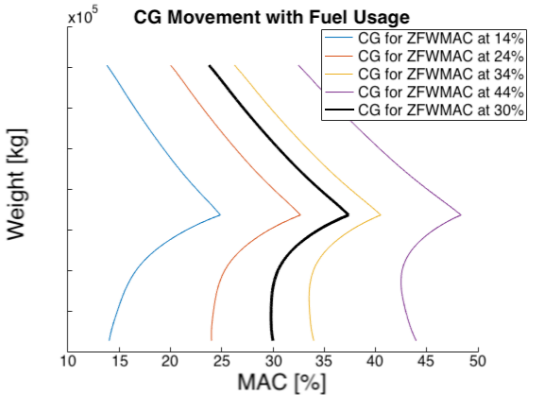

(b) Computed Fuel Vector

Figure 4.8.: 777-300ER Fuel Vectors

4.2.6. Whole Flight

Having validated all parts of the model, the whole model can be validated to ensure all sections provide validated results when used together. For this, the NRT-AMS route, flown by a Boeing 777-200ER was chosen for discussion, due to its frequent use in this chapter. The results can be found in table 4.5.

Table 4.5.: Whole flight Fuel Validation Indication

Date [-]	**Actual Fuel** [kg]	**Computed Fuel** [kg]	**Accuracy** [-]
01-Dec-2017	84825	81320	0.96
02-Dec-2017	80690	79510	0.989
03-Dec-2017	83780	81530	0.97
04-Dec-2017	84020	83580	0.99
05-Dec-2017	76030	75100	0.99
06-Dec-2017	75200	73180	0.97
07-Dec-2017	77780	78720	1.01
10-Dec-2017	77980	77830	1.00
13-Dec-2017	80500	78060	0.97
14-Dec-2017	80100	77710	0.97
15-Dec-2017	80920	79740	0.99
19-Dec-2017	83740	80510	0.96
22-Dec-2017	83400	87100	1.04
24-Dec-2017	83590	81040	0.97
26-Dec-2017	79660	76890	0.97
27-Dec-2017	80840	77690	0.96
28-Dec-2017	75640	74240	0.98
29-Dec-2017	77940	76150	0.98

Table 4.5 shows that over a whole month, the accuracy is within 4.5%. The average accuracy is 98%, with a mean absolute deviation of 1.5%. Similar results are obtained for other routes flown by the Boeing 777-200ER. This is considered accurate enough for this research, validating the methods of each flight phase.

4.2.7. Standard Flight

Knowing the fuel burn computation is validated, the average flights are used and evaluated. Once again, the Boeing 777-200ER flight from Tokyo to Amsterdam, on December 2^{nd} is considered.

Going through the results of each waypoint is done in a similar fashion as was done in previous sections. Due to no validation data being available, the order of magnitude per waypoint is checked for its realism. The resulting table can be found in appendix B. Comparing the total calculated fuel consumption of the standardised flight (80300kg) with the total fuel discussed in section 4.2.6 (79510kg) gives a difference of 790kg. This is a difference of 1%.

A second means of validation was performed. Flights with similar ZFW and ZFWMAC values have been used to compare to the average flight. This also resulted in results

within a few percent of the real flight. This is less accurate, since a lot can vary between flights. Despite this, the method was determined to be accurate and discussion of the analysis of all the waypoints is deemed unnecessary.

4.3. Simplified Model

To enable the development of the simplified model, a function that reduces the root mean square error was used to determine the coefficients of a general function. The resulting coefficients are used to define the three dimensional function needed to determine the fuel burn. Figure 4.9 shows the resulting values of varying ZFWMAC locations and ZFW values, marked with circles. It also shows lines depicting the result of using the derived function using the coefficients. Amsterdam to Tokyo was used since the return flight had a less clearly visible relation, due to the points being located near each other. It is more difficult to see the relation if three out of four points are near each other, hence AMS-NRT is preferred for visualisation, since it does not encounter this issue.

Figure 4.9 shows the simplified method of deriving the fuel burn is close to the calculated results. For the purpose of the simplified model, the resulting average accuracy being within 4%, is seen as sufficiently accurate. Any inaccuracy in the fuel burn calculation has a small impact, since the change in fuel burn is required. Due to the smooth curves, fuel differences due to shifted CGs are more accurate and deemed valid.

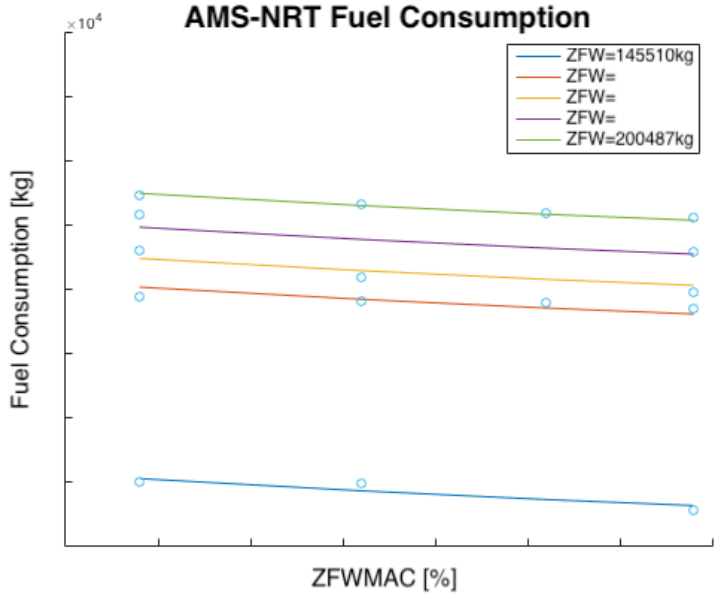

Figure 4.9.: ZFWMAC-Fuel Burn Indication for Varying ZFWs

To get to these plots, some validation had been performed before figure 4.9 could be

constructed. Firstly, outliers have been removed using the mean absolute deviation method introduced in section 4.1.1. This is visible in figure 4.9 by a few points, marked by a circle, missing. In this figure, these points were removed since the mean absolute deviation is small. Investigation showed the datapoints to deviate very little, but still enough to be removed. Despite this drawback, some flights had more significant outliers which required removal. The outliers of these flights are due to the provided aircraft data not always giving a full spectrum. If requested data is outside the range of the input data, the nearest known data is used. This occasionally causes such an outlier, especially when close to the minimal or maximal ZFW or ZFWMAC.

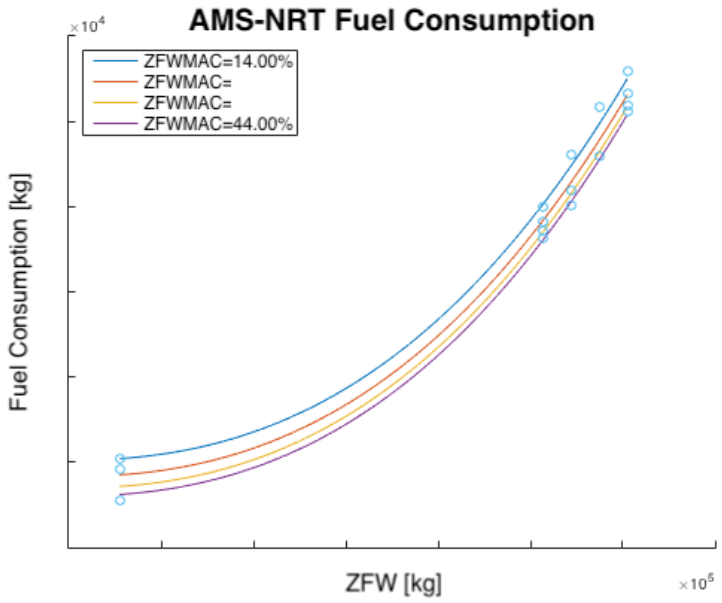

Figure 4.10.: ZFW-Fuel Burn Indication for Varying ZFWMACs

The second validation is related to deriving the order of the simplified function to derive the fuel consumption. Due to theory stating a quadratic relation between the C_L and C_D of the tail, a quadratic relation was assumed for the ZFWMAC-fuel burn. Despite the high accuracy, also other relations were tested. Due to a quadratic relation requiring less data points to derive a function, and due to its accuracy, a quadratic function was chosen. This accuracy of the relation is also shown in figure 4.9.

In a similar fashion the most accurate relation between the ZFW and fuel burn , with a low amount of coefficients, was determined to be a cubic relation. The result of this can be seen in figure 4.10, although with differenc ZFW values than figure 4.9. It contains the same data as figure 4.9, only depicting a different x-axis. Only near the maximum ZFWs and forward ZFWMACs larger deviations show. Due to the good accuracy, the relation was kept cubic.

Finally, due to developing a 3 dimensional function, interactions between both input

variables (ZFW and CG) was considered. These showed high accuracy at the validation points, but unrealistic behaviour between these points. Considering that the extensive calculations incorporate influence of the ZFW and CG on each other, it was discarded in the simplified function.

The validation of the Excel file, the main deliverable for KLM of this research, is considered next. It consists only of checking if the computations are the same as the results displayed in figures 4.9 and 4.10. As such, this is a small check, only to see if the functions have been implemented correctly and requires no further discussion since the functions have been validated.

4.4. Verification

Knowing each section of the calculation is validated, a test version of the simplified model was handed over to KLM Loadcontrol. By doing this, any errors could be found and adjusted, as could also be done for practical issues. It also served verification purposes. Feedback from KLM were positive, but the model did not provide means to quickly and easily derive the routes with the highest potential savings. As such, this was later added to the model, which considered each route and aircraft combination. The average ZFWMAC and ZFW were used to determine a basis fuel consumption. Getting the fuel burn for the identical case, only moving the CG by 2 and 5 percentage points will give a second fuel burn. Subtracting these two fuel burns indicates how much fuel can potentially be saved. Ranking these will give the routes with the highest potential, as is requested by KLM.

Since KLM put larger preference on the average ZFW and ZFWMAC points being accurate, it was decided to have the extensive tool calculate the fuel burn at average ZFW and ZFWMAC. These points are saved to the simplified tool, while the rest of the ZFWMAC-ZFW combinations are used to derive the function and coefficients.

4.5. Conclusion

Having performed the validation of the whole model and all intermediate steps, the tool is deemed valid. This was achieved by making alterations and additions to the tool. Examples of the additions and alterations are the removal of outliers and update of the CN1 values. By doing so, the accuracy of the tool when entering real flight data was within 5% and at roughly 2% on average. Using the average flight profile, realistic results were obtained when comparing to flights with similar inputs.

The simplified model was validated next, with the coefficients being checked for giving accurate results. Small variations existed, but proved not to provide significant inaccuracies. Through the introduction of a test version of the simplified tool, verification

was achieved, while small errors or exceptions encountered were resolved.

5. Results

With the method established, the modules validated and the result verified, the results obtained are discussed. Since all results obtained are saved into the simplified model, the discussed results can also be found in the simplified module. Each discussed result is computed using the extensive model, unless mentioned otherwise. By logging the results in the simplified module, it provides accuracy where KLM requires it.

First, the highest savings potential per aircraft type will be discussed. This is followed by the discussion of the result of potential CG improvements, made for individual research and motivation. Finally, all sub-question related research is treated, answering any questions not answered yet.

5.1. Savings Potential

As determined in section 4.4 and section 3.3, the highest savings potential routes provide the routes that can obtain the highest fuel savings by shifting the ZFWMAC by 2 and 5 percentage points. The savings are computed for two identical flights, with only the ZFWMAC differing. If required, the Excel file provides sufficient data to also analyse the effect of changing the other inputs.

Considering all routes and aircraft combinations, in appendix C is obtained. It shows the most fuel consuming aircraft to have the most savings potential, which is within expectations. Due to the comparison between all aircraft being unrepresentative, each aircraft will be treated separately in the following sections. The top 5 for each aircraft will be treated per aircraft type and provide discussion if it showed any interesting results.

5.1.1. Boeing 777-200ER

Looking at the Boeing 777-200ER, the route with the largest savings potential is from Singapore (SIN) to Amsterdam, for winter. The top five is displayed in table 5.1, with the savings at 5% and 2% ZFWMAC shift. Interesting to note is that the longest routes do not always provide the highest savings potential. This is caused by the average ZFWMAC being very forward for some shorter routes. Due to the parabolic tendency of the fuel-CG relation, a forward ZFWMAC can have a larger decrease in drag than a

aft ZFWMAC. As such, Amsterdam-Atlanta (AMS-ATL) shows up in the top 5 of most savings potential routes.

A second interesting result is that the 2% savings potential show a larger change per percentage point than at 5%. This is a reflection of the parabolic relation between the CG and trim drag established in section 2.3.1. This results in the gains being bigger when shifting in the forward CG range.

Table 5.1.: Boeing 777-200ER Top 5 Potential Savings Indication

Ranking	1	2	3	4	5
Origin	SIN	KIX	TPE	NRT	AMS
Destination	AMS	AMS	AMS	AMS	ATL
Season [-]	Winter	Winter	Winter	Winter	Winter
Average Consumption [kg]	94300	75700	94800	82400	51300
Average ZFW [kg]	211200	212400	215600	210800	211900
Average ZFWMAC [%]	32	29	32	32	32
5% CG Shift Savings [kg]	820	800	750	690	660
2% CG Shift Savings [kg]	330	330	310	290	280
Percentage of Total at 5% shift [%]	0.9	1.1	0.8	0.8	1.3
Percentage of Total at 2% shift [%]	0.4	0.4	0.3	0.4	0.5

Table 5.2.: Boeing 777-200ER Fleet-wide Performance Indication

Average ZFW [kg]	208700
Average ZFWMAC [%]	33
Average Savings at 5% CG Shift [kg]	360

From table 5.1, it already shows, but when considering all Boeing 777-200ER results, a clear trend is visible showing higher fuel burn in winter when flying in western direction. This is due to the encountered winds in easterly direction being stronger in winter, lengthening the flight time (Dispatch, 2017). This, in return, means any percentage savings is encountered longer, meaning larger savings when only considering a shift in CG. Since flights in winter are generally less full, it is easier to shift cargo and therefore optimise the CG location (Koninklijke Luchtvaart Maatschappij, 2011). It should be mentioned that adding weight will cause an increase in fuel burn, undoing the savings by a shift in CG. Therefore, adding weight to shift the ZFWMAC aft when the cargo hold allows this, is not advised.

To get a quick impression of the results for a single route, figure 4.9 from section 4.3 was reconsidered, depicting the Boeing 777-200ER on the Amsterdam to Tokyo route during winter. This figure did not show the expected, quadratic relation between CG and fuel burn discussed in section 2.3.1. This relation is present, although barely visible. Different flights were looked at, often with the same problem. Cause is the small influence of the CG on the total fuel burn, making it hard to see. Also, due to including all ZFW values when deriving the function, the relation can be more linear on average. Figure 5.1b has been added, since it has the relation more clearly visible.

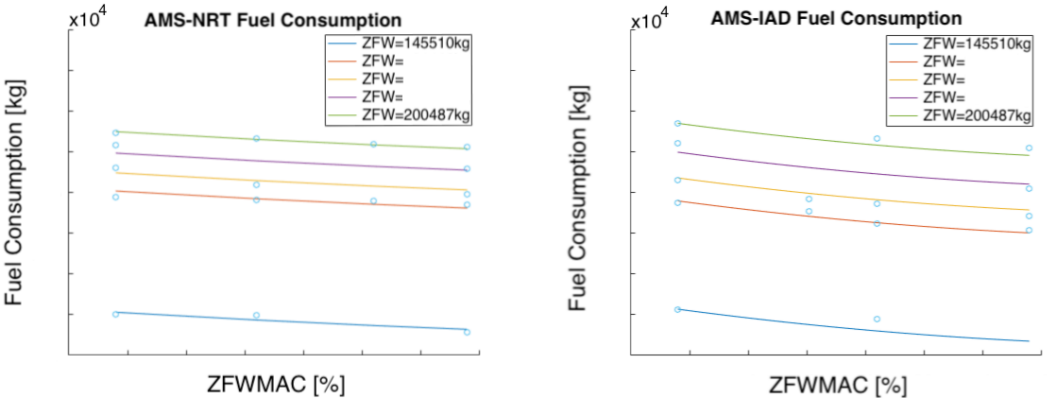

(a) Amsterdam-Tokyo (b) Amsterdam-Washington D.C.

Figure 5.1.: ZFWMAC-Fuel Burn for Varying ZFWs

Investigating figures 5.1a and 5.1b prompted an unexpected observation. For lower ZFWs, the CG has a larger, percentage wise impact on the fuel burn. Since this was not encountered in the research done prior to the execution of the research, this was somewhat surprising. Appendix E shows the derivation to check this occurrence, concluding that the relation between ΔD_{wing} and ΔD_h is constant when ignoring aerodynamic moments. Including the aerodynamic moments explains the higher percent-wise savings when shifting the CG aft in empty aircraft.

5.1.2. Whole Fleet

At the request of KLM, the six other aircraft types within the fleet are analysed with the same tool. These are the Boeing 747-400, 747-400 Combi, 777-300ER, 787-9, Airbus A330-200 and A330-300. The results are available in the following paragraphs.

Overall, it can be concluded that flights heading west, especially during winter, have higher saving potentials. In addition, the longer routes will have higher savings than shorter routes, and Airbus aircraft show to be more sensitive to CG changes, partially due to the trim tank. These observations have also been provided as a general rule of thumb for KLM. Due to the similarities in results, no individual discussion of the results

will be treated. Only the savings at 5% are displayed, since including the 2% savings was done for the 777-200ER since it showed the nonlinear increase in fuel consumption. This relation is also present in other aircraft, but is considered additional information, which is not necessary. Main focus of this research is the quantification of the fuel savings.

Boeing 777-300ER

Moving from the Boeing 777-200ER to the 777-300ER is a relatively small step. The aircraft belongs to the same family, with the 777-300ER being larger. At KLM it is configured to carry as many passengers as the Boeing 747-400, making these two aircraft the largest in their fleet. Due to its higher efficiency, it is used more and more often compared to the Boeing 747-400. The higher efficiency does mean a lower savings potential, as can be seen in table 5.3 (and comparing with table 5.5).

Table 5.3.: Boeing 777-300ER Top 5 Potential Savings Indication

Ranking	1	2	3	4	5
Origin	KUL	AMS	SIN	AMS	TPE
Destination	AMS	PTY	AMS	SIN	AMS
Season [-]	Winter	Winter	Winter	Winter	Summer
Average Consumption [kg]	119700	98500	123700	111600	118500
Average ZFW [kg]	252700	246700	248500	253700	254800
Average ZFWMAC [%]	32	35	33	31	32
5% CG Shift Savings [kg]	1010	1000	980	940	920
Percentage of Total at 5% shift [%]	0.8	1.0	0.8	0.8	0.8

Table 5.4.: Boeing 777-300ER Fleet-wide Performance Indication

Average ZFW [kg]	247700
Average ZFWMAC [%]	33
Average Savings at 5% CG Shift [kg]	570

Boeing 747-400

The Boeing 747-400, together with the Combi version, is the oldest and largest type in the fleet of KLM with long range capabilities. Due to its age and use of four engines, it is also the most fuel consuming aircraft within the fleet. Due to this, it is used less intensively whenever possible, and preferably on shorter routes with high passenger demand. As such, it is frequently encountered on routes that required an aircraft change, since a 747 is often available and will always be able to carry the load planned for the flight. As such, the results in table 5.5 is for routes not frequently flown by the 747-400. Note how the average savings potential in table 5.6 for this type is much smaller than encountered in table 5.5. This is caused due to the aircraft being deployed on shorter routes due to its high fuel consumption. The higher savings potentials are mainly achieved on flights where the 747 substituted a different type, or on routes no longer served.

Table 5.5.: Boeing 747-400 Top 5 Potential Savings Indication

Ranking	1	2	3	4	5
Origin	PVG	AMS	AMS	AMS	AMS
Destination	AMS	PBM	SXM	YUL	IAH
Season [-]	Winter	Winter	Winter	Summer	Winter
Average Consumption [kg]	133600	101800	96900	66730	104346
Average ZFW [kg]	255400	256900	255100	250200	254100
Average ZFWMAC [%]	29	33	32	27	22
5% CG Shift Savings [kg]	2800	2700	2550	2440	2040
Percentage of Total at 5% shift [%]	2.1	2.6	2.6	3.3	1.8

Table 5.6.: Boeing 747-400 Fleet-wide Performance Indication

Average ZFW [kg]	25900
Average ZFWMAC [%]	26
Average Savings at 5% CG Shift [kg]	1050

Boeing 747-400 Combi

The Boeing 747-400 Combi is a Boeing 747, but adapted to carry cargo at the rear section of the main deck. Due to cargo being more dense than passengers, while having the same design characteristics as the full passenger version, this type consumes most fuel of all aircraft in the fleet. This is, however, not reflected in the potential savings. Despite the heavy load capability in the rear, the ZFWMAC does differ much from the full passenger version. The large variance is due to the 747 combi being frequently used as substitute. Not all airports can offload the main deck cargo, while ballast should be present to balance the aircraft. In these cases, the minimal amount of ballast is added to keep the CG within limits, resulting in a forward ZFWMAC. This consumes less fuel than adding more ballast to shift the ZFWMAC aft, as discussed in 5.1.1.

The cause of the low savings potential, which has not been determined, was found somewhere else; the flight distance. The 747 Combi tends to be dispatched on shorter flights compared to the full passenger 747. This reflects in the results displayed in table 5.7 and the average savings in table 5.8 being almost 3 times smaller.

Table 5.7.: Boeing 747-400 Combi Top 5 Potential Savings Indication

Ranking	1	2	3	4	5
Origin	NRT	AMS	NBO	CTU	AMS
Destination	AMS	YUL	AMS	AMS	NBO
Season [-]	Winter	Summer	Winter	Winter	Summer
Average Consumption [kg]	134100	74300	94100	114600	87700
Average ZFW [kg]	264600	248400	267200	261500	257900
Average ZFWMAC [%]	33	23	26	34	32
5% CG Shift Savings [kg]	2530	2520	2330	1780	1780
Percentage of Total at 5% shift [%]	3.3	1.9	3.4	1.6	2.0

Table 5.8.: Boeing 747-400 Combi Fleet-wide Performance Indication

Average ZFW [kg]	264860
Average ZFWMAC [%]	32
Average Savings at 5% CG Shift [kg]	800

Boeing 787-9

Being the newest addition to the fleet of KLM, the 787-9 is praised for its high efficiency (The Boeing Company, 2006). Due to this, and its relatively small size compared to other long haul aircraft within the fleet, one would expect the potential savings to be smaller than the other aircraft. However, looking at table 5.9 and comparing to other aircraft, this is not evident. The aircraft seems to have similar fuel saving quantities as the Boeing 777-200ER with respect to the CG. Both aircraft types are often being used on the same routes, making comparing slightly easier. It is therefore found that the Boeing 787-9 is influenced more by the CG than the 777-200ER.

Table 5.9.: Boeing 787-9 Top 5 Potential Savings Indication

Ranking	1	2	3	4	5
Origin	AMS	GIG	KUL	MRU	XMN
Destination	GRU	AMS	AMS	AMS	AMS
Season [-]	Summer	Winter	Winter	Winter	Winter
Average Consumption [kg]	70000	62800	77900	67800	74000
Average ZFW [kg]	189000	182000	182200	177300	188300
Average ZFWMAC [%]	31	36	32	34	32
5% CG Shift Savings [kg]	830	810	780	770	680
Percentage of Total at 5% shift [%]	1.2	1.3	1.0	1.1	0.9

Table 5.10.: Boeing 787-9 Fleet-wide Performance Indication

Average ZFW [kg]	185200
Average ZFWMAC [%]	33
Average Savings at 5% CG Shift [kg]	290

Airbus A330-200

With all Boeing aircraft discussed, the two Airbus types are up next. The Airbus A330-200 is slightly smaller than the Boeing 787-9, but of an older design. This reflects in the potential fuel savings being larger for the A330-200. Both the 787-9 and A330 family are used on long haul flights, although the A330 is most frequently used on medium haul routes in Africa or Eastern America. This reflects in the top 5 in table 5.11 containing the longest routes, with all medium haul routes falling outside the top 5. This is reflected by the average savings potential being considerably lower than the values encountered in the top 5.

Both the Airbus A330-200 and A330-300 have a trim tank to influence the CG in flight. This has been included in these results, while the magnitude of the savings by the trim tank is discussed in section 5.2. Due to the trim tank mainly influencing the CG in flight (Airbus SE, 2017a), it is not included in the ZFWMAC figures presented in table 5.11.

Table 5.11.: Airbus A330-200 Top 5 Potential Savings Indication

Ranking	1	2	3	4	5
Origin	AMS	AMS	AMS	AMS	AMS
Destination	YYC	AUA	JRO	HAV	DFW
Season [-]	Winter	Winter	Winter	Winter	Summer
Average Consumption [kg]	57700	61500	51500	66700	62500
Average ZFW [kg]	175200	166300	166800	168500	170700
Average ZFWMAC [%]	36	39	37	38	35
5% CG Shift Savings [kg]	1100	1060	930	910	900
Percentage of Total at 5% shift [%]	1.9	1.7	1.8	1.4	1.4

Table 5.12.: Airbus A330-200 Fleet-wide Performance Indication

Average ZFW [kg]	168800
Average ZFWMAC [%]	37
Average Savings at 5% CG Shift [kg]	450

Airbus A330-300

The final aircraft being considered is the Airbus A330-300. Like the A330-200, it is used on medium haul routes, and occasionally on long haul routes. This use on medium haul routes is more clearly seen in table 5.13 than in table 5.11. Table 5.13 shows Dubai (DXB), which has a significantly lower savings potential than higher ranking routes. This trend continues outside the top 5, showing the medium haul routes having significantly lower potentials than the top 4. The average savings for a 5% shift is therefore significantly smaller than the top 5. Once again, the trim tank has been included in the results, as was done for the A330-200.

Table 5.13.: Airbus A330-300 Top 5 Potential Savings Indication

Ranking	1	2	3	4	5
Origin	AMS	AMS	AMS	DEL	DXB
Destination	BON	YUL	YEG	AMS	AMS
Season [-]	Winter	Winter	Winter	Summer	Winter
Average Consumption [kg]	63200	46800	56100	55500	45400
Average ZFW [kg]	175000	183700	180300	191100	186300
Average ZFWMAC [%]	31	33	37	28	28
5% CG Shift Savings [kg]	1140	1100	1020	890	830
Percentage of Total at 5% shift [%]	1.8	2.4	1.8	1.6	1.8

Table 5.14.: Airbus A330-300 Fleet-wide Performance Indication

Average ZFW [kg]	179000
Average ZFWMAC [%]	33
Average Savings at 5% CG Shift [kg]	400

5.1.3. Short Range

As was mentioned at the beginning of chapter 3, short range flights are not considered. To check the short flights are indeed not worth the effort, two routes were checked for this. Due to the main focus of this research being placed on the Boeing 777-200ER, a short range flight was investigated for this type. The particular aircraft is analysed for Cairo (CAI) from Amsterdam (AMS) during summer, which is about 3300km apart. The second flight is a leg between two cities served in a triangular routing between Amsterdam, Bonaire (BON) and Aruba (AUA). Bonaire and Aruba are 194km apart. Both types have their highest savings potential routes added for comparison purposes.

Both types have their number one potential route as a comparison available in table 5.15. It can be concluded that 27kg of fuel is not worth the hassle of optimising the ZFWMAC for. Plus, it can be seen that the CG has a smaller percentage-wise impact, most likely due to the large portion of take-off and landing on the route. These phases use flaps and landing gear, which have a considerably larger impact on the drag than the CG.

Table 5.15.: Short Range Comparison Indication

Aircraft Type	777-200ER	777-200ER	A330-300	A330-300
Origin	SIN	AMS	AMS	BON
Destination	AMS	CAI	BON	AUA
Season [-]	Winter	Summer	Winter	Winter
Average Consumption [kg]	94300	21400	63200	4000
5% CG Shift Savings [kg]	820	200	1140	26
10% CG Shift Savings [kg]	1420	340	2500	47
Percentage of Total at 5% shift [%]	0.9	0.9	1.8	0.7
Percentage of Total at 10% shift [%]	1.5	1.6	4.0	1.2

5.2. A330 Trim Tank

As discussed in section 3.2.5, the results for the Airbus A330 are including trim tank. Out of interest, the program was run with an empty trim tank, since it is used on every flight in the calculations. This showed, that an A330-300 flying from Amsterdam to Bonaire using the average values during winter saved 330kg of additional fuel due to the trim tank. Over all A330-200 flights, about 220kg is saved (0.45%) and 200kg (0.39%) for the A330-300.

The savings for the A330-200 are larger, partially due to the average range, but also since the both types share the same horizontal tail. Due to the shorter fuselage, the A330-200 will have to generate a larger downforce. As discussed in chapter 2, the relation between lift and drag coefficient is parabolic, explaining the A330-200 having a larger fuel savings. Note that the application of a full or empty trim tank can have an influence too. The tool does not allow half full trim tanks, despite the FCOM stating the trim tank does empty the tank in increments. It also states certain conditions under which the trim tank is not filled or emptied, which also have not been incorporated.

5.3. Snowball Effect

Within aerospace engineering a so-called snowball effect exists. It encompasses the effect that due to reducing fuel burn, less fuel can be taken aboard. This in turn means the aircraft will fly more efficiently, reducing fuel burn, which in turn means even less fuel is needed to be taken on board.

This effect has not been included in the research, since the Loadcontrol department has no influence on fuel decisions. Therefore, the effect of shifting the CG means no fuel has to be added or removed once the load plan has been finalised. However, as discussed in chapter 6, Dispatch does use the ZFWMAC of the preliminary load plan to add or subtract fuel to the total fuel. Therefore, it was decided to perform an analysis of one route, including these iterations to see the impact. The fuel penalty table of Dispatch has not been used to update the fuel loaded. The computed fuel savings were preferred, since these were higher for the highest ranking routes. As such, this research shows the highest savings possible, as was also the goal of this whole research. Once again, taking the Amsterdam-Tokyo route for the 777-200ER, during winter and summer, results in table 5.16.

Table 5.16.: Boeing 777-200ER Savings Including Snowball Effect Indication

Origin	AMS	NRT	AMS	NRT
Destination	NRT	AMS	NRT	AMS
Season [-]	Winter	Winter	Summer	Summer
Average ZFW [kg]	212500	210800	214900	209400
Average ZFWMAC [%]	32	32	33	32
5% CG Shift Savings [kg]	280	690	340	320
5% CG Shift Savings Including Snowball [kg]	320	740	400	370
Percentage Savings [%]	0.3	0.8	0.5	0.4
Percentage Savings Including Snowball [%]	0.4	0.9	0.6	0.4

By including the snowball effect, between 0% and 0.1% of additional fuel can be saved for a Boeing 777-200ER flying between Amsterdam and Tokyo. Despite this seeming small, it is fuel that is easy to save. On a yearly basis, it can mean 122000kg of fuel on average, if a daily flight takes place per aircraft, assuming 300 days of availability. One can imagine the effect of doing this over the whole fleet.

5.4. Conclusion

With the developed model, seven aircraft types have been investigated and their highest potential routes were provided. Potential savings discussed varied between 2500kg and 590kg for a shift of 5 percentage points of the ZFWMAC. Over all flights, the longest flights provide higher savings potential. Flying in western direction has a considerable impact due to headwinds, especially during winter. These two conditions, together with the average ZFWMAC and ZFW performance, can push the longest routes out of the top 5.

Striking trends found during the research were the percentage wise high savings for flights with a low take-off weight. Higher take-off weights have a lower savings expressed in percentages of the total fuel. Despite this, the quantity of fuel saved is smaller compared to heavier flights.

A second remarkable discovery was the hardly visible parabolic relation between CG location and fuel consumption for the two variable function. This was determined to be due to the inclusion of all ZFWs when deriving the function.

Next to the major results and their observations, the snowball effect is investigated to see the additional impact. This results in roughly 0% and 0.1% additional savings flying between Amsterdam and Tokyo. This comes down to about 40kg. The Airbus trim tanks have been included, but investigating their effects separately showed a 0.4% to 0.5% additional savings. Finally, short range flights proved to have small potential fuel savings. As such, they can be ignored by KLM.

With the KLM fleet at the time of writing and assuming each aircraft flies one route per day, 335 days per year, about 10 million kilograms of fuel, or €5.5 to €7 million in fuel, can be saved. That is, if the ZFWMAC is shifted by 5 percentage points and loads are not increasing. No costs to enable the CG shift have been included in this figure.

6. Flight Planning Process

During the research, shifts at departments related to the loading of aircraft have been followed. This to understand the task of each department which has an influence on the CG and fuel consumption. This chapter will discuss the process related to baggage and cargo handling and the fuel planning influencing the CG. It is, in general, discussed chronologically, with each section giving the unit of time as indication. Due to confidentiality, the exact deadline is not provided, with some deadlines being left out or switched, leaving only the general process available. The tasks to finalise will be discussed briefly, with any link to this research, observations or improvements finalising the discussion. This provides KLM recommendations throughout the process and how this can be adjusted or improved.

A Hours

At A hours to departure, the flight is created in ALTEA FM, the program developing the loadplan, loadsheet and balance of the flight. At this instance, it is only created, since the tailnumber assigned to the flight is not yet known. No fuel figures and initial weight and balance planning is added to the flight at this instance. At this point, bookings are still open and the loads are therefore not fixed.

Observation and Advise
Due to the early stage, many variables are estimated or not entered. As such any planning done during this stage is very inaccurate. As such, it is only created digitally, without any human interaction. It is advised to consider using algorithms to determine the expected load, based on the booked passenger numbers. This can be used to make a preliminary, estimated load plan, potentially reducing man hours at a later stage.

B Hours

The expected available space is determined for cargo. This is based on algorithms predicting the amount of baggage passengers will check in. The leftover space in the cargo holds is made available for cargo, which can determine the cargo taken along on the flight. With this knowledge, the containers and pallets are loaded.

Observation and Advise
This is the first instance where a qualitative estimate of the weight and balance of the

flight can be made. The number of passengers are nearing the final numbers and the amount of pallets that can be taken along can be estimated with reasonable accuracy. Due to ALTEA FM including a statistically determined amount of fuel, an initial estimation of the ZFWMAC can be made.

Figure 6.1 is applicable from this instance on, with the current stage being at the left of the figure. Any changes made during these first stages can have a large impact on the CG, since there is plenty of time to make them possible. At later stages, only small changes are performed, unless absolutely necessary. Therefore, the possible impact is quantified as small, since large changes are mostly not performed.

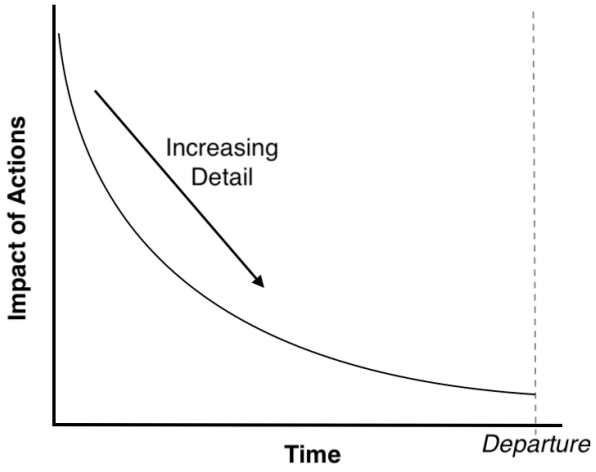

Figure 6.1.: Quantitative Impact-Time Diagram

The need and ability to shift the CG aft on the considered flight can be communicated with the cargo department. By doing so, certain pallets can be loaded with the heaviest cargo, such that they can be placed aft in the aircraft, if desired. It is advised to investigate this, since B hours are available for this initial loading scheme. Occasionally, this is already done, making one wonder why not more often.

A Minutes

At A minutes to departure, the cargo department sends their booking weights to ALTEA. Following this action, a forecast of the ZFW is sent to Dispatch. This does not include adjusted ZFWMAC information. In turn, Dispatch is able to make a preliminary flight plan.

Observation and Advise
At this stage only the total weights are known, the details of the pallets are not. As

such, no ZFWMAC related data can be obtained. Due to this, it is advised to see if any details on the pallets can be determined at this stage. Preliminary or estimated details can aid in developing a preliminary load plan, which means more time is available until departure. As shown in figure 6.1, at the earlier stages larger changes are possible due to the abundance of time.

B Minutes

Most passengers with baggage have been checked in by this point, meaning most of the weights of the luggage is known. In addition, passengers have been classified as Male, Female or Child, each having a dedicated average weight. This updates the weight and balance of the flight, with baggage containers estimates gradually being adjusted to actual values. At this moment, dispatch needs the final load data, as to make the flightplan for the flight plan.

Due to estimates still being (partly) used at this instance, if a larger than specified difference occurs between actual and planned weight, dispatch must be notified. The updated data is used to check if the flightplan and fuel quantity is still valid, and is adjusted if necessary.

On long haul flights, it can occur that the aircraft is limited in the amount of passengers and freight taken aboard. Some airports can have only one departure direction due to numerous reasons. With certain wind directions, the aircraft is limited in the take-off weight, reducing the cargo and passengers taken aboard. Similarly, it frequently occurs that freight is left at the airport on westward flights which are limited in their MZFW. Such flights are extra sensitive to differences in planned and actual weights, and require more attention.

Observation and Advise
Due to the actual loading taking place shortly after this deadline, this is the last instance to make large changes. One can imagine that once some load is on board, it will not be taken off board unless absolutely necessary. This is also depicted in figure 6.1, with the possible impact decreasing with time. The current point is roughly halfway to departure.

During loading at the gate, it is allowed to make changes, but this hardly happens as it is discouraged. It is therefore advised to have time available at this stage to make a good final planning. The time saved by reducing man-hours at previous deadlines can be used here. After this moment, dispatch will not include the effect of an aft CG in the fuel planning. This research excludes the ability to take less fuel on board due to an aft CG, but with the fuel penalty table, more fuel can be saved than provided in this research. It is advised to check how the CG is used within flight planning software of Dispatch. Also, the tables used by Dispatch for the ZFWMAC will have to be updated to increase accuracy, since their values do not correspond to those in this research. Differences between this research and the tables of dispatch are attributed to this research providing the results

per destination, whereas dispatch uses averages. Any existing CG effects within the used software should be investigated, compared with this research and compared with the table used by dispatch. Doing this research prevents double application of the CG related fuel penalty, and enables the more accurate to be used or even updated.

The results of this research show that on certain flights, hundreds of kilograms of fuel can be saved. On flights limited in their take-off weight, these savings in fuel can result in an extra passenger taken on board, meaning additional revenue next to the savings. Dispatch needs to include this in their planning, and therefore this is the last instance where this can be done without delays.

A second advise is to have $CG - \Delta Fuel$ tables for all aircraft available for dispatch, or ensure the software incorporates this. Currently, only some aircraft have these tables available, reducing the savings impact of aft CGs.

C Minutes and D Minutes

The final weights of the mail and express packages are released. At this instance, if the weight is more than a specified difference, spread over a predefined amount of pallets, an update is sent to dispatch. Large differences are rare and often insignificant to the total weight and balance of the aircraft. However, from a safety point of view, it should be checked.
At D minutes to departure, the final check of all cargo and baggage on board is conducted, along with the amount of passengers. This must be approved by the flight crew.

Observation and Advise
These deadlines are the only deadlines without a significant advise. Only advise that can be given is that any changes in the weight and balance, due to the express packages and post, can be used to finalise the amount of fuel needed. However, due to regulations, this requires additional work by the Dispatch and Loadcontrol departments, resulting in delays. Therefore, this advice is likely to be unfeasible.

E Minutes

With the acceptance of the flight plan by the cabin crew and all weights known, the aircraft is fuelled. Occasionally, the aircraft has been partially fuelled before this time, based on the final flight plan, stopping in time to prevent the removal of fuel at a later stage. After fuelling, the final fuel figures are shared with the flight crew.

Observation and Advise
Once the fuel is on board, removal is very often not seen as an option. If fuel can be saved by a certain action, it will not result in the highest potential savings. Due to this,

it is advised to aim for all CG related actions being finalised at this stage. This will maximise the savings, more than in this research.

F Minutes and G Minutes

The flight is closed, nothing is changed and the flight is ready for push-back, with the flight crew performing the last checks and paperwork. At F minutes the final cargo and passengers should be reported, such that at G minutes the loadsheet can be sent to the cockpit. The planned and actual cargo and passenger weights should be within a second predefined value, and if it does not comply, a new loadsheet should be sent. If the differences are larger than the predefined maximum over a certain number of containers or pallets, the flight planning must be redone by dispatch, causing delays. Causes can be missing pallets or containers, or baggage from passengers missing their connection.

Observation and Advise
To get a feeling of the accuracy of estimations of the load, it is interesting to create a database of loaded and planned cargo and baggage. By doing this, KLM will be able to determine how feasible it is to include CG optimisation.

A second note is related to differences. Being at the left of figure 6.1, differences should be small. Any large change will cause delays and is unwanted. As such, the predefined difference is very uncommon, and if the flight is lighter than planned, no changes to the flight plan have to be made. It is advised to keep track of these occurrences, since the knowledge can be used for improvement. Due to the second predefined limit being critical at this point, it is stressed to focus on focusing on these occurrences first, since this will occur more frequently.

H Minutes

H minutes before departure the Boeing 747 will perform a balance measurement by measuring the deflection of the nose gear. The weight is checked with the nose and main gear deflections.

Observation and Advise
Just like the previous deadline, monitoring the differences between planned and actual loads can help shed light on what parts can be improved most.

This deadline only applies to the Boeing 747. It can be interesting to have similar measurements on other aircraft. Its data can be used to make comparisons between measured and calculated weight distributions. The possibility to use the horizontal tail setting to determine the distribution is also interesting, and will be further discussed in section 7.2.

Conclusion

Based on the analysis of the time line, a general advise has been created. Three major subjects were identified, namely:

- Initial CG related savings
- Final CG related savings
- Data monitoring

The first point considers the first stages of flight planning, up to E minutes to departure. An initial load plan is developed and used with the flight plan to determine the required fuel. At this stage, the loadplan is not final since the current checked in luggage and the planned cargo does not consist all the load. It is therefore not of the highest accuracy achievable, since cargo and baggage can still be added at this stage. Based on the estimated load plan, a fuel adjustment is applied based on the planned ZFWMAC, meaning the snowball effect comes into play. This can be performed up to E minutes before departure, since the aircraft can be fuelled from this moment on. At this stage, however, the final load plan has not been finalised, so changes in the CG are possible, reducing the potential fuel savings. It is advised to reconsider this deadline. Delaying the deadline means higher accuracy and more accurate fuel planning, but this has to be agreed with the fuelling department. If possible, consider fuelling to, say, 90% and leave the last part until a later moment when the accuracy is higher. It can also be investigated if the load related deadlines can be brought forward, ensuring higher accuracy at an earlier stage.

Moving to the second point, which applies from E minutes to departure, changes in CG will not cause a change in fuel taken on board. The snowball effect is thus not applicable, but an additional shift aft of the CG will still save fuel. This is the stage at which the results of this research is aimed. The exact weight of the load is known at this stage, meaning the loadcontroller can focus effectively on aft CG if desired. Large, fuel consumption increasing changes are no longer allowed, since the fuel quantity has been frozen. Thus, at this stage it is wise to know what the allowable changes are, and how to maximise these to save fuel.

Finally, the last point is separate from the deadlines related to the first two points, as it is data related. It is focused on department improvements in the future, instead of considering singular flights. With aircraft determining their weight and balance before take-off, this provides valuable comparison data. The expected and calculated load and load scheme can be compared to the actual values. By doing so, any shortcomings in the calculated values can be focused on, improving the load schemes and fuel burns for future flights. It is advised to start a project to investigate this data, as it can be used in the future to improve the process and identify issues.

7. Conclusion, Discussion and Recommendations

This chapter contains the conclusions, discussions and recommendations drawn from the research. As can be read in previous chapters, the CG reduces fuel burn up to 2800kg, including the confidentiality factor, if moved aft. By computing the fuel consumption at multiple ZFWMAC and ZFW values, a function was derived. The simplified tool uses this function to enable quick determination of the fuel saved when shifting the ZFWMAC for the considered flight.

7.1. Conclusion

Means to reduce fuel burn are investigated by airlines, due to increasing fuel costs. The positive effect of an aft CG is one of the known means to reduce fuel burn. However, despite literature discussing this effect, no readily available method to derive a quantification are available. At the request of KLM, a quantification has been made of this relation, applicable to their fleet and practices.

Using the developed model, which is able to calculate the fuel consumption within 5% accuracy, it was found that about 0% to 4% of fuel can be saved if shifting the CG 5 percentage points. The exact figure mainly depends on the aircraft type, ZFW and ZFWMAC, although season can also have an influence. Generally, long routes heading west show the highest savings potential, especially during winter. Due to the nonlinear relation between CG and fuel consumption, results can vary, with a shift in the forward range of the CG range giving larger changes in fuel consumption. Same can be said for the ZFW, only with ZFW changes near the maximum allowable ZFW giving larger changes in fuel consumption. Taking all aircraft types and their average savings at a 5 percentage point shift in ZFWMAC will result in €5.5 to €7 million saving in fuel costs annually. This is excluding additional costs due to non-compliance with current logistical requirements.

7.2. Discussion and Recommendations

This section will discuss the results and provide any recommendations. Chapter 6 gave operational recommendations, while this section considers the three modules used in

this research. These modules used assumptions and simplifications, as can be read in previous chapters. These result in a decrease in accuracy of the fuel burn calculations. The effects of these assumptions and simplifications will be discussed in this chapter, and recommendations are derived from them for future research. First, a look will be taken at the flight profile generation, followed by the fuel burn calculations. The simplified model is treated next, followed by the turnaround time and associated costs. The discussion and recommendations for future research is the final section.

7.2.1. Flight Data Module

The flight data module searches outliers in the routing and removes these before developing the standard flight profile. In chapter 4 it already showed that the Amsterdam to Tokyo route did not have significantly deviating routes. However, due to the outliers considering the mean absolute deviation, some routes are removed, although them not visually deviating from the others. This shows a limitation of the outlier detection, and further investigation is advised to see if certain cases can occur when adding a larger amount of data compared to the validation data.

A second point of attention are the discussed wind days. Chapter 4 discussed the occurrence of the cargo not being loaded due to high wind speeds. Despite this, the flight data does show the cargo loaded, resulting in large differences between actual and calculated fuel burn. The model assumed that this situation occurs if the data showed a difference of at least 10% between actual and calculated fuel. These days are discarded before deriving the average flight profile. However, more attention might be required when more detail is required, since a 9% difference might be observed during wind days. This 9% will cause an outlier in the analysis, resulting in other outliers being kept despite them being outliers too. This also shows some inaccuracies that can occur with the used outlier method.

7.2.2. Fuel Burn Module

With the standard flight profiles, the fuel burn is calculated. One can observe that the method assumed that a climb is initiated directly after a waypoint. After achieving the required flight altitude, the module will model a cruise until the next waypoint. The order can be the other way round, or climb can be initiated between the waypoints. This effect is not considered, and will cause some deviating fuel burn calculations with respect to actual flight.

A second note is made regarding the thrust setting during climbs. Especially with constant TAS, the thrust is set constant to a certain value. Chapter 4 already discussed how two settings were used instead of one. Due to the actual aircraft providing the most efficient thrust setting under the encountered ambient temperatures, this can vary.

As such, the model does not always provide the correct thrust setting, causing slight differences between calculated and actual fuel burn.

Descend proved to be difficult to model and consists of the third note, as discussed in chapter 4. The same effect as during climb is an issue, since descent does not necessarily start at the waypoint. Also, expedited descents can occur, where spoilers are used to increase drag and reduce lift. This increases the rate of descent, but has not been incorporated in the model. The same principle goes for the use of flaps during take-off and landing, which enable lower flight speeds but have not been included in the model.

Finally, the validation showed that the CG can move outside the limits when burning fuel for certain ZFWMACs. Also, it might be near impossible to achieve the furthest aft limit for the ZFWMAC due to logistical constraints. These effects are considered practical limitations and have been touched upon briefly. Thorough research considering these practical limits have not been included in the scope of this research. KLM will ensure the CG is within the safety limits, but it is up to them to decide where the CG will be within these limits, while applying this research.

7.2.3. Simplified Model

The simplified model does not use complex calculations. As such, the approach of finding a function to the results will cause deviations in fuel computations compared to the complex calculations. Especially near ZFW and ZFWMAC limits, the simplified model can deviate from the complex calculations. Due to this, a warning has been added, warning the user of the situation. Despite this, this often occurs near the limits, which are not to occur frequently for the ZFWMAC.

As was also discussed in the previous section, the practical limitations of the ZFWMAC are not thoroughly included in the research. This is also the case for the simplified model. However, the loadcontrollers will encounter these limitations when using their planning software, and it is therefore not deemed necessary to add a second warning in the simplified model.

The last remark on the simplified model is related to the fuel burn prediction. As was mentioned in section 4.3, at times the fuel prediction can be off. Despite this, the change in fuel consumption can still be accurate, since the change is considered and not the overall fuel consumption. To prevent the tool being used for fuel predictions, these fuel consumption results are hidden for the user. If required, the main tool in this research can be used to make fuel burn predictions, but this would require a different simplified tool to be developed, which will be more accurate considering fuel burn.

7.2.4. Further Research

During research, subjects for future research were encountered. Currently, Loadcontrol is investigating the loading themes and setting a minimal limit for the program stating when to choose aft CG over logistic optimal loading. With the results of this research, the ZFWMAC shift at which it becomes cheaper to apply an aft CG can be determined. Doing this per route and incorporating the associated costs to achieve this will enable the loading program to automatically determine when to choose the aft CG theme. It is recommended to look into this possibility, but it is stressed that this can only be done effectively if detailed costs to achieve a shifted CG are known.

A second possible research opted by Loadcontrol is a research on the ZFWMAC performance per route. Having a clearer picture on why certain routes perform poorly can aid in improving the CG. Combining with the results of this report provides a justification for any changes in the loading process on certain routes. It also justifies why such researches are of interest, since improving CG performance is recommended. When performing this research, it is also advised to research how much ZFWMAC shift is possible per route. By doing these together, it is directly visible which routes will keep on performing poorly and which have a high savings potential.

Within the maintenance department, a research related to the tail setting is considered. The tail setting is related to the CG location. The idea is to use this to get more accurate balance reports of an aircraft, frequently updating these between the actual weighing of an aircraft. It is recommended to combine this with this research, as to provide more accurate CG data and savings calculations.

References

Airbus SE. (2004). *Getting to grips with fuel economy.* `http://ansperformance.eu/references/library/airbus-fuel-economy.pdf`.

Airbus SE. (2013). Flight Crew Operating Manual [Computer software manual]. Toulouse, France.

Airbus SE. (2017a). Aircraft Flight Manual [Computer software manual]. Toulouse, France.

Airbus SE. (2017b). *Eco-efficiency, The A350 XWB: an Xtra green aircraft.* `http://www.a350xwb.com/eco-efficiency/`.

A. K. Kundu, D. R., M. A. Price. (2016). *Theory and Practice of Aircraft Performance.* New Jersey: John Wiley & Sons.

Anderson, D. (2006). *Fuel Conservation, Operational Procedures for Environmental Performance.* Seattle, United States.

Anderson, J. (2005). *Introduction to Flight* (fifth ed.). Singapore: McGraw-Hill.

Benson, T. (2014). *Propulsion System Analysis* (Tech. Rep.). Cleveland, United States: National Aeronautics and Space Administration.

Blake, W. (2009). *Jet Transport Performance Methods.* Seattle: The Boeing Company.

Buijtenen, J., Visser, W., Shakariyants, S. & Montella, F. (2011). Gas Turbines, Propulsion and Power, AE2–203 [Computer software manual].

Buisson, D. & Moline, A. (1988). *Process and system for determining the longitudinal position of the center of gravity of an aircraft provided with an adjustable horizontal stabilizer and application to the monitoring of said center of gravity near the focus of the aircraft* (No. US 4937754 A). United States.

Cavcar, M. (2010). *The International Standard Atmosphere (ISA)* (Tech. Rep.). Eskisehir, Turkey: Anadolu University.

Chatterji, G., Sridhar, B. & Bilimoria, K. (1996). *En-route Flight Trajectory Prediction for Conflict Avoidance and Traffic Management* (Tech. Rep.). Moffett Field, United States: National Aeronautics and Space Administration Ames Research Center.

Chatterji, G. B. (2011). *Fuel Burn Estimation Using Real Track Data* (No. 11). American Institute of Aeronautics and Astronautics.

Cheng, F. & Gulding, J. (2016). *Computing Wind-Optimal Routes for Flight Performance* (Tech. Rep.). Washington D.C., United States: Federal Aviation Administration.

Civil Aviation Authority. (2016). *Check flight handbook.* `https://www.skybrary.aero/bookshelf/books/876.pdf`.

Collins, B. P. (1982). *Estimation of Aircraft Fuel Consumption* (Tech. Rep.). Reston, United States: American Institute of Aeronautics and Astronautics.

Dispatch, K. L. M. (2017). *Untitled Manuscript.* unpublished private communication (oral).

EUROCONTROL. (2009). *Base of Aircraft Data (BADA) Aircraft Performance Modelling Report* (Tech. Rep.). Bretigny-sur-Orge, France: EUROCONTROL Experimental Centre.

EUROCONTROL Experimental Centre. (2014). User Manual for the Base of Aircraft Data (BADA) [Computer software manual]. Bretigny-sur-Orge, France.

Graham, D., Nelson, R. & Olive, E. (1980). *Trim control system for reduced drag* (No. US 4382282 A). United States.

International Air Transport Association. (2017). *IATA Fact Sheet-Fuel.* `http://www.iata.org/pressroom/facts_figures/fact_sheets/Documents/fact-sheet-fuel.pdf`.

Jara-Díaz, S., Cortés, C. & Mora, G. (2012). *Transportation Research Part E: Logistics and Transportation Review* (Tech. Rep.). Santiago de Chile, Chile: Universidad de Chile.

Jardine, C. N. (2012). *NCEP/NCAR Reanalysis Monthly Means and Other Derived Variables: Pressure Level* (Tech. Rep.). Oxford, United Kingdom: Earth System Research Laboratory.

KLM Royal Dutch Airlines. (2017). *Seating Plans.* `https://www.klm.com/travel/nl_en/prepare_for_travel/on_board/seating_plans/index.htm`.

Koninklijke Luchtvaart Maatschappij. (2017). *Untitled Internal Email.* unpublished private communication (email).

Koninklijke Luchtvaart Maatschappij. (2018). *Untitled Internal Email.* unpublished private communication (email).

Koninklijke Luchtvaart Maatschappij and The Boeing Company. (2018). *Untitled Internal Email.* unpublished private communication (email).

Koninklijke Luchtvaart Maatschappij, O. I. S. (2011). *Basic Index and MAC/RC Formula* (Tech. Rep.). Schiphol, The Netherlands: Koninklijke Luchtvaart Maatschappij & The Boeing Company.

Lee, H., Aminpour, H. & Morgenstein, J. (2003). *Aircraft with active center of gravity control* (No. US 6913228 B2). United States.

Loadcontrol, K. L. M. (2017). *Untitled Manuscript.* unpublished private communication (oral and email).

Marianne. (2014). *Lost but lovely: The haversine.* `https://plus.maths.org/content/lost-lovely-haversine`.

Miller, S. (2010). *Adaptive Wing Structures for Aeroelastic Drag Reduction and Loads Elevation* (Tech. Rep.). Manchester, United Kingdom: University of Manchester.

Mongeau, M. & Bès, C. (2003). *Optimization of Aircraft Container Loading* (Tech. Rep.). Toulouse, France: Université Paul Sabatier and Airbus France.

Mulder, J., van Staveren, W., van der Vaart, J. & de Weerdt, E. (2014). *Flight dynamics lecture notes.* Delft University of Technology - University Lecture Slides.

NOREBBO. (2014). *Boeing 787-9 blank illustration templates.* `https://www.norebbo.com/2014/04/boeing-787-9-blank-illustration-templates/`.

Peckham, D. H. (1974). *Range Performance in Cruising Flight.* Springfield: National Technical Information Service.

Quito International Airport. (2018). *Know your airport, Physical Characteristics.* `http://www.aeropuertoquito.aero/en/15-conozca-su-aereopuerto/254-know-your-airport.html?highlight=WyJhbHRpdHVkZSJd`.

Raymer, D. (1992). *Aircraft design: A conceptual approach.* Washington D.C.: American Institute of Aeronautics and Astronautics.

Renteux, J.-L. (1987). *Aircraft Modelling Standards for Future ATC Systems* (Tech. Rep.). Bretigny-sur-Orge, France: EUROCONTROL Division E1.

Rising, J. & Henke, K. (1983). *L-1011 testing with relaxed static stability* (No. 1). Lockheed California Company.

Roberson, W. & Johns, J. (2008). *Fuel Conservation Strategies: Descent and Approach.* `http://www.boeing.com/commercial/aeromagazine/articles/qtr_02_10/pdfs/AERO_FuelConsSeries.pdf`.

Rolls-Royce plc. (2017). *World's Most Efficient Large Aero-Engine.* https://www.rolls-royce.com/products-and-services/civil-aerospace/airlines/trent-xwb.aspx.

Royal Schiphol Group. (2018). *Capacity Decleration Summer Season 2018.* `http://slotcoordination.nl/wp-content/uploads/2017/09/S18-AMS-Capacity-declaration.pdf`.

Ruijgrok, G. (2009). *Elements of airplane performance.* Delft: Vereniging voor Studie- en Studentenbelangen te Delft.

Senzig, D., Flemming, G. & Iovinelli, R. (2009). *Modelling of Terminal-Area Airplane Fuel Consumption* (Tech. Rep.). Reston, United States: American Institute of Aeronautics and Astronautics.

Smith, S. (1996). *A Computational And Experimental Study of Nonlinear Aspects of Induced Drag* (Tech. Rep.). Washington D.C., United States: National Aeronautics and Space Administration.

Stevens, B. & Lewis, F. (1992). *Aircraft Control and Simulation.* New Jersey: John Wiley & Sons.

The Boeing Company. (2004). Performance Engineers Manual Boeing 777-200ER / GE90-94B [Computer software manual]. Seattle, United States.

The Boeing Company. (2006). *Boeing 787 From the Ground Up.* `http://www.boeing.com/commercial/aeromagazine/articles/qtr_4_06/AERO_Q406_article4.pdf`.

The Boeing Company. (2010). Aircraft Flight Manual [Computer software manual]. Toulouse, France.

The Boeing Company. (2017). Propulsion (1): Jet Engine Basics [Computer software manual]. Seattle, United States.

The Boeing Company. (2018). *Untitled Manuscript.* unpublished private communication (email).

The International Aviation Safety Association. (2018). *A330 Fuel System Trickery.* `http://www.iasa.com.au/folders/images/airtransat/vol1ch28sec20Top4000-eff1.htm`.

Torenbeek, E. (1982). *Synthesis of subsonic airplane design.* Delft: Delft University of Technology.

Transport Canada. (2012a). *Cruise Performance* (Tech. Rep.). Ottawa, Canada: Government of Canada.

Transport Canada. (2012b). *Long Range Cruise* (Tech. Rep.). Ottawa, Canada: Government of Canada.

van Ginneken, D., Voskuijl, M. & van Tooren, M. J. (2010). *Automated Control Surface Design and Sizing for the Prandtl Plane* (Tech. Rep.). Delft, Netherlands: Delft University of Technology and Pisa University.

Verschuren, P. & Doorewaard, H. (2010). *Designing a Research Project.* The Hague: Eleven International Publishing.

Voskuijl, M. (2011). *Introduction aerospace engineering: Flight mechanics lecture notes.* Delft University of Technology - University Lecture Slides.

A. Additional Theoretical Framework

This appendix discusses some details not thoroughly discussed in chapter 2 (Theory). It is followed by variables and conditions also not discussed in chapter 2. Next to the treated subjects giving added detail are subjects not included in the developed model for this research. Also, some light is shed on details which make this research less accurate, as discussed in chapter 7.2.

A.1. Forces and Moments

In a similar fashion as chapter 2, the forces and moments are derived. This time, a more extensive derivation is discussed, which served as a basis for chapter 2.

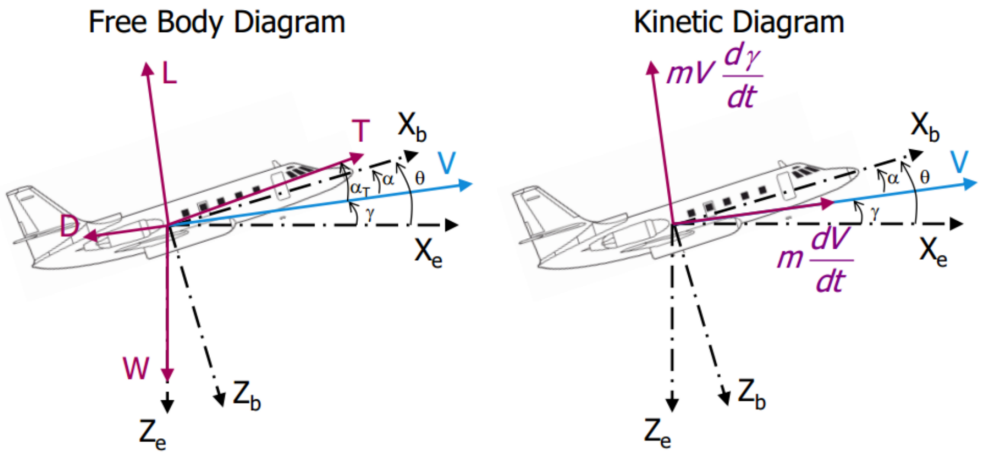

Figure A.1.: Free Body Diagram and Kinetic Diagram (Voskuijl, 2011)

Figure A.1 shows the free-body diagram and kinetic diagram for a point mass model. It served as the basis of chapter 2, which uses a simplified figure.

As discussed in chapter 2, the effect of the horizontal tailplane lift is, amongst others, dependent on the CG location. The free-body diagram in chapter 2 is derived using Torenbeek (Torenbeek, 1982), who discusses the use of figure A.2.

Figure A.2 shows the rigid body free-body diagram. It shows the forces contributing to the pitching moment, excluding the fuselage contribution. Note that the tail contribution

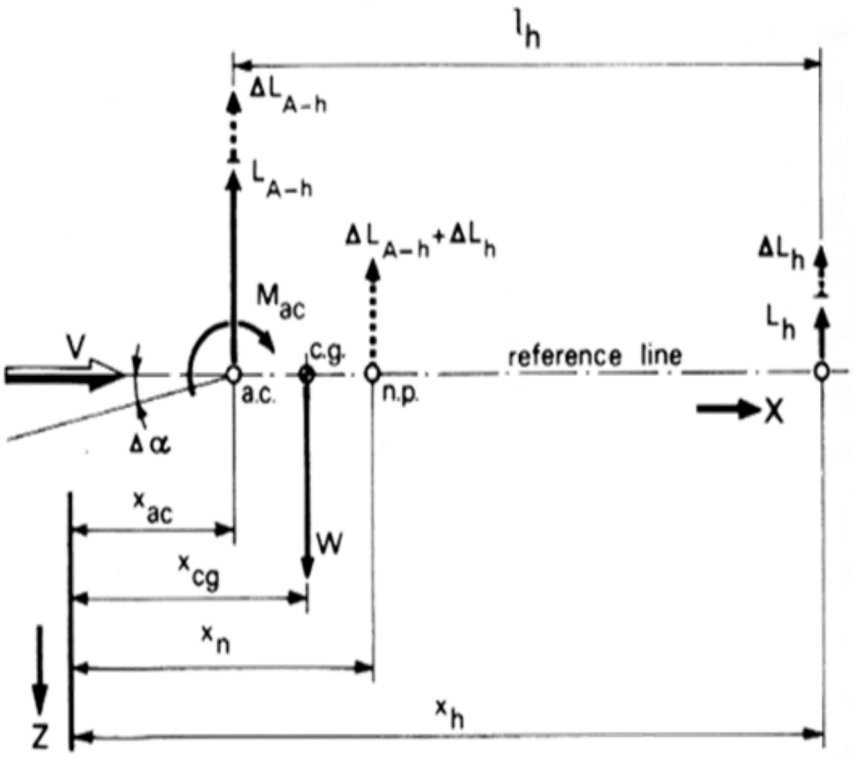

Figure A.2.: Moment Equilibrium (Torenbeek, 1982)

is drawn upward, but in fact is downward, as was shown in figure 2.1.

Torenbeek discusses the effect of a perturbation causing a change in angle of attack α, which will result in a change in lift. The resultant force acts through the so called neutral point. Around the neutral point, the resulting moment due to the perturbation is zero, by definition (Torenbeek, 1982).

A.2. Additional Modelling Details

As was discussed in chapter 3, details were left out of the research to reduce complexity. During initial research they were investigated to see the possibility of including them. The following sections discuss details that are not included, but can be for future applications. Their discussion also provides a short overview of any causes of reduced accuracy.

A.2.1. Flaps and Landing Gear

Flaps and landing gear are both needed during takeoff and landing. Whereas the landing gear only causes additional drag, flaps increase lift and drag, such that the aircraft can fly at lower speeds. Both effects are available through plots provided by OEMs and can be applied in similar ways as the main lift and drag polars. Due to the short time spent using these devices, they can be neglected for long haul flights.

A.2.2. Takeoff and Landing Procedure

Next to the flaps and landing gear during takeoff and landing, the aircraft requires acceleration and deceleration during these phases. Depending on airline procedures, this can change fuel consumption with respect to that of the OEM. This is yet another aspect that can be incorporated in a future model. That is, only if required when the takeoff and landing phases are added for additional detail or when a significant part of the total flight.

A.2.3. Turns and Sideslip

Chapter 3 mentioned that the theory is applicable to two dimensional flights. Side forces and turns were left out, but these are encountered by an aircraft. Examples are turns to align with a runway and follow a specified route, or sideslip to prevent down drifting. These effects make the flight less efficient. Sideslip means the vertical tail will cause a sideways force, which also causes drag, similar to the horizontal tail. During a banked turn, the aircraft requires additional lift generation to maintain altitude, as depicted by equation A.1 (Ruijgrok, 2009).

$$L = \frac{W}{cos\phi} \tag{A.1}$$

Due to the effect being a too small detail and too difficult to obtain data for, it will not be further investigated in this research. The turns require the inclusion of terms in all directions, while the model is built to only consider two dimensional flight. Turns would introduce side forces (from the fuselage to the wingtips), which adds an extra dimension and unnecessary complexity. The same applies to side-slipping flights.

A.2.4. Altitude offset airport

Since not all airports are located at the same altitude, the model can be extended to incorporate this. It will require the adjustment of the original altitude from sea level to

that of the airport. It will however mean the altitude affects the takeoff performance, another detail which is initially left out.

A.2.5. Fuel Penalties

A final addition would be fuel penalties. If a computation matching a certain aircraft is required, aircraft specific details are required. Such details can be the additional fuel consumption due to broken parts or engines not being clean. Due to a general result being required for this research, this has been left out, also reducing complexity. However, if required for future research, this can be added to the model. The PEM and similar manuals have fuel penalties for such occurrences.

A.3. Additional Details

This final section consists of details not used during the research and not related to the fuel burn computation. However, it sheds some light on a detail on the total picture. Therefore, it is added to the appendix.

A.3.1. Fuel Build-up

To get a better understanding of the fuel contribution per flight section, a short description of the fuel build-up is given. Multiple reports can be found on the subject of researching fuel burn, of which Airbus was used (2004). The build-up of total fuel consumption can be extracted from these references, and is defined as follows:

- Start-up fuel
- Taxi fuel
- Trip fuel
  - Take-off fuel
  - Cruise fuel
  - Landing fuel
- Reserve fuel
- APU fuel

Due to the focus of this research being on long-haul flights, the initial focus is on the cruise fuel. Cruise consists of the majority of a long-haul flight (up to 95% according to the provided KLM data), while taxi is excluded due to it being non-flying. The total trip

fuel, the fuel from standstill between take-off and landing, can be done as an extension of the base model if required and time permits.

Any fuel required for the Auxiliary Power Unit (APU) can be neglected. The percentage is insignificant compared to the total fuel consumption, plus the APU is mostly used on ground and not during flight. In the unusual case of the APU being used during flight, it is done during take-off to improve performance (Airbus SE, 2004), which is a small part of the total flight. The small contribution of take-off to the total fuel consumption, combined with the small percentage of fuel used by the APU, makes it neglectable.
The reserve fuel can also left out of consideration. It is assumed to remain the same. The regulations are the same, and the needed quantity will decrease slightly due to more efficient flight. The effects are assumed too insignificant for the scope of this research.

B. Fuel Burn Validation

As was mentioned in chapter 4, for validation the calculated fuel was compared with the actual fuel burn. The considered flight is on December 2^{nd}, 2018, flying from Tokyo to Amsterdam. For each waypoint, the flight phase, calculated fuel burn, actual fuel burn and the accuracy is given.

This table was removed due to confidentiality.

B.1. Standard Flight Fuel Consumption

For validation of the standardised route, with the ZFW and ZFWMAC being equal to the average, the standardised flight fuel burn can be computed. Similarities are expected and seen with the previous table, since that table is based on input data close to the averages. Due to rounding, certain waypoints seem to have identical fuel burn values, despite these actually being slightly different.

This table was removed due to confidentiality.

C. Largest Potential Route Results

Below in the table, are the route-aircraft combinations with the highest savings potential for KLM.

This table was removed due to confidentiality.

D. Results per Season

Since the results in chapter 5 had a strong tendency to present routes in winter as the highest potential, summer routes were also considered. This to present what the top 5 routes are per season. The results are shown in the tables below. As discussed in chapter 5, the longer routes, heading east will have the largest savings potential. Exceptions are mostly due to a poor performing ZFWMAC or significantly different ZFW. Due to certain aircraft types flying certain routes only during one season, it can occur that results might be different or unexpected between summer and winter. An example can be significantly different average savings during winter, since the type is only flown on short routes during this season.

This table was removed due to confidentiality.

E. Lift-Horizontal Tail Drag Relation

As was mentioned in chapter 5, at lower ZFW the CG has a larger percent-wise influence on the fuel consumption. In terms of total quantity, larger savings are present at large ZFWs, due to the considerably larger total fuel consumption. This difference in percentage between forward and aft CGs was not expected, but this result is checked with theory to see its origin. Figure E.1 is used as a basis (same as figure 2.1), and static conditions are considered.

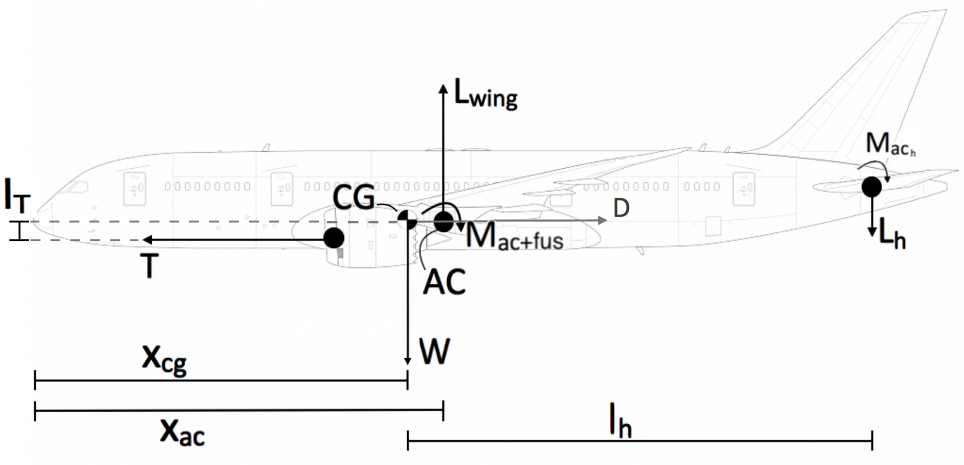

Figure E.1.: Free-Body Diagram (not to scale), *adapted from Norebbo (2014)*

Two new variables are defined, being d_1 and d_2. d_1 is the distance between the AC and CG, meaning $d_1 = x_{ac} - x_{cg}$. Similarly, d_2 does the same, only between the CG and horizontal tail AC, thus $d_2 = x_{ac_h} - x_{cg}$.
The relation between the change in lift, ΔL, and change in horizontal tail lift, ΔL_h, is found by setting the moment around the CG equal to zero. For simplicity, the thrust moment is assumed to be zero, while the aerodynamic moment of the horizontal tail is set equal to zero due to the symmetric airfoil. Doing this results in equation E.1.

$$\Delta L_h = \frac{\Delta L d_1 - \Delta M_{ac}}{d_2} \tag{E.1}$$

The air density, flight velocity and aircraft specific values like the wing area and zero-lift drag coefficient will remain the same values. As such, equation E.2 can be rewritten to

equation E.3, depicting the change in lift. One can conclude that $\Delta C_{D_{wing}}$ is proportional to $\Delta C^2_{L_{wing}}$.

$$C_{D_{wing}} = C_{D_0} + \frac{C^2_{L_{wing}}}{\pi A e} \tag{E.2}$$

$$\Delta C_{D_{wing}} = \frac{\Delta C^2_{L_{wing}}}{\pi A e} \tag{E.3}$$

To obtain the lift coefficients of the tail and wing, equations E.4 and E.5 are used. The relation in equation E.1 has been used in the derivation of C_{L_h}.

$$\Delta C^2_{L_{wing}} = \frac{\Delta L^2}{\frac{1}{4}\rho^2 V^4 S^2} \tag{E.4}$$

$$\Delta C^2_{L_h} = \frac{\Delta L^2_h}{\frac{1}{4}\rho^2 V^4 S^2} = \frac{(\Delta L d_1 - \Delta M_{ac})^2}{\frac{1}{4}\rho^2 V^4 S^2 d_2^2} \tag{E.5}$$

Substituting equations E.4 and E.5 in equation E.3 gives equations E.6 and E.7.

$$\Delta C_{D_{wing}} = \frac{4\Delta L^2}{\pi A e \rho^2 V^4 S^2} \tag{E.6}$$

$$\Delta C_{D_h} = \frac{4(\Delta L d_1 - \Delta M_{ac})^2}{\pi A e \rho^2 V^4 S^2 d_2^2} \tag{E.7}$$

Finally, from equations E.6 and E.7 equation E.8. $\frac{\Delta C_{D_h}}{\Delta C_{D_{wing}}}$ is close to zero due to the small drag generated by the horizontal tail compared to the wing.

$$\frac{\Delta C_{D_h}}{\Delta C_{D_{wing}}} = \frac{\Delta L^2 d_2^2}{\Delta L^2 d_1^2 - 2\Delta M_{ac}\Delta L d_1 + \Delta M_{ac}^2} \tag{E.8}$$

If ΔM_{ac} were zero, equation E.8 would simplify to $\frac{d_2^2}{d_1^2}$, showing a constant relation between $C_{D_{wing}}$ and C_{D_h}. This is not what is seen in the results, showing M_{ac} has an influence that cannot be neglected.

Keeping ΔM_{ac} in the relation explains the difference being investigated. C_M is required to be negative for pitching stability, meaning M_{ac} acts in the opposite direction shown in figure E.1 (Ruijgrok, 2009). As such, any influence of ΔM_{ac} will contribute to a larger horizontal tail drag coefficient. Consulting a general $C_m - \alpha$ plot of a cambered wing, it can be seen that C_m does not vary as significant as C_L (J. Anderson, 2005). As such,

the main terms influencing the result of equation E.8 are thus the change in lift and its related terms.

Due to ΔM_{ac} being small, but not neglectable, the observation made in 5.1.1 is explained. Depending on the airfoil characteristics, ΔM_{ac} will vary in size. For heavier aircraft, L will be larger, with M_{ac} also being larger in absolute terms. Depending on the slope of C_m, it will cause the trim drag to be a larger or smaller percentage of the total drag. Referring to the results of the Boeing 777-200ER, it can thus be concluded that at higher weights, the trim drag will be a smaller percentage of the total drag.

F. Problem and Research Question

In chapter 1, two options during loading were mentioned. Both result in associated costs; optimising for logistics reduces effort and turnaround time during loading and unloading. Optimising the CG results in a lower fuel burn. This requires decisions to be made as to reduce overall costs.

Despite this trade-off being known within KLM, not much detail is known on the exact costs. As such, the focus has been on optimising for logistical efforts, with the aft CG being of a lower importance. With rising fuel costs (Jara-Díaz et al., 2012), the interest in more detail on the CG-fuel relation is created.
With this in mind, the first solution is to contact the OEM. Boeing does provide data on the relation, if requested, but with the fuel burn increase given in rounded percentages and large ranges of CG locations. In other words, if the CG were to be shifted by
As will be further discussed in chapter 2, not only the CG is of influence on the trim drag (and hence, total drag). The weight of the aircraft and the altitude are of influence too. As such, one can see that the rough table provided by Boeing, also lacks influencing details.

Since KLM also uses Airbus aircraft, this OEM should also be considered. However, no information at all is provided to account for the CG-fuel burn relation. This since the Airbus A-330 family, used by KLM, has a trim tank in the tail to influence the CG in flight (Airbus SE, 2017a).

An additional reason why OEMs do not provide much detail on the relation is since it is not required. When an aircraft is tested, it is done "ensure that the aircraft's flight characteristics and its functioning in flight do not differ significantly from the normal characteristics for the type and to check the flight performance against the appropriate sections of the flight manual" (Civil Aviation Authority, 2016). This does not include the detailed monitoring of the fuel consumption for many CG locations; as long as the results do not differ significantly from the computations and ensure safe flight. Additionally, focus is put on the stability during testing at various CG positions (Civil Aviation Authority, 2016).

Considering literature, not much additional information on the subject can be found. Despite references noting the benefit of an aft CG (Buisson & Moline, 1988), (Graham, Nelson & Olive, 1980), (Lee et al., 2003), detail is not available. Statements like "a displacement of the CG of less than 75cm in a long-range aircraft yields, over a 10.000km flight, a saving of 4000kg of fuel" (Mongeau & Bès, 2003) shed some light on achievable

quantities. However, detail on how these results were obtained is not provided, making application for KLM difficult.

F.1. Research Objective

Based on the previous section and the introduction (chapter 1), a direction for this research can be seen. With these chapters and this direction, the research objective was determined to be:

To add a model, for practical application by operators, to existing literature.

This model will enable the investigation of fuel consumption under variable inputs, especially with varying CG locations. It should incorporate data of KLM flights to give results specifically for the operator. This data is also used to validate the fuel consumption computed by the model. Any effects other than the drag should be investigated for the incorporation in the model. These can comprise indirect effects.

Since this research is performed at the request of KLM, and their request for practical implementation, a sub-objective was determined:

To develop a simplified tool or model for easy and quick implementation by KLM.

This sub-objective was added, since the main model will be too complex for quick implementation. It will also require too much input and computing for the destined use. This is a requirement that should not be forgotten or neglected.

F.2. Research Question

Based on the objective, one can derive the following research question:

What is the influence of the Centre of Gravity position on fuel consumption and how can this be modelled to give a simplified for economic advantage for an airline?

F.2.1. Sub-questions

Next to this main question, one can derive sub-questions. The first sub-questions were defined to aid in understanding any aspects related to the main question. The last three sub-questions are introduced due to the practical aspect of this research.

1. What flight phases are influenced by the CG, and how?
2. What variables have an influence on the trim drag aside from the CG location?
3. Are there limiting factors to the positioning of the CG?

4. What other factors are influenced when focusing on optimising the CG?
5. What set of variables are needed to model an actual flight?
6. How can the model be used to determine the CG influence on fuel consumption?
7. How can this model be used by an operator? What simplifications are needed?
8. What are the differences between aircraft types and influences on the CG considering trim tanks?

G. Use of Tool

For any research related to or continuing this research, the extensive and flight data tools will be available. To ease the use, this appendix is written to help any user. If this document is not sufficient, or questions arise, please contact the developer, Martijn Zondag.

This appendix consists of a short explanation on what script to run. Note that due to confidentiality, the PEM data are not included, as are the flight data. To enable replication, enough data is kept available to run the provided route. Some data has been altered, due to confidentiality. This provides the structure and order of magnitude for the input data required and the ability to perform a test run.

G.1. How To Run

Running the tool is simple. Open the main.m and ensure the correct flight input files (in .xlsx) are entered. This does assume all aircraft performance data discussed in section G.2 has been entered. Running the script will automatically call the data analyser and create a standard profile. This profile is then evaluated for the fuel consumption at various ZFWMAC and ZFW values. It is advised to run the flight data analyser separately and have the results saved, before running the fuel burn calculations. This prevents any error due to bad input data causing the whole program to quit.

The provided file also contains a readme file, containing additional notes and explanation on how to run the program.

G.2. Input Data

The PEM provides numerous data required for the tool. To get a quick reference, the following data should be obtained from the PEM for each respective script:

- Lift-Drag coefficient polar(s)
- CG influence on drag coefficient (k-factor)
- Thrust specific fuel consumption
- General thrust curves (Thrust setting-Thrust relation)

- Idle thrust fuel flows
- Idle thrust force
- Thrust required plots

In addition, the PEM provided means to derive the drag from the drag coefficients. This has been applied, but is advised to read as to understand the computations. Also, lift-drag coefficient figures have not been included, but can be if deemed necessary.